



UNIVERSIDADE FEDERAL DE PERNAMBUCO

CENTRO DE TECNOLOGIA E GEOCIÊNCIAS
ESCOLA DE ENGENHARIA DE PERNAMBUCO

DEPARTAMENTO DE OCEANOGRAFIA
PROGRAMA DE PÓS-GRADUAÇÃO EM OCEANOGRAFIA

***INFLUÊNCIA DOS FATORES AMBIENTAIS E ESPAÇO-
TEMPORAIS NA ABUNDÂNCIA, REPRODUÇÃO E
COMPORTAMENTO DO AGULHÃO-VELA, Istiophorus platypterus
(Shaw & Nodder, 1791) NO OCEANO ATLÂNTICO***

Bruno Leite Mourato

Orientador: Dr. Fabio Hissa Vieira Hazin


Tese apresentada ao Programa de Pós-graduação
em Oceanografia da Universidade Federal de
Pernambuco, como parte dos requisitos para
obtenção do título de Doutor em Oceanografia.

**Recife – PE
Junho de 2012**

Catálogo na fonte
Bibliotecária Margareth Malta, CRB-4 / 1198

M929i	<p>Mourato, Bruno Leite.</p> <p>Influência dos fatores ambientais e espaço-temporais na abundancia, reprodução e comportamento do Agulhão-Vela, <i>Istiophorus platypterus</i> (Shaw & Nodder, 1791) no Oceano Atlântico / Bruno Leite Mourato. - Recife: O Autor, 2012.</p> <p>viii, 152 folhas, il., gráfs., tabs.</p> <p>Orientador: Prof. Dr. Fabio Hissa Vieira Hazin.</p> <p>Tese (Doutorado) – Universidade Federal de Pernambuco. CTG. Programa de Pós-Graduação em Oceanografia, 2012.</p> <p>Inclui Referências Bibliográficas.</p> <p>1. Oceanografia. 2. Agulhão-Vela. 3. Desova. 4. Fecundidade. 5. Tamanho 6. Padronização de CPUE. 7. Telemetria via-satélite. 8. Oceano Atlântico. I. Hazin, Fabio Hissa Vieira. (Orientador). II. Título.</p> <p>UFPE</p> <p>551.46 CDD (22. ed.)</p> <p>BCTG/2012-257</p>
-------	---

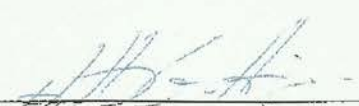
**INFLUÊNCIA DOS FATORES AMBIENTAIS E ESPAÇO-
TEMPORAIS NA ABUNDÂNCIA, REPRODUÇÃO E
COMPORTAMENTO DO AGULHÃO-VELA, *Istiophorus platypterus*
(Shaw & Nodder, 1791) NO OCEANO ATLÂNTICO**



Prof. Dr. Fábio Missa Vieira Hazin (Orientador; Titular)

Prof. Dr. Douglas Francisco Marcolino Gherardi (Titular)

Prof. Dr. Paulo Eurico Travassos (Titular)



Prof. Dr. Humberto Gomes Hazin (Titular)

Prof. Dr. Alberto Ferreira Amorim (Titular)



Prof. Dr. Thierry Frédou (Suplente)

Prof. Dr. Manuel Flores (Suplente)

Resumo

No presente trabalho foram investigados vários aspectos relacionados à dinâmica populacional, ecologia e pesca do agulhão-vela no Atlântico equatorial e sudoeste. As análises incluíram: (1) biologia reprodutiva; (2) modelagem da distribuição de tamanho e captura por unidade de esforço (CPUE) em relação aos efeitos ambientais e espaciais; (3) movimentos e utilização do habitat determinado por telemetria via-satélite e; (4) análise da CPUE de agulhão-vela capturado pela pesca esportiva no Brasil. A proporção sexual de agulhão-vela varia espaço-temporalmente na área de estudo e o comprimento de primeira maturação sexual estimado foi 147,21 cm de mandíbula inferior até a forquilha (MIF). A fecundidade variou entre $0,44 \times 10^6$ ovócitos hidratados para uma fêmea de 156 cm MIF e $2,26 \times 10^6$ ovócitos hidratados para uma fêmea de 183 cm LJFL. O Atlântico equatorial oeste não é uma área de desova, enquanto que a costa sudeste brasileira, ao contrário, se constitui em uma área de desova importante para a espécie, principalmente de dezembro a fevereiro. Altas densidades de adultos também foram observadas a oeste de 40°W, em ambas as partes da área de estudo, norte e sul. Por outro lado, uma tendência oposta foi observada em relação aos juvenis, que parecem estar associados a águas com temperatura da superfície do mar (TSM) superiores a 28°C com uma profundidade da camada de mistura mais profunda (> 50m), no lado ocidental, particularmente entre 10° - 20°S e 25° - 35°W. A modelagem da CPUE revelou uma agregação sazonal elevada ao longo da costa sudeste brasileira durante o pico de desova, enquanto que o centro-oeste do Atlântico, ao sul de ~ 15°S, bem como a costa norte brasileira, podem representar importantes áreas de alimentação durante o inverno. Os modelos também revelaram que a TSM e a velocidade do vento foram as variáveis mais importantes na variação da CPUE. Os resultados da telemetria via-satélite indicaram um claro padrão de utilização do habitat vertical, predominantemente concentrado próximo da superfície do mar com uma preferência relativamente estreita de temperatura. A "rota mais provável" sugerem que os agulhões-vela marcados não se deslocaram significativamente do local de marcação. Por fim, na presente tese, novos insights sobre a estrutura populacional da espécie no Oceano Atlântico foram apresentados e discutidos. Embora a separação do estoque do noroeste parece ser clara, ainda há uma grande incerteza sobre o grau de mistura entre os estoques do sudoeste e leste.

Palavras-chave: *Agulhão-vela; época de desova, proporção sexual, fecundidade, predição espacial, estrutura de tamanho, padronização de CPUE, telemetria via-satélite, Oceano Atlântico*

Abstract

In the present dissertation it was investigated several aspects related to the population dynamics, ecology and fishery of sailfish in the equatorial and southwestern Atlantic. The analysis included: (1) reproductive biology; (2) modeling of size distribution and catch rates in relation to environmental and spatial effects; (3) movements and habitat utilization determined by pop-up satellite tagging and; (4) catch rates of sailfish caught by spot fishery. Sex ratio of sailfish caught in the western equatorial south Atlantic varies temporally and spatially and estimate length at first sexual maturity was 147.21 cm Lower Jaw Fork Length (*LJFL*). Batch fecundity estimates ranged from 0.44×10^6 hydrated oocytes for a 156 cm *LJFL* female to 2.26×10^6 hydrated oocytes for a 183 cm *LJFL* female. The western equatorial Atlantic Ocean, off Brazilian coast is not a spawning ground for sailfish, while the southeast Brazilian coast, in contrast, seems to be an important spawning area for the species, with the spawning season happening mainly from December to February. High densities of adults were also observed to the west of 40°W, both at northern and southern parts of the studied area. An opposite trend was observed in relation to juveniles, which appear to be associated with waters with SSTs higher than 28°C and deep mixed layer (>50m) in the western side, particularly between 10° - 20°S and 25° - 35°W. Catch rate predictions revealed a seasonally high aggregation of sailfish off the southeast Brazilian coast during peak spawning while the mid-west Atlantic to the south of ~15°S as well as the Brazilian north coast may represent important winter feeding grounds. The oceanographic model revealed that SST and wind velocity were the most important variables describing catch rate variation. Regarding pop-up tags, the results indicate a clear pattern of vertical habitat utilization of sailfish, with the majority of the time spent being predominantly concentrated near the sea surface with a relatively narrow temperature range preference. In brief, the “most probable tracks” suggest that tagged sailfish did not move significantly away from the tagging site. Finally, in the present dissertation, new insights regarding the stock structure of sailfish in the Atlantic Ocean were presented and discussed. Although the separation of the northwest sailfish stock seems to be clear, there is still a large uncertainty about the degree of mixing between southwestern and eastern sailfish.

Key words: *Sailfish, spawning season, sex ratio, fecundity, spatial prediction, catch at size, catch rate standardization, pop-up satellite tagging, Atlantic Ocean.*

Agradecimentos

Aloha! agradeço primeiramente a Deus por ter me dado saúde, paz e paciência para concluir mais uma etapa da minha vida acadêmica. Deixo aqui registrado os meus profundos agradecimentos a todos que contribuíram para realização deste trabalho, especialmente as seguintes pessoas e entidades:

- A minha família pela confiança e por tudo o que fizeram e fazem até hoje para eu ter chegado aqui. Um obrigado especial aos meus pais, Margarida e Alberto por todo apoio prestado e confiança ao longo de todos esses anos.
- Um obrigado especial a minha companheira Bianca pelo companheirismo, suporte e parceria ao longo desses anos.
- Ao meu orientador Prof. Fábio Hazin pela amizade cultivada ao longo dos anos. Muito obrigado pela oportunidade e confiança, valeu professor! Serei sempre grato.
- Aos professores Alberto Amorim e Carlos Arfelli por tudo que fizeram ao longo desses anos, pelos inúmeros bate-papos e explicações sobre biologia pesquisa de grandes peixes pelágicos. Muito obrigado!
- Aos pesquisadores Keith Bigelow e Michael Musyl pela hospitalidade, confiança e ensinamentos durante o estágio no Havaí. *Mahalo's!!!!*
- Aos amigos Felipe Carvalho e Humberto Hazin, que além de serem grandes amigos, são um exemplo de conduta profissional a ser seguida! Obrigado por tudo “brothers”.
- Ao Prof. Paulo Travassos pela amizade, sugestões e críticas no desenvolvimento deste trabalho.
- Aos professores e pesquisadores Debie Murie, George Burgess e David Kerstetter por me acolherem na Flórida e pelas valiosas sugestões no desenvolvimento deste trabalho.
- Ao meu grande amigo Bruno Macena pelos inúmeros quebra-galhos, bate-papos científicos, dias de surfe em Maracaípe (rs!). Valeu irmão!
- Ao meu grande amigo Igor da Mata pela hospitalidade em Recife e inúmeros quebra-galhos! Muito Obrigado

- Ao meu parceiro de muitos anos Fábio Caltabelota pelos inúmeros bate-papos sobre “ciência pesqueira”, “surfe” e *other matters*. Vamos adiante.....aloha.
- Aos amigos Diogo Nunes, Bruno Oliveira, André Afonso, Rodrigo Barreto, Danielle Viana, Dráusio Vêras. Muito obrigado!
- À colega Patricia Pinheiro pelo auxílio prestado ao longo desses anos. Obrigado Paty!
- Aos professores da Universidade Federal de Pernambuco - UFPE/Departamento de Oceanografia. Um obrigado especial à Myrna Lins pelos inúmeros “quebra-galhos” prestados nesses anos.
- À Universidade Federal Rural de Pernambuco - UFRPE, especialmente ao Departamento de Pesca e Aquicultura pela utilização de suas instalações.
- Ao Conselho Nacional de Desenvolvimento Científico e Tecnológico - CNPq, do governo brasileiro pela bolsa de estudo e confiança depositada em mim para o desenvolvimento deste manuscrito.
- Ao *Joint Institute for Marine and Atmospheric Research - University of Hawaii* pela bolsa auxílio concedida durante o estágio no Havaí.
- Ao *NOAA Fisheries Pacific Islands Fisheries Science Center* pela hospitalidade e utilização de suas instalações durante o estágio no Havaí.
- Ao Ministério da Pesca e Aquicultura (MPA) pelo auxílio e aporte de recursos que sem dúvida viabilizaram o desenvolvimento do presente trabalho.
- Aos colegas “brasilienses” do MPA, em especial ao Felipe Pereira pelo auxílio prestado na formatação deste manuscrito e ao Rafael Roma pelos inúmeros *sessions* radicais no DF. Obrigado pela hospitalidade na minha chegada em Brasília.
- A todos os membros do Sub-Comitê Científico do Comitê Permanente de Gestão da Pesca de Atuns e Afins do MPA que de alguma forma apoiaram e auxiliaram no desenvolvimento do presente trabalho.
- Aos membros da comissão examinadora deste trabalho, Dr. Douglas Gherardi, Dr. Thierry Frédou, Dr. Alberto Amorim, Dr. Manuel Flores, Dr. Paulo Travassos e Dr. Humberto Hazin

pela disponibilidade, atenção prestada e pelas críticas construtivas apontadas para o melhoramento do presente manuscrito.

- A todas as pessoas do Laboratório de Oceanografia Pesqueira (LOP), Laboratório de Tecnologia Pesqueira (LATEP) e Laboratório de Ecologia Marinha (LEMAR) do departamento de Pesca e Aquicultura (DEPAq) da UFRPE, que auxiliaram e ajudaram de alguma forma a realização desta pesquisa.

E a todos que de alguma forma contribuíram para realização deste trabalho.

*Dedico este trabalho aos meus pais, Margarida e Alberto,
pelo apoio, confiança e paciência demonstrados ao longo
desses anos.*

Índice

Chapter 1 - Introdução Geral	11
1.1. Introdução.....	11
1.2. Identificação do problema abordado na tese	13
1.3. Objetivos	14
1.3.1. Objetivo geral.....	14
1.3.2. Objetivos específicos	15
1.4. Organização da tese.....	16
Chapter 2 - Spawning seasonality, sexual maturity, sex ratio and fecundity of sailfish in the equatorial and southwestern Atlantic Ocean	18
2.1. Introduction	19
2.2. Material and Methods.....	20
2.2.1. Sample collection and area of study	20
2.2.2. Assessing the reproductive activity	21
2.2.3. Reproductive parameters population	21
2.2.4. Spawning pattern and annual fecundity	22
2.3. Results	22
2.3.1. Size composition and sex ratio	22
2.3.2. Ovary development and spawning season	23
2.3.3. Spawning pattern	24
2.3.4. Length at first sexual maturity and batch fecundity.....	24
2.4. Discussion	25
2.4.1. Size distribution and sex ratio	25
2.4.2. Ovarian development and spawning season	25
2.4.3. Reproductive population parameters	27
Chapter 3 - Environmental and spatial effects on the size distribution of sailfish in the Atlantic Ocean	43
3.1. Introduction	43
3.2. Material and methods	45
3.2.1. Size data	45
3.2.2. Environmental data	45
3.2.3. Modeling	46
3.3. Results	47
3.4. Discussion	48
Chapter 4 - Spatio-temporal trends of sailfish catch rates in relation to spawning season and environmental factors in the equatorial and southwestern Atlantic Ocean	55
4.1. Introduction	55
4.2. Material and Methods.....	57

4.2.1.	Catch and effort data.....	57
4.2.2.	Environmental data	57
4.2.3.	Generalized additive model fitting procedures	58
4.3.	Results	59
4.3.1.	Modeling	60
4.3.2.	Selection and significance of variables in the models	60
4.3.3.	Spatiotemporal trends of catch rates	61
4.3.4.	Environmental effects on catch rate.....	61
4.4.	Discussion	62
4.4.1.	Modeling approach	62
4.4.2.	Spatiotemporal trends of catch rates	63
4.4.3.	Impact of environmental factors	64
Chapter 5 - Movements and habitat utilization of Atlantic sailfish off Southeast Brazil, determined by pop-up satellite tagging.....		80
5.1.	Introduction	81
5.2.	Material and Methods.....	83
5.2.1.	Field Operation and PSAT tag programming	83
5.2.2.	Horizontal distribution	85
5.2.3.	Vertical distribution	85
5.3.	Results	86
5.3.1.	Tag deployments and performance	86
5.3.2.	Vertical habitat use and temperature preference.....	86
5.3.3.	Horizontal movements	89
5.4.	Discussion	90
5.4.1.	Tag performance	90
5.4.2.	Vertical distribution	90
5.4.3.	Horizontal movements	93
Chapter 6 - Catch rates of Atlantic sailfish caught by sport fishery in southern Brazil.....		116
6.1.	Introduction	116
6.2.	Material and Methods.....	117
6.2.1.	Catch and effort data.....	117
6.2.2.	Modeling	118
6.3.	Results	119
6.3.1.	Exploratory analysis.....	119
6.3.2.	Standardization of catch rate.....	119
6.4.	Discussion	120
Chapter 7 - General conclusions and recommendations		134
Chapter 8 - References		139

Índice de tabelas

Table 2.1 - Sex ratio, χ^2 and p value from chi-squared test by area and month of sailfish caught in the southwestern and equatorial Atlantic Ocean.....	29
Table 2.2 - Sex ratio, χ^2 and p value from chi-squared test by area and size class of sailfish caught in the southwestern and equatorial Atlantic Ocean.....	29
Table 2.3 - Maturity classification of female sailfish ovaries from samples collected from the southwestern and equatorial Atlantic Ocean. GI represent the gonadal index.	30
Table 4.1 – Summary of model diagnostics used to select the error distribution of the spatiotemporal and oceanographic models for sailfish caught by Brazilian longline fleet in the southwestern Atlantic Ocean from 2004 to 2008. Deviance explained (%): Explained deviance by each model; AIC: Akaike Information Criterion and; BIC: Bayesian Information Criterion. 67	
Table 4.2 - Deviance analysis in the spatiotemporal models of sailfish caught by Brazilian longline fleet in the southwestern Atlantic Ocean from 2004 to 2008. Resid. df: residual degrees of freedom; df: degrees of freedom; Resid. Dev.: Residual deviance; $P(> \chi)$: Chi-square test p value; Dev.expl. (%): Explained deviance by each model and; AIC: Akaike Information Criterion.	68
Table 4.3 - Deviance analysis in the oceanographic models of sailfish caught by Brazilian longline fleet in the southwestern Atlantic Ocean from 2004 to 2008. Resid. df: residual degrees of freedom; df: degrees of freedom; Resid. Dev.: Residual deviance; $P(> \chi)$: Chi-square test p value; Dev.expl. (%): Explained deviance by each model and; AIC: Akaike Information Criterion.	69
Table 4.4 - Standardized sailfish catch rates and standard deviations (in parenthesis) associated of spatiotemporal and oceanographic models for spawning and non-spawning periods.....	70
Table 5.1 - Summary of depth and temperatures bins used to program the pop-up tags in the present study.	95
Table 5.2 – Mean, minimum, maximum temperatures and depths with the respective standard deviation experienced by tagged sailfish during the tracked period by fish and period.....	96

Table 5.3 - Movement parameter estimates for tagged sailfish determined from the Kalman Filter state-space model (KFTRACK). Blank spaces indicate models in which the parameters were set to zero, i.e. have no influence on the model, and were not estimated. u and v are advection parameters in longitude and latitude, respectively; D is all estimated diffusive parameters, b_x , b_y , b_{sst} are the bias estimates for longitude, latitude and SST, respectively; σ_x , σ_y , σ_{sst} are the standard deviations, a_0 is the upper bound for the latitude variance, b_0 is the estimated number of days prior to the equinox (when latitude error is maximal), and $nlogL$ is the loglikelihood function. u and v are expressed in nautical mile (nm) day⁻¹, D in nm² day⁻¹, b_x , b_y , b_{sst} , σ_x , σ_y , and σ_{sst} in degrees, and a_0 and b_0 in days..... 97

Table 6.1 - Deviance analysis of the fitted model for the standardization of sailfish catch rate caught by the Brazilian sport fishery in the Atlantic Ocean from 1996 to 2008. Resid. df: residual degrees of freedom; df: degrees of freedom; Resid. Dev.: Residual deviance and; $P(>|\chi|)$: Chi-square test p value..... 122

Table 6.2 - Estimations of coefficients, standard errors (SE), t-statistic and P-value of the t-test. 122

Índice de figuras

Figure 2.1 - Spatial distribution of longline sets from where sailfish were sampled by the Brazilian Pelagic Longline Observer Program from vessels operating in the southwestern and equatorial Atlantic Ocean between 2002 and 2006. Blue circles represent the longline sets sampled in the area 2..... 31

Figure 2.2 - Size frequency distributions of female and male of sailfish collected from the southwestern and equatorial Atlantic..... 32

Figure 2.3 - Mosaic plot showing the number of females and males of sailfish caught in the southwestern and equatorial Atlantic Ocean by month and area..... 33

Figure 2.4 Sex-ratio-at size (proportion of female) of sailfish caught in the southwestern and equatorial Atlantic Ocean by area..... 34

Figure 2.5 - Histological sections of ovaries of the Sailfish *Istiophorus platypterus* in different maturity phases. A: Immature (Scale bar = 100 μ m), B: Developing (Scale bar = 300 μ m), C:

Spawning capable (Scale bar = 350 μm), D: Actively spawning (Scale bar = 1000 μm), E: Regressing (Scale bar = 250 μm), F: Recovering (Scale bar = 100 μm). The oocyte stages: Og (oogonia), PG (primary growth oocyte), primary vitellogenic oocyte (Vtg1), secondary vitellogenic oocyte (Vtg2), tertiary vitellogenic oocyte (Vtg3), germinal vesicle migration (GVM), germinal vesicle breakdown (GVBD), hydrated oocyte (HO), post-ovulatory follicle (POF), alpha atresia (α -at) and beta atresia (β -at). Staining by Hematoxylin/Eosin. 35

Figure 2.6 - Ovarian weight by size class and maturity stage of females of sailfish caught in the southwestern and equatorial Atlantic Ocean. The dotted line represents the length at first sexual maturity. 36

Figure 2.7 - Relative frequency of the different maturity stages of female of sailfish caught in the southwestern and equatorial Atlantic by area and month. 37

Figure 2.8 – Box-plot of the gonadal index of female of sailfish caught in the southwestern and equatorial Atlantic by area and month. 38

Figure 2.9 - Box-plot of the gonadal index of female of sailfish caught in the southwestern and equatorial Atlantic by maturity stage. 39

Figure 2.10 - Size frequency distribution of whole oocytes of female of sailfish caught in the southwestern and equatorial Atlantic. The oocyte stages: PG (primary growth oocyte), primary vitellogenic oocyte (Vtg1), secondary vitellogenic oocyte (Vtg2), tertiary vitellogenic oocyte (Vtg3), germinal vesicle migration (GVM), germinal vesicle breakdown (GVBD), hydrated oocyte (HO) and post-ovulatory follicle (POF). 40

Figure 2.11 - Proportion of mature female of sailfish caught in the southwestern and equatorial Atlantic at 5 cm length intervals. *Left panel:* Fitted curve (red line) illustrate the optimal logistic curve fitted by maximum likelihood and observed values (blue points). *Right panel:* Approximate 95% confidence intervals from the likelihood profiles for parameter $LJFL_{50}$ of the proportion of maturity for sailfish. 41

Figure 2.12 - Relationship between the batch fecundity and lower jaw fork length for females of sailfish caught in the southwestern and equatorial Atlantic. 42

Figure 3.1 - Spatial Distribution of length frequency (LJFL) data obtained through the ICCAT *Data Record* from 1998 to 2007. The legend represents the number of fishes measured. 51

Figure 3.2 - Contribution of each variable added on the final model (model contribution). SST, sea surface temperature, CHO, chlorophyll- α concentration, DML, deep mixed layer and bathymetry, BATH in explanation of total variance.....	52
Figure 3.3 - Partial response curves showing the effects of the predictor variables added on the size model of adult sailfish in the South Atlantic from 1998 to 2007. SST, sea surface temperature, CHO, chlorophyll- α concentration, DML, deep mixed layer and BATH, bathymetry. Dashed lines represent the 95% confidence interval limits.	53
Figure 3.4 - Spatial prediction for the proportion of adult sailfish, using data from ICCAT <i>data record</i> from 1998 to 2007.	54
Figure 4.1 - Distribution of the Brazilian fishery longline sets in the Atlantic Ocean, from 2004 to 2008.	71
Figure 4.2 - Sailfish catch per set for the Brazilian longline fishery in the Atlantic Ocean from 2004 to 2008. Spawning period (left panel) and non-spawning period (right panel).	72
Figure 4.3 - Histogram of standard residuals (left panels) and quantile–quantile (QQ) plots of the deviance residuals (right panels) of the spatio-temporal models fitting sailfish catches using negative binomial error distribution.....	73
Figure 4.4 - Histogram of standard residuals (left panels) and quantile–quantile (QQ) plots of the deviance residuals (right panels) of the oceanographic models models fitting sailfish catches using negative binomial error distribution.	74
Figure 4.5 - Spatial predictions of catch rate for sailfish in the Brazilian longline fishery based on negative binomial spatio-temporal models (2004–2008). Spawning period (left panel) and non-spawning period (right panel). The color scale and contour lines represent the magnitude of the model predictions.....	75
Figure 4.6 - Standardized catch rate using a negative binomial error distribution of sailfish caught by the Brazilian longline fleet from 2004 to 2008. Black points represent the annual nominal catch rates.	76

Figure 4.7 – Partial residuals showing the effect of month on catch rate of sailfish caught by the Brazilian longline fleet from 2004 to 2008. Spawning period (left panel) and non-spawning period (right panel)	77
Figure 4.8 - Partial response curves showing the effects of the oceanographic variables on catch rate of sailfish caught by the Brazilian longline fleet from 2004 to 2008 for the spawning period. Shaded area represents the 95% confidence interval limits and the dotted line displayed on the plots indicates the mean catch rate estimated by the model.	78
Figure 4.9 - Partial response curves showing the effects of the oceanographic variables on catch rate of sailfish caught by the Brazilian longline fleet from 2004 to 2008 for the non-spawning period. Shaded area represents the 95% confidence interval limits and the dotted line displayed on the plots indicates the mean catch rate estimated by the model. The dotted line displayed on the plots indicates the mean catch rate estimated by the model	79
Figure 5.1 - Pop-up Satellite Archival Tag (PSAT), Wildlife Computers Inc (Redmond, WA, USA) MK10 PAT model. Lower panel shows the sailfish II in the moment of tagging.....	98
Figure 5.2 - Optimal placement of PSAT taghead in sailfish is shown in red. The area comprises the base of the dorsal fin between spaces of the interneural and neural spines	99
Figure 5.3 - The depth histograms, showing relative frequency of time spent that represent the entire dataset for each fish and period.	100
Figure 5.4 - The temperature histograms, showing relative frequency of time spent that represent the entire dataset for each fish and period.	101
Figure 5.5 - Cumulative frequency at depth (right) and temperature (left) for each sailfish.....	102
Figure 5.6 - Proportions of time spent by Delta T relative to the surface temperature for each fish and period.....	103
Figure 5.7 - Cluster analysis of the frequency distributions of the proportion of time at depth and temperature for each fish and period.	104
Figure 5.8 - Depth records by 3 h (sailfish I and II) and 6 h (sailfish III e IV) during the tracked period for each sailfish.....	105
Figure 5.9 - Depth records by period during the tracked period for each sailfish.	106

Figure 5.10 - Minimum and maximum daily temperature and depth experienced by sailfish ...	107
Figure 5.11 - Minimum and maximum daily temperature and depth experienced by sailfish II	108
Figure 5.12 - Minimum and maximum daily temperature and depth experienced by sailfish III	109
Figure 5.13 - Depth and temperature profiles experienced by tracked sailfish. Left panel shows the profiles for each fish separately and right panel shows all records pooled together.	110
Figure 5.14 - The depth histograms, showing relative frequency of time spent that represent the entire dataset for each fish and period.	111
Figure 5.15 - Most-probable track for sailfish I (upper right) fitted with (red line) Kalman Filter State-Space Model. The upper left panel shows a comparison between the raw gelocation marked by crosses and fitted track. Shaded blue are represents the confidence interval of the estimates. The lower panels show how well the model fits the two different information sources (longitude- left, latitude-right). Blue and dashed line represents the fitted track and the confidence intervals, respectively. Deployment point is marked by ‘▲’, and known recapture/pop-up position is marked by ‘▼’.....	112
Figure 5.16 - Most-probable track for sailfish II (upper right) fitted with (red line) Kalman Filter State-Space Model. The upper left panel shows a comparison between the raw gelocation marked by crosses and fitted track. Shaded blue are represents the confidence interval of the estimates. The lower panels show how well the model fits the two different information sources (longitude- left, latitude-right). Blue and dashed line represents the fitted track and the confidence intervals, respectively. Deployment point is marked by ‘▲’, and known recapture/pop-up position is marked by ‘▼’.....	113
Figure 5.17 - Most-probable track for sailfish III (upper right) fitted with (red line) Kalman Filter State-Space Model. The upper left panel shows a comparison between the raw gelocation marked by crosses and fitted track. Shaded blue are represents the confidence interval of the estimates. The lower panels show how well the model fits the two different information sources (longitude- left, latitude-right). Blue and dashed line represents the fitted track and the confidence intervals, respectively. Deployment point is marked by ‘▲’, and known recapture/pop-up position is marked by ‘▼’.....	114

Figure 5.18 - Most-probable track for sailfish IV (upper right) fitted with (red line) Kalman Filter State-Space Model. The upper left panel shows a comparison between the raw gelocation marked by crosses and fitted track. Shaded blue are represents the confidence interval of the estimates. The lower panels show how well the model fits the two different information sources (longitude-left, latitude-right). Blue and dashed line represents the fitted track and the confidence intervals, respectively. Deployment point is marked by ‘▲’, and known recapture/pop-up position is marked by ‘▼’.....	115
Figure 6.1 - Proportion of positive catch for sailfish in the Brazilian sport fishery in the Atlantic Ocean from 1996 to 2008.	123
Figure 6.2 - Sailfish catch per number of boats registered per tournament day for the Brazilian sport fishery in the Atlantic Ocean from 1996 to 2008.	124
Figure 6.3 - Grey bars empirical distribution of catch per number of boats registered per tournament per day; Red line represents the theoretical negative binomial distribution and; Blue line represents the theoretical Poisson distribution.....	125
Figure 6.4 - Fishing grounds of recreational fishery in southern Brazil representing two different fishing areas about approximately 90 miles from coast, as follows: A: 23° to 24°S/ 41° to 42°W for Rio de Janeiro and B: 24° to 25°S/ 44° to 45°W for São Paulo	126
Figure 6.5 - Number of tournament days monitored and total catch by year in the Brazilian sport fishery in the Atlantic Ocean from 1996 to 2008. Blue line represents the fishing effort and green line represents the total catch.....	127
Figure 6.6 - Proportion of species regularly caught year in the Brazilian sport fishery in the Atlantic Ocean from 1996 to 2008.....	128
Figure 6.7 - Percentage of total catch and total catch (n) by year in the Brazilian sport fishery in the Atlantic Ocean from 1996 to 2008. Blue line: Sailfish (%); Red line: Blue marlin (%); Green line: Tunas (%); Yellow line: White marlin (%) and; Black line: Total catch (n).....	129
Figure 6.8 – Box plot of nominal sailfish catch (n° of fish/n° of boats/day) for each factor and level in the Brazilian sport fishery in the Atlantic Ocean from 1996 to 2008	130

Figure 6.9 – Box plot of partial residuals for each select factor and level of the selected model for the standardization of sailfish caught by the sport fishery in Atlantic Ocean (1996-2008).	131
Figure 6.10 – Diagnostics plots of the fitted model for the standardization of sailfish caught by the Brazilian sport fishery in Atlantic Ocean (1996-2008). Red line represents the smooth fit and in the leverage plot dashed red line represents the Cook’s distance	132
Figure 6.11 – Nominal (black points) and standardized catch rate (blue line) of sailfish caught by the Brazilian sport fishery in Atlantic Ocean. Dashed line represents the standard errors of standardized catch rate estimates.	133

Chapter 1 - Introdução Geral

1.1. Introdução

O agulhão-vela, *Istiophorus platypterus*, pertencente à Ordem Perciformes e à Família Istiophoridae (Nakamura, 1985), possui distribuição circumglobal, encontrando-se amplamente distribuído em águas tropicais e temperadas. No oceano Atlântico a espécie ocorre, baseado em dados de captura, entre 40°N a 40°S, na porção oeste, e entre 50°N e 32°S, na porção leste (Ueyagnagi *et al.*, 1970; Ovchinnikov, 1971; Beardsley *et al.*, 1975; Nakamura, 1985). A presença da espécie no Mar Mediterrâneo tem sido também relatada, embora tais registros, além de raros, tenham se baseado em espécimes jovens, gerando dúvidas a respeito de sua identificação (Nakamura, 1985). É uma espécie oceânica, epipelágica e migradora, sendo geralmente encontrada em águas quentes acima da termoclina (entre 21 e 28°C), embora realize incursões eventuais em águas mais profundas (Nakamura, 1985). Apresenta um padrão migratório associado ao deslocamento sazonal das isotermas de superfície, situando-se normalmente em temperaturas acima de 26°C (Ueyagnagi *et al.*, 1970).

Entre as espécies de peixe de bico, o agulhão-vela é a que apresenta hábitos menos oceânicos. No Atlântico oeste tropical é freqüentemente encontrado sobre a plataforma continental, sobretudo no Golfo do México, Mar do Caribe e costa nordeste do Brasil. Embora, ocasionalmente, possa formar cardumes ou pequenos grupos, variando entre três e trinta indivíduos, é geralmente encontrado isolado, sem formar agregações (Beardsley *et al.*, 1975; Nakamura, 1985). É uma espécie heterossexual, não havendo características morfológicas externas ou coloração diferenciada entre machos e fêmeas, embora os espécimes maiores usualmente sejam do sexo feminino. Pode atingir um comprimento máximo de aproximadamente 348 cm e 100 kg de peso, com os machos alcançando a maturidade com 110 cm e as fêmeas com 130 cm (Jolley Jr., 1977; Nakamura, 1985).

O agulhão-vela é o um dos principais alvos da pesca recreacional e esportiva em todo o mundo, sendo uma das espécies mais capturadas por esta pescaria, devido a sua natureza menos oceânica entre os peixes de bico. Por outro lado, a pesca oceânica com espinhel de superfície direcionada para os atuns e o espadarte, representa o maior impacto sobre os estoques de agulhão-vela ao redor do mundo. Além disso, os estoques da espécie também tem sofrido

impacto de pescarias de pequena escala direcionadas ao dourado (*Coryphaena Hippurus*) no sudeste do Brasil e no Mar do Caribe. Entre os peixes de bico, o agulhão-vela é a espécie mais capturada e comercializada no Caribe. Em Barbados, por exemplo, a espécie perfaz 73% da captura total de peixes de bico (Mohammed *et al.* 2003). No Atlântico leste tropical, a espécie também é capturada incidentalmente na pesca de cerco europeia (Gaertner *et al.* 2002) e na pesca artesanal com redes de emalhar frente a costa de Gana e Senegal (ICCAT, 2009). Sendo assim, os estoques da espécie vêm sendo submetidos a uma intensa pressão pesqueira, a qual nas últimas décadas se intensificou de forma acentuada, não apenas pelo crescimento da pesca de espinhel e de pequena escala, mas também pela crescente popularização da pesca esportiva.

Em função do seu comportamento altamente migratório, a espécie é capturada por vários países e diferentes artes de pesca, o que faz com que a avaliação e o manejo de seus estoques só sejam possíveis por meio de esforços conjuntos de várias nações. No caso da pesca de atuns e afins no Atlântico, a organização responsável pela avaliação e manejo dos estoques de agulhões é a Comissão Internacional para a Conservação do Atum Atlântico (ICCAT - *International Commission for the Conservation of Atlantic Tunas*), constituída atualmente por quase 48 países. Historicamente a ICCAT tem adotado a hipótese da existência de dois estoques distintos de agulhão-vela (oeste e leste) separados arbitrariamente pelos meridianos associados à cordilheira meso-oceânica do Atlântico (40° W no Atlântico norte e; 20°W no Atlântico sul). Como os estoques de agulhão-vela encontram-se atualmente em níveis muito baixos de biomassa, apresentando sinais claros de sobrepesca, particularmente para o estoque leste, há uma necessidade urgente de adoção de medidas de ordenamento que garantam a sua conservação, as quais, entretanto, para que sejam efetivas, dependem fortemente da disponibilidade de dados de captura e esforço, além de informações biológicas, os quais são ainda, infelizmente, bastante escassos. Além disso, a necessidade de uma melhor definição da estrutura populacional dos agulhões no âmbito da ICCAT é tão grande que desde 1987 vem se desenvolvendo o Programa de Investigação Intensiva sobre os Agulhões, incluindo trabalhos de marcação e recaptura, distribuição e abundância, genética, levantamento das características de seus habitats, de idade e crescimento, de distribuição e de biologia reprodutiva.

Segundo as estatísticas da ICCAT, a captura de agulhão-vela no oceano Atlântico leste teve um aumento significativo entre as décadas de 50 e 60, passando de 95 t em 1957 para

1714 t em 1969. A partir de 1970 a captura continuou a aumentar atingindo o pico em 1976, com 6.250 t, seguido por uma tendência decrescente até 1981, com 3.050 t. Em 1983 a captura voltou a aumentar, atingindo 4.892 t, passando por um período de decréscimo gradativo até 1999, quando alcançou 2.724 t. De 2000 em diante a captura de agulhão-vela se estabilizou em aproximadamente 3.000 t/ano. O lado leste do oceano Atlântico sempre foi responsável pela maior parcela da captura dessa espécie, sobretudo, entre meados da década de 70 e o início da década de 90, quando foram registradas as maiores capturas (média de ~71% do total capturado no Atlântico). A partir da década de 90, a participação de ambos os lados do Atlântico se equilibraram em um patamar semelhante, embora o Atlântico oriental ainda apresente uma ligeira predominância nas capturas.

1.2. Identificação do problema abordado na tese

Historicamente o manejo dos recursos pesqueiros tem sido embasado em modelos de dinâmica populacional que levam em consideração apenas as alterações da abundância dos recursos ao longo do tempo (Hilborn e Walters, 1992). Tais modelos consideram as variáveis demográficas (abundância populacional) e ambientais de forma estacionária e correlacionadas dentro de uma escala temporal (*i.e.* médias anuais calculadas para extensas áreas geográficas) (Ciannelli *et al.*, 2008). Entretanto, apesar desses modelos fornecerem sinais de como os mecanismos denso-dependentes influenciam a dinâmica populacional dos recursos explorados, eles podem, ao mesmo tempo, potencialmente distorcer a interpretação acerca das interações entre o ambiente e a abundância dos recursos (Brill e Lutcavage, 2001), já que na maioria dos casos, em razão da falta de dados, a variabilidade populacional é considerada espacialmente homogênea.

Os organismos aquáticos, de uma maneira geral, apresentam uma elevada sensibilidade às variações das condições ambientais, decorrente de sua maior vulnerabilidade ao meio no qual estão imersos. Por essa razão, flutuações ambientais podem retardar ou acelerar, significativamente, a recuperação de um determinado estoque pesqueiro. Além disso, as mudanças no regime ambiental também podem determinar períodos de aumento da produção de alguns recursos importantes em algumas áreas e o declínio equivalente para outras populações, com consequências potencialmente negativas para o setor pesqueiro. A constante mudança espaço-temporal do meio ambiente é que condiciona a concentração das principais espécies de

atuns e afins numa determinada área e época do ano, onde as condições oceanográficas são favoráveis à reprodução ou à alimentação dessas espécies (Fréon e Misund, 1999), principalmente de espécies pelágicas que realizam grandes migrações, como é o caso do agulhão-vela.

Apesar do impacto das variações ambientais sobre a captura e distribuição dos recursos pesqueiros ter sido bastante discutido na arena internacional, em conjunção com a necessidade crescente de se buscar cada vez mais um manejo pesqueiro baseado no ecossistema (*ecosystem-based fisheries management*) (Pikitch *et al.*, 2004), estudos sobre o agulhão-vela com essa abordagem no Atlântico sul são particularmente raros. Por exemplo, na costa sudeste e sul do Brasil, concentrações de agulhão-vela têm sido observadas apenas nos meses quentes, entre setembro e março, quando a espécie concentra-se nessa região para realizar a desova (Arfelli e Amorim, 1981, Mourato *et al.*, 2009a). Na costa norte e nordeste, o agulhão-vela é capturado ao longo do ano, embora com rendimentos bem menores do que no sudeste e sul do Brasil durante o verão (Mourato *et al.*, 2009a) e com participação relativa na produção total da frota atuneira sediada no nordeste, de apenas 1,5%, representando cerca de 13% dos agulhões capturados (Hazin *et al.*, 1994).

Sendo assim, a presente tese visou suprir as lacunas desta área do conhecimento para o oceano Atlântico sul, estudando-se a relação entre a heterogeneidade espacial das capturas de agulhão-vela e a variação das condições ambientais, de forma a se compreender se elas interferem na capturabilidade no espinhel pelágico, bem como no ciclo migratório e sua relação com a época de desova da espécie.

1.3. Objetivos

1.3.1. *Objetivo geral*

O objetivo geral deste estudo foi aprofundar os conhecimentos sobre a dinâmica populacional do agulhão-vela no Atlântico sul, incluindo estudos sobre sua abundância relativa, distribuição, uso do habitat, comportamento e biologia reprodutiva. Para este propósito, primeiramente foi abordado os aspectos relativos à biologia reprodutiva da espécie, analisando-se um número considerável de amostras com ampla abrangência geográfica, o que permitiu identificar e delinear com maior precisão as áreas de desova da espécie no Atlântico sudoeste

equatorial. Em seguida, foram analisados dados de captura e esforço de pesca, bem como uma série temporal de dados de distribuição de frequência de comprimentos em conjunção com diversas variáveis ambientais (temperatura da superfície do mar, profundidade do topo da termoclina, concentração de clorofila, etc.) através de modelos robustos de regressão não-linear. A partir dessa análise, foi possível identificar os padrões de distribuição espaço-temporal das capturas e sua relação com a época de desova da espécie, bem como descrever o padrão de distribuição e preferências ambientais de indivíduos adultos e sub-adultos/juvenis no Atlântico sul. Além disso, objetivando-se identificar com maior precisão os movimentos migratórios e utilização do habitat da espécie, também foi utilizada a metodologia de telemetria via satélite, por meio das marcas *PSAT (Pop-up Satellite Archival Tags)*. Essa análise possibilitou um melhor entendimento dos movimentos verticais e sua relação com a vulnerabilidade e capturabilidade da espécie no espinhel pelágico, bem como o tempo de residência em determinadas áreas e sua relação com a época de desova da espécie no Atlântico sul. Por fim, foi efetuada uma discussão geral sobre os principais resultados obtidos, levando-se em consideração os aspectos relacionados com o manejo pesqueiro da espécie, bem como a estrutura do estoque da espécie no Atlântico sul.

1.3.2. *Objetivos específicos*

Os objetivos propostos específicos da presente foram:

❖ *Descrever os aspectos relacionados à biologia reprodutiva no Atlântico sul*

- Caracterizar e identificar a área, a época e o tipo de desova.
- Estimar a proporção sexual;
- Caracterizar os aspectos macroscópicos e microscópicos do desenvolvimento gonadal das fêmeas e dos machos;
- Classificar os estádios de desenvolvimento gonadal;
- Estimar o tamanho de primeira maturação sexual (L_{50});
- Estimar o índice gonadal (IG);
- Determinar a fecundidade;

❖ ***Estudar a distribuição e abundância relativa do agulhão-vela no oceano Atlântico relacionando as informações de pesca com as variáveis ambientais.***

- Realizar a modelagem dos dados de comprimento de agulhão-vela no oceano Atlântico Sul, identificando-se as áreas com maior concentração de jovens e adultos bem como a influência de algumas variáveis ambientais na distribuição dos mesmos;
- Avaliar e prever as áreas de maior probabilidade de captura de agulhão-vela, identificando-se as variações espaço-temporais da abundância relativa do agulhão-vela em relação à época de desova
- Relacionar os efeitos das variáveis temporais, espaciais e ambientais com a CPUE do agulhão-vela capturado pela frota atuneira brasileira, identificando-se os fatores de maior influência.

❖ ***Avaliar os movimentos, uso do habitat e comportamento do agulhão-vela no oceano Atlântico sul.***

- Analisar o padrão de distribuição vertical e horizontal do agulhão-vela com as principais variáveis ambientais, particularmente a temperatura da água, com o uso de PSATs (*Pop up Satellite Archival Tags*).

❖ ***Avaliar a série temporal de CPUE de agulhão-vela capturado pela pesca esportiva na costa sudeste e sul do Brasil***

- Apresentar a padronização da CPUE (Captura por Unidade de Esforço) do agulhão-vela capturado pela pesca esportiva sediada na costa sudeste e sul do Brasil, por meio da aplicação de modelos lineares generalizados.

1.4. Organização da tese

Para o cumprimento dos objetivos propostos a tese foi dividida em sete capítulos, sendo que cada um abordou um diferente aspecto, como indicado abaixo:

- ***Capítulo I*** – Apresenta, de forma sucinta e objetiva, a qualificação do problema a ser abordado na tese, incluindo uma explanação dos principais objetivos propostos, bem como uma introdução geral sobre a biologia, ecologia e pesca do agulhão-vela no Oceano Atlântico;

- **Capítulo II** – Trata dos aspectos relacionados com a biologia reprodutiva do agulhão-vela no Atlântico Sul, incluindo o seu desenvolvimento gonadal, proporção sexual, identificação de áreas de desova, e comprimento médio de primeira maturação sexual.
- **Capítulo III** – Consiste na aplicação do método GRASP (*Generalized Regression Analysis and Spatial Prediction*) aos dados de comprimento de agulhão-vela no oceano Atlântico Sul, identificando-se as áreas com maior concentração de jovens e adultos bem como a influência de algumas variáveis ambientais na distribuição dos mesmos;
- **Capítulo IV** – Descreve as variações espaço-temporais da abundância relativa do agulhão-vela em relação à época de desova e às condições ambientais;
- **Capítulo V**- Aborda o uso da telemetria via satélite para descrever e avaliar as possíveis rotas migratórias da espécie, incluindo a sua relação com o período reprodutivo e variação sazonal das condições ambientais, particularmente com a temperatura da água do mar, além do seu comportamento e padrão de uso do habitat;
- **Capítulo VI** – Inclui a padronização da CPUE (Captura por Unidade de Esforço) do agulhão-vela capturado pela pesca esportiva sediada na costa sudeste e sul do Brasil, por meio da aplicação de modelos lineares generalizados;
- **Capítulo VII** – Consistirá em uma análise final da tese com uma discussão abrangente dos principais resultados, incluindo algumas considerações e recomendações para o manejo das pescarias nas quais a espécie ocorre.

Considerando-se que os capítulos da tese foram estruturados em formato de artigo científico, os quais visam à publicação em periódicos e jornais científicos especializados, os textos dos próximos capítulos foram redigidos na língua inglesa.

Chapter 2 - Spawning seasonality, sexual maturity, sex ratio and fecundity of sailfish in the equatorial and southwestern Atlantic Ocean

Abstract

The biological samples examined in the present study were collected by observers of the National Observer Program of the Brazilian Ministry of Fisheries and Aquaculture, from 2006 to 2009, on board of tuna longliners based in the ports of Natal (RN) and Cabedelo (PB) (Area 1). Additionally, gonad samples were also obtained from small longliners, based in the port of Cabo Frio (RJ), located in the southeast coast of Brazil, and from tuna longliners based in São Paulo State (Santos- SP) (Area 2). All specimens were measured for lower jaw-fork length (*LJFL*) and to assign maturity phases, the microscopic characteristics of histological sections, the distribution of oocyte diameters and the gonadal index (GI) were considered. A total of 250 specimens were examined from Area 1, 168 of which were females, ranging in *LJFL* from 104 to 210 cm, and 82 were males, ranging from 134 to 185 cm. A total of 375 specimens were examined from area 2, 171 of which were females, ranging in *LJFL* from 122 to 197 cm, and 204 were males, from 104 to 197 cm *LJFL*. The ovaries of 280 females could be classed into six ovarian development phases based on microscopic characteristics and the most advanced group of oocytes. The relationship between the fraction mature and size can be described by a logistic curve with lengths at 50% and 95% maturity (*LJFL*₅₀ and *LJFL*₉₅) of 147.31 ± 1.01 cm *LJFL* (estimate \pm standard error, SE) and 168.18 ± 1.01 cm *LJFL*. Batch fecundity estimates ranged from 0.44×10^6 hydrated oocytes for a 156 cm *LJFL* female to 2.26×10^6 hydrated oocytes for a 183 cm *LJFL* female. According to the results, the western equatorial Atlantic Ocean, off Brazilian coast (Area 1), is not a spawning ground for sailfish, since most of the specimens were classified as immature or developing, with few spawning capable females and the total absence of actively spawning specimens. The southeast Brazilian coast, in contrast, seems to be an important spawning area for the species, with the spawning season happening mainly from December to February.

2.1. Introduction

In the Atlantic Ocean, sailfish is widely distributed in subtropical and tropical waters and occasionally in temperate waters, occurring also in the Mediterranean Sea. Geographical limits for its distribution, based on commercial catches, is approximately 40°N in the western North Atlantic, 50°N in the eastern North Atlantic, 40°S in the western South Atlantic, and 32°S in the eastern South Atlantic (Beardsley *et al.*, 1975; Nakamura, 1985). The impact of fishing on billfish stocks in the south Atlantic is currently on focus of considerable international concern. Major recreational fisheries for billfishes (*Istiophoridae*) exist throughout the world's tropical oceans, thus placing them among the most sought-after big gamefish (IGFA, 2001). Besides, although billfishes are not a target species, they are also caught in great numbers by commercial fisheries, including both industrial, such as the tuna longline fishery, and artisanal (ICCAT, 2009).

The first assessment of sailfish stocks in the Atlantic Ocean was conducted by the Standing Committee on Research and Statistics (SCRS) of the International Commission for the Conservation of Atlantic Tunas (ICCAT) in 2009. Conclusions of the assessment indicated evidences of overfishing, particularly on the east side of the Atlantic Ocean. However, the results were interpreted with considerable caution due to data deficiencies and the resulting uncertainty in the assessment (ICCAT, 2009). It was clear also that there remains considerable uncertainty regarding the stock structure of the sailfish in the Atlantic Ocean. These uncertainties linger on mainly due to the lack of adequate information about catch and effort data, since most countries often report their fishery statistics to the ICCAT without distinguishing between sailfish and spearfish and landings data for these two species are usually combined.

Furthermore, the current stock assessment model used to assess population status of sailfish in the Atlantic Ocean is hampered by the lack of information on life history of this species, such as age, growth and reproductive biology. It is important, for instance, to quantify the reproductive potential of sailfish for a better understanding of the population dynamics of this species. In addition, the delineation of spawning grounds is fundamental for the potential establishment of time-area closures to protect and ensure the spawning and consequently the recruitment of heavily exploited species. Besides, the identification of the spawning grounds, including their degree of spatiotemporal isolation, might help the delineation of different stocks.

Up to now, the available information on the reproductive biology of sailfish in the Atlantic Ocean is restricted to gonad assessments and larval surveys, most of which conducted in the North Atlantic (Voss, 1953; Jolley, 1977; de Sylva and Breder 1997; Post *et al.*, 1997; Luthy 2004; Richardson *et al.*, 2009a and b). The available information for the south Atlantic is restricted to gonad weights from few individuals caught off the coast of Brazil, according to which the majority of spawning activity takes place off the southeast coast, during summer months (Arfelli and Amorim, 1981; Hazin *et al.*, 1994). However, detailed information on ovarian development, sex ratio, size at maturity, fecundity or spawning is not yet available.

In this context, the general goal of the present chapter was to examine the reproductive dynamics of sailfish in the equatorial and southwestern Atlantic Ocean in order to provide life history information useful for stock assessment, including the spatial and temporal variation in reproductive activity, based on histological analysis of gonads and gonad weight indices. Reproductive parameters estimated included: length/season/region-specific sex-ratios, size at maturity, batch fecundity and spawning frequency.

2.2. Material and Methods

2.2.1. Sample collection and area of study

The biological samples examined in the present study were collected by observers of the National Observer Program of the Brazilian Ministry of Fisheries and Aquaculture, from 2006 to 2009, on board of tuna longliners based in the ports of Natal (RN) and Cabedelo (PB), located in northeast coast of Brazil. Additionally, gonad samples were also obtained from small longliners, based in the port of Cabo Frio (RJ), located in the southeast coast of Brazil, and from tuna longliners based in São Paulo State (Santos- SP) (Figure 2.1). In order to evaluate the spatial variability of the reproductive activity, the analysis was conducted in two separate areas: a) Area 1, for samples obtained from longliners based in Northeast Brazil, which operated in the equatorial and southwestern Atlantic Ocean; and b) Area 2, for those collected from vessels based in São Paulo and Rio de Janeiro, operating off the southeast coast of Brazil (Figure 2.1). All specimens were measured for lower jaw-fork length (*LJFL*), being then dissected for the collection of gonads, which were then frozen and stored in freezers, up to the time of landing. Sex was initially determined from the macroscopic characteristics of the gonads.

2.2.2. Assessing the reproductive activity

In the laboratory, the gonads were thawed, individually weighted (± 0.1 g) and measured for the total length and width. A sub-sample was kept in 10% neutral formalin solution for posterior microscopic analysis. To assign maturity phases to the examined specimens, the microscopic characteristics of histological sections, the distribution of oocyte diameters and the gonadal index (GI) were considered (West, 1990; Arocha, 2002; Brown-Peterson *et al.*, 2011).

Histological sections were prepared from gonad tissue samples embedded in paraffin, sectioned at approximately 5 μ m, and stained with Harris's haematoxylin and eosin. Histological examination assisted the field-classified sex, especially for small specimens. Each ovary was staged according to the microscopic characteristics and the most advanced group of oocytes (MAGO) present in the sample, including: primary growth oocytes, cortical alveolar, vitellogenic oocytes, germinal vesicle migration or hydrated. Post-ovulatory follicles (Hunter *et al.* 1985; Murua *et al.*, 2003) were identified and atresia of vitellogenic oocytes was recorded to aid in the determination of the reproductive condition. Additionally, to confirm that the sailfish is a multiple spawner, the frequency distribution of diameter of approximately 300 oocytes from eleven females with gonads with hydrated oocytes (actively spawning females) was analyzed. The diameters (mm) of whole oocytes were obtained randomly from each female, with the assistance of a stereomicroscope with a micrometer.

The sex ratio was analyzed by month and LJFL, with the statistical significance of the differences being tested by the chi-square test (χ^2 , $\alpha=0.05$). After assigning the maturity stages, the monthly mean GI was estimated for adult specimens (excluding the immature specimens), for determination of spawning period. The GI was calculated based on Cayré and Laloé (1986), as follows: $GI = \left(\frac{GW}{LJFL^3} \right) \cdot 10^4$, where GW is gonad weight (g).

2.2.3. Reproductive parameters population

The length at which 50% of all individuals were sexually mature (L_{50}) was estimated only from specimens caught during the spawning season and from the spawning area. Females were defined as mature if they presented cortical alveolar, vitellogenic oocytes, germinal

vesicle migration, or hydrated oocytes. The probability that the i^{th} fish was mature (P_i) was modeled using a logistic curve, described by Sun *et al.* (2009), as:

$$P_i = 1 / \left(1 + e^{-\ln(19) [(LJFL_i - LJFL_{50}) / (LJFL_{50} - LJFL_{95})]} \right),$$

where $LJFL_i$ = the LJFL of fish i ; and $LJFL_{50}$ and $LJFL_{95}$ = the LJFLs at which 50% and 95% of the specimens reached maturity, respectively. $LJFL_{50}$ and $LJFL_{95}$ were estimated by maximizing a log-likelihood function, and by assuming a binomial error distribution, with R software.

Batch fecundity (BF) was estimated gravimetrically by the hydrated oocyte method using fixed ovarian samples, which contained hydrated oocytes. Three subsamples (1.0 g) were taken from each ovary, teased apart to release the oocytes, and washed thoroughly to release the hydrated oocytes. BF was then back-calculated by the product of gonad weight and oocyte density, where oocyte density was the mean number of oocytes per gram of three ovarian tissues with no early postovulatory follicles (Hunter *et al.*, 1985). Regression analyses were conducted to quantify the relationships between batch fecundity and LJFL.

2.2.4. Spawning pattern and annual fecundity

The spawning interval was estimated by the *hydrated oocyte method* (Hunter and Macewicz, 1985) and was restricted to samples collected in the Area 2 during the peak spawning season (Arocha and Barrios, 2009), from December to February. The spawning interval (in days) was calculated by dividing the total number of mature females for all years combined by the number of actively spawning females. For the hydrated oocyte method to be a useful proxy for spawning frequency two assumptions were considered. The first was whether or not spawning occurs in the evening and the second was whether the spawning area represents a closed population (Arocha and Barrios, 2009). Annual fecundity was estimated as the product of average batch fecundity, the spawning fraction, and the duration of the spawning season.

2.3. Results

2.3.1. Size composition and sex ratio

Area 1

A total of 250 specimens were examined from Area 1, 168 of which were females, ranging in LJFL from 104 to 210 cm (Figure 2.2), and 82 were males, ranging from 134 to 185 cm (Figure 2.2). Most of the females measured from 160 to 190 cm LJFL, with a mode in 170 cm, while most of the males showed a LJFL between 150 and 170 cm, with a mode at 160cm. The overall sex ratio was 2.04 females to 1 male, which differed significantly ($\chi^2 = 29.584$; $p < 0.05$) from the expected proportion of 1:1. Females predominated in almost all months, except for May, but only in September and October the difference was statistically significant (Table 2.1, Figure 2.3). An apparent predominance of females was observed in all size classes (Figure 2.4), but only in LJFL larger than 160 cm the differences were statistically significant (Table 2.2).

Area 2

A total of 375 specimens were examined from area 2, 171 of which were females, ranging in LJFL from 122 to 197 cm (Figure 2.2), and 204 were males, from 104 to 197 cm LJFL (Figure 2.2). The LJFL frequency distribution of females showed a higher frequency of specimens between 150 and 180 cm, with a mode in 160 cm. For males, the LJFL frequency distribution showed a mode in 160 cm, with most specimens ranging from 150 to 170 cm. The estimated sex ratio for all samples was 0.84 female to 1 male, which not differed significantly from the expected proportion of 1:1. The monthly sex ratios were not significantly different from the expected ratio of 1:1 ($p > 0.05$) for any month (Table 2.1). A slight predominance of males was however observed (Figure 2.3). The sex ratio by size also showed a predominance of males in almost all size classes, except for 160 and 190 cm LJFL classes which not differed significantly ($p < 0.05$) from the expected proportion of 1:1 (Table 2.2, Figure 2.4).

2.3.2. Ovary development and spawning season

The ovaries of 280 females could be classed into six ovarian development phases based on microscopic characteristics and the most advanced group of oocytes (Table 2.3, Figure 2.5). The gonad weight of the females classified as immature ranged from 32 to 180g (Figure 2.6). The LJFL of immature females ranged between 104 and 173 cm. Developing females, in turn, had a LJFL between 136 and 210 cm and GW from 51 to 1334g. Spawning capable females had a LJFL between 146 and 197 cm with a GW ranging from 250 to 2,752g. Actively spawning

females, with a LJFL between 156 and 194 cm, had a GW from 700 to 2,105g. Regressing females presented a LJFL between 159 and 181 cm, with a GW ranging from 163 to 1,195g (Figure 2.6). Recovering females had a LJFL between 157 and 210 cm and GW from 93 to 355g.

Actively spawning females were absent in Area 1, and only 2% of the females in this area were in the spawning capable phase. The great majority of the specimens analyzed were in developing phase (57%). Immature and recovering phases accounted, respectively, for 22% and 17%. In contrast, in area 2, most of the specimens were spawning capable or actively spawning, representing, respectively, 42% and 14% of the sample. In Area 1, females with developing ovaries occurred in all sampled months, while immature females were more frequent in January and February (Figure 2.7). In area 2, females with spawning capable or regressing ovaries were more frequent from December to February while the proportion of immature and developing females was very low (Figure 2.7). The monthly GI showed higher mean values in Area 2, from December to February (close or more than two) (Figure 2.8). In contrast, the monthly mean GI in Area 1 presented much smaller values, being always less than one (Figure 2.8).

2.3.3. *Spawning pattern*

The smallest group had oocytes smaller than 0.4 mm, composed by primary growth oocytes, cortical alveolar, primary and secondary vitellogenic oocytes (Figure 2.10). The next larger group was composed of tertiary vitellogenic oocytes, ranging from 0.4 to 0.9 mm (Figure 2.10). The third group was the largest and corresponded to the germinal vesicle migration oocytes, germinal vesicle breakdown oocytes and hydrated oocytes, measuring 0.8-1.6 mm (Figure 2.10). During the peak of the spawning season (December to February), an average of 22% of the actively spawning females was spawning daily which indicates that the average interval between spawning and a new batch of eggs is around 4.4 days.

2.3.4. *Length at first sexual maturity and batch fecundity*

The relationship between the fraction mature and size can be described by a logistic curve with lengths at 50% and 95% maturity ($LJFL_{50}$ and $LJFL_{95}$) of 147.21 ± 1.01 cm LJFL (estimate \pm standard error, SE) and 168.18 ± 1.01 cm LJFL (Figure 2.11), respectively. The logistic regression was (Figure 2.11):

$$P_i = 1 / \left(1 + e^{-\ln(19) [(LJFL_i - 147.31) / (147.31 - 168.18)]} \right) \quad (\text{Pseudo-}R^2 = 0.77, n = 222, 5 \text{ cm classes}).$$

Only 15 of the actively spawning females fit the criteria for estimating batch fecundity (*BF*) (hydrated oocytes present, without early postovulatory follicles). The *LJFL*s of these individuals ranged from 155 to 183 cm, and their gonad weights ranged from 548 to 2,752 g. Batch fecundity estimates ranged from 0.44×10^6 hydrated oocytes for a 156 cm *LJFL* female to 2.26×10^6 hydrated oocytes for a 183 cm *LJFL* female (Figure 2.12). The regression equation was: $BF = 9.026E-13 * LJFL^{8.122}$ ($n = 15$, pseudo- $R^2 = 0.62$). The annual fecundity was estimated to range between 9 and 46 million eggs (average of 21 million).

2.4. Discussion

2.4.1. Size distribution and sex ratio

Sex ratio of sailfish caught in the western equatorial south Atlantic varies temporally and spatially. We observed a general predominance of females in western equatorial Atlantic along the year while the opposite was noticed in the southeast Brazilian coast during the spawning season, in warmer months. The predominance of males may be consistent with sexual differences in migratory or reproductive behaviors, such as the greater propensity for males to aggregate in group-spawning pelagic species (Hunter and Macewicz, 1986). Around Florida, for example, sailfish is known to move inshore, into shallow waters, where the females, swimming sluggishly with their dorsal fins extended and accompanied each by one or more males, may spawn near the surface, during the warm season (Voss, 1953; Jolley, 1977). Moreover, temporal changes in sex ratios may partly reflect different availabilities or catchabilities resulting from sexual differences in behavior that change seasonally (e.g. during spawning periods). Similar results were also observed by Chiang *et al.* (2006a) in the eastern Taiwan, but they differ from the findings by Hernandez and Ramirez (1998) for the sailfish in the Pacific Coast of Mexico, where the proportion of female sailfish was higher than 50%.

2.4.2. Ovarian development and spawning season

The histological analysis of the ovaries and the method of most advanced group of oocytes, used to develop a maturity classification scheme for female sailfish in this study,

allowed a more precise identification of maturity phases than the traditional macroscopic techniques (*i.e.* Mourato *et al.* 2009). Histological studies provide very precise information on oocyte development, although their interpretation may be confused because different authors use different terminology for the same structures (West, 1990). Previous studies on histology-based maturity classifications for sailfish have identified five (Jolley 1977; Hernandez and Ramirez, 1998) to seven different reproductive stages (De Sylvia and Breder, 1998; Chiang *et al.*, 2006a). Differences in histological staging classification, especially for highly migratory species, make it difficult to compare reproductive parameters between studies in different regions of the world. In this study, we adopted a standardized terminology for describing reproductive development in fishes suggested by Brown-Peterson *et al.* (2011) which is applied for majority of determinate and indeterminate spawner fishes. The use of histology to assign the stages of ovary maturation permitted a clear differentiation of six different phases of maturity, which showed similar oocyte microscopic characteristics as those observed by Chiang *et al.* (2006a), for Pacific sailfish in Taiwanese waters.

Spawning season and areas for the Atlantic sailfish were defined and identified by the combination of several methods, including: (1) the identification of actively spawning females with the use of histology analysis; (2) high GSI values; and (3) the position where actively spawning females were caught. According to the results shown in the present study, the equatorial and western equatorial Atlantic Ocean, off Brazilian coast (Area 1), is not a spawning ground for sailfish, since most of the specimens were classified as immature and developing, , with few spawning capable females and the total absence of actively spawning specimens. This is also supported by the low values of gonad index, when compared to the fish caught off southern Brazil (Area 2). The southeast Brazilian coast, in contrast, seems to be an important spawning area for the species, with the spawning season happening mainly from December to February. The vast majority of females caught in this area, during this period of the year, were either spawning capable or actively spawning, with high values of gonad indices. Important concentrations of mature specimens in this area were previously reported by various authors (Arfelli and Amorim, 1981; Mourato *et al.*, 2009; Pimenta *et al.*, 2005).

The presence of different batches of growing oocytes, including hydrated eggs in the oocyte size-frequency distribution and the presence of different generations of oocytes in

histological sections of spawning capable females, suggests that sailfish in the study area (Area 2) can spawn more than once during a spawning season. Moreover, asynchronous oocyte development was observed due to presence of all types of oocyte stage (previtellogenic and vitellogenic oocytes) in sections of ovaries, and mainly in spawning capable and actively spawning females. The presence of post-ovulatory follicles (recent spawned less than 24 hs) and hydrated oocytes (imminent spawning less than 12 hs) simultaneously in histological section of ovaries from females in actively spawning phase is an evidence of multiple spawning behavior. Similar findings were also reported by several authors in different regions of the world (Jolley, 1977; Hernandez *et al.*, 2000; Chiang *et al.*, 2006b).

2.4.3. Reproductive population parameters

The L_{JFL50} for female sailfish was estimated at 147.31 cm, and the smallest size at which any female was mature was 136.0 cm L_{JFL} . In general, there is a lack of exhaustive studies on sailfish sexual maturity. Prior reported estimates of body size at sexual maturity for female sailfish in the Atlantic Ocean in general agree with the estimates of the present study, but dissimilarities likely reflect the different measures used to gauge sexual maturity used in other works. A first attempt to estimate the L_{50} of sailfish in South Atlantic was reported by Mourato *et al* (2009), obtaining a L_{JFL} of the 154.9 cm, based on macroscopic assessment of gonads. Jolley (1977) reported that female sailfish caught in the western North Atlantic attains sexual maturity between 147 and 160 cm L_{JFL} (13 to 18 kg). Arocha and Marcano (2006) reported an L_{50} for females sailfish caught between 5°N and 25°N in western North Atlantic of 180.2cm L_{JFL} , but the analysis were derived from macroscopic and microscopic assessment of gonads without histological calibration. Probably the estimate of L_{50} reported by Arocha and Marcano (2006) have included fish of relatively bigger size caught off Caribbean waters, as well as a lower number of immature fish, which may have deviated the size at maturity upwards.

The present estimates of L_{50} for female sailfish caught by Brazilian longliners are also smaller than those of sailfish caught in several regions of the Pacific. In the Mexican Pacific coast, Hernandez and Ramirez (1998) estimated that 50% of the females mature at 175 cm $EOFL$ (eye-orbit fork length) (198.5 cm L_{JFL}), based on histological analysis of gonads. In the western Pacific, Chiang *et al.* (2006a) reported a L_{50} of 167 cm L_{JFL} , also based on histological examination.

The difference between the present results and the other studies cited above might be a combined result of different stocks, different environmental conditions, or sampling bias resulting from sample size and timing, i.e. whether estimates include fish caught throughout the entire year and fisheries range or during spawning season and area only, such as in the present case. The different fisheries strategies are also a likely source of variation, due the non-selective nature of fishing gears.

In the present study, the power regression function provided a good relationship between batch fecundity with LJFL, with fecundity increasing with female size. Several authors have reported similar results, with fecundity increasing with the size of the sailfish, from eastern Africa (Merret, 1970), eastern Pacific (Hernandez *et al.*, 2000), western Pacific (Chiang *et al.*, 2006b), and northwest Atlantic (Voss, 1953; Jolley, 1977). Despite the length range of spawned females collected in this study (155-183 cm *LJFL*) was slightly smaller to that reported by studies done in the Pacific Ocean, the batch fecundity estimated in the present work ($0.44\text{--}2.26 \times 10^6$) had a similar range from those reported by Hernandez-Herrera *et al.* (2000) ($0.42\text{--}2.52 \times 10^6$) and by Chiang *et al.* (2006b) ($0.2\text{--}2.48 \times 10^6$), for Pacific sailfish. However, it differed slightly from the estimates ($0.75\text{--}1.6 \times 10^6$) observed by Jolley (1977) for the Atlantic.

This study presents the first attempt to estimate important parameters (i.e. size at maturity, fecundity) of the sailfish in the equatorial and southwestern Atlantic, which can be useful for future stock assessments of the species in the Atlantic Ocean. Moreover, the results presented here seem to confirm the hypothesis that sailfish spawning in the equatorial and southwestern Atlantic is rather limited both geographically and temporally, being greatly restricted to the southeast coast of Brazil, between November and February, with the peak of the spawning season happening in January. Further studies are however still needed, including tagging experiments, in order to better understand the reproductive cycle of the sailfish in the South Atlantic, and particularly how it is coupled with seasonal migratory movements performed by the species.

Table 2.1 - Sex ratio, χ^2 and p value from chi-squared test by area and month of sailfish caught in the southwestern and equatorial Atlantic Ocean

Month	Area 1			Area 2		
	Sex Ratio	χ^2	$p(\text{chi})$	Sex Ratio	χ^2	$p(\text{chi})$
Jan	3	2	0.1573	0.68	3.1	0.0747
Feb	3	3	0.0832	0.75	0.5	0.4497
Mar	2.2	2.2	0.1336	-	-	-
Apr	0.7	0.2	0.5930	-	-	-
May	1.6	0.5	0.4795	-	-	-
Jun	1.6	1	0.3173	-	-	-
Jul	2.6	3.5	0.0593	-	-	-
Aug	1.4	0.7	0.3938	0.5	0.6	0.4142
Sep	3.7	14.5	0.0001	-	-	-
Oct	2.1	4.5	0.0325	-	-	-
Nov	1.5	1.2	0.2733	0.76	1.8	0.1698
Dec	2.2	3.8	0.0498	1.12	0.4	0.5211

Table 2.2 - Sex ratio, χ^2 and p value from chi-squared test by area and size class of sailfish caught in the southwestern and equatorial Atlantic Ocean.

LJFL class	Area 1			Area 2		
	Sex Ratio	χ^2	$p(\text{chi})$	Sex Ratio	χ^2	$p(\text{chi})$
100	-	-	-	-	-	-
110	-	-	-	-	-	-
120	-	-	-	0.5	0.8	0.3657
130	1.5	0.2	0.6547	0.4	1.6	0.2059
140	1.3	0.1	0.7	0.3	3	0.0832
150	1.1	0.1	0.715	0.5	8.1	0.0043
160	1.1	0.1	0.7456	0.6	7.2	0.0071
170	1.9	8.2	0.0040	1.8	9	0.0027
180	2.4	5.4	0.0195	4.6	7.1	0.0076
190	-	-	-	4	1.8	0.1797
200	-	-	-	-	-	-
210	-	-	-	-	-	-

Table 2.3 - Maturity classification of female sailfish ovaries from samples collected from the southwestern and equatorial Atlantic Ocean. GI represent the gonadal index.

Ovary Maturity Phases	Microscopic characteristics	GI (mean and standard error)
Immature (Figure 2.5A)	Only oogonia and primary growth oocytes (PG). No vitellogenic oocytes, no cortical alveolar (CA), rarely occurring atresia.	0.15 (± 0.14); Figure 2.9
Developing (Figure 2.5B)	Initial presence of cortical alveolar. Even showing oogonia and primary growth oocytes. Some primary (Vtg1) and secondary (Vtg2) vitellogenic oocytes. But no presence of tertiary vitellogenic oocytes (Vtg3).	0.54 (± 0.43); Figure 2.9
Spawning capable (Figure 2.5C)	All oocyte stages present. Many Vtg3 oocytes. No hydrated oocytes (HO) present and no post-ovulatory follicles (POF).	2.51 (± 1.07); Figure 2.9
Actively spawning (Figure 2.5D)	Oocyte maturation begins. Even showing all oocytes stages. But, germinal vesicle migration (GVM) and germinal vesicle break-down (GVBD), and HO oocyte are abundant. When recent spawning occurred show some post-ovulatory follicles.	2.59 (± 0.68); Figure 2.9
Regressing (Figure 2.5E)	Cessation of spawning season. Many vitellogenic oocytes are undergoing resorption. Oocytes in α -atresia and β -atresia are dominant. Some POFs are observed in beginning of regression, but rare in the late regression.	1.13 (± 0.52); Figure 2.9
Recovering (Figure 2.5F)	No vitellogenic oocyte present. Residual atresia in late stages. Only oogonia and primary growth oocytes. When fully recovered shows some cortical alveolar growing to next spawning season	0.32 (± 0.16); Figure 2.9

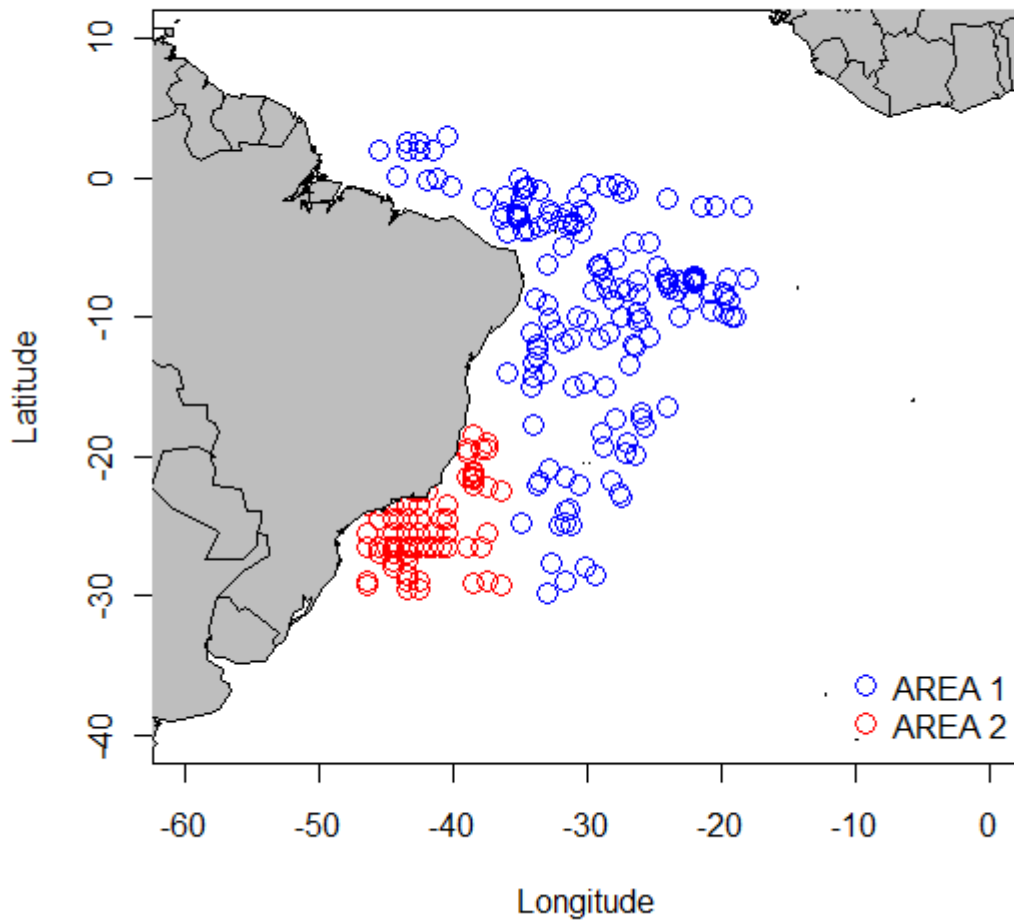


Figure 2.1 - Spatial distribution of longline sets from where sailfish were sampled by the Brazilian Pelagic Longline Observer Program from vessels operating in the southwestern and equatorial Atlantic Ocean between 2002 and 2006. Blue circles represent the longline sets sampled in the area 2.

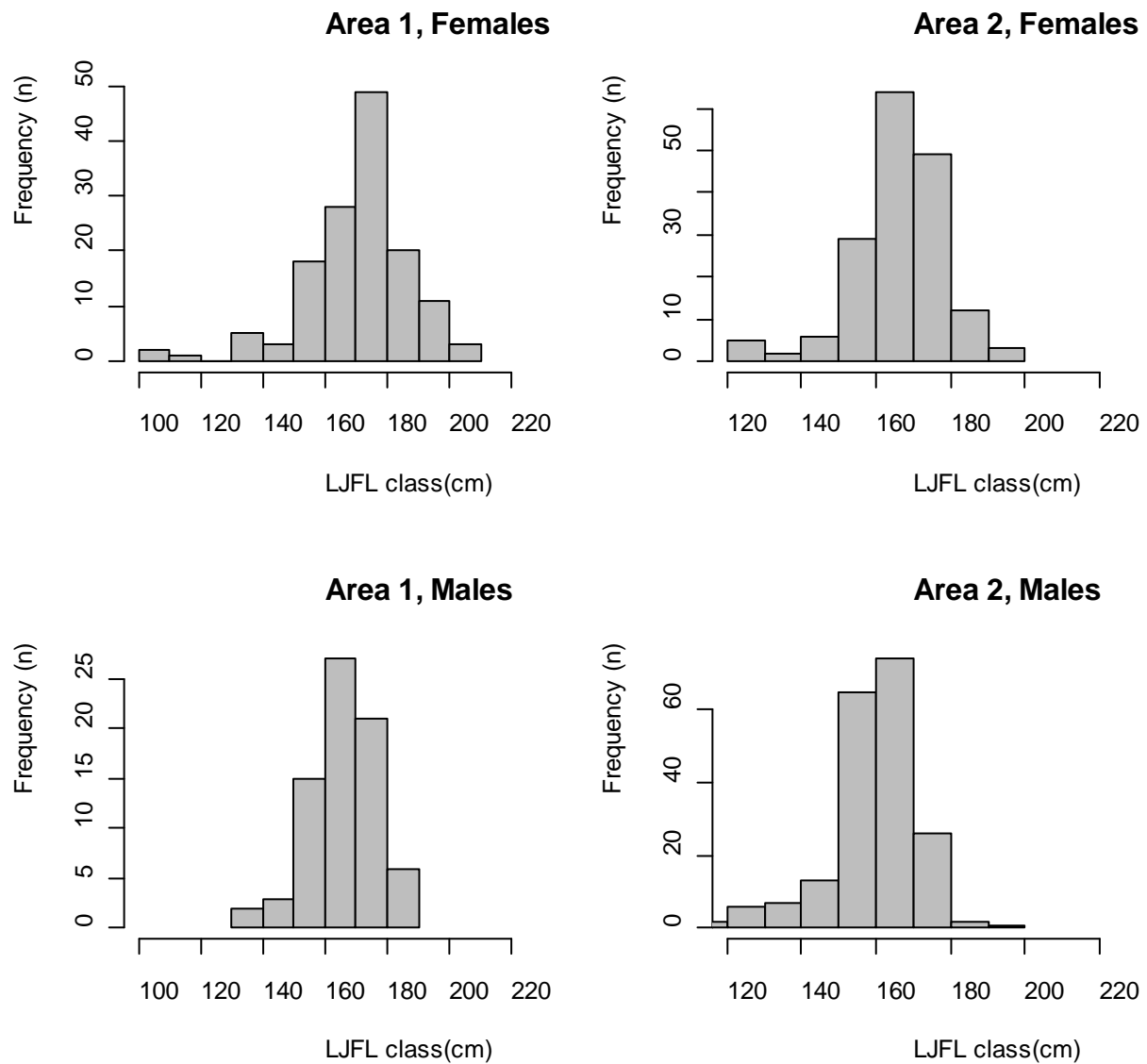


Figure 2.2 - Size frequency distributions of female and male of sailfish collected from the southwestern and equatorial Atlantic.

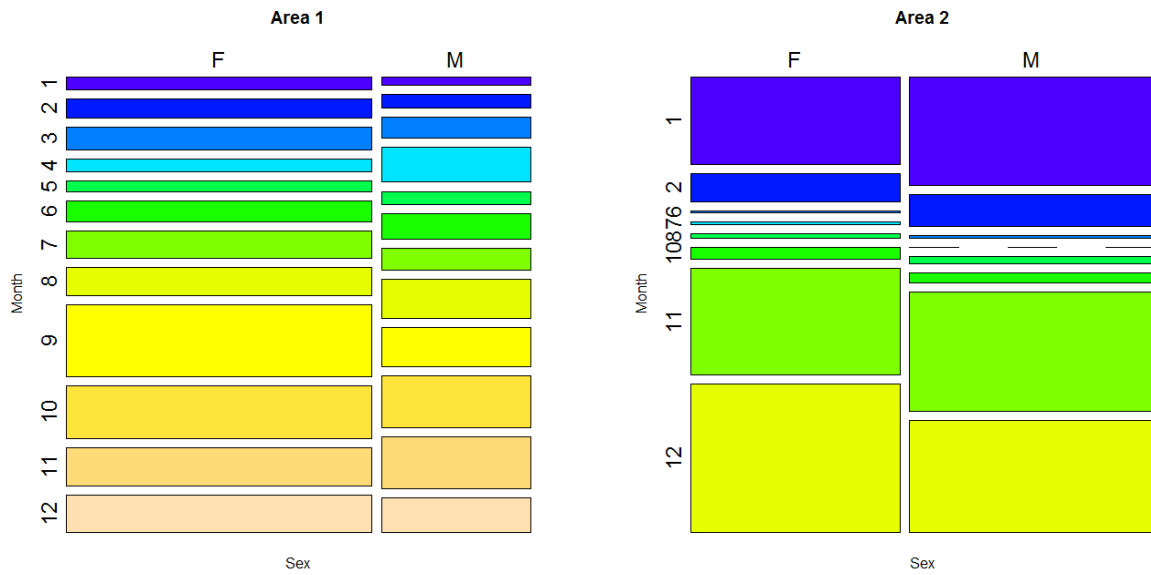


Figure 2.3 - Mosaic plot showing the number of females and males of sailfish caught in the southwestern and equatorial Atlantic Ocean by month and area

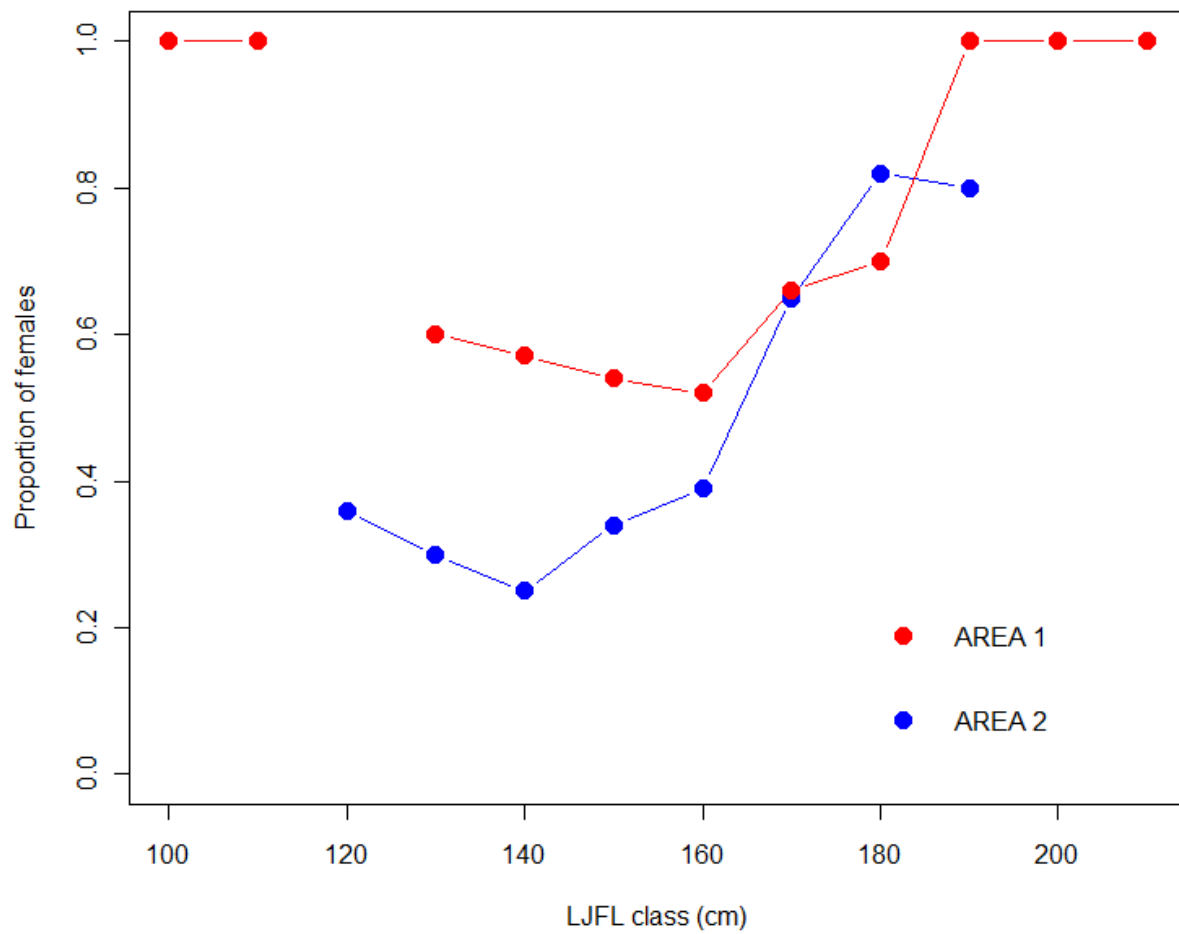


Figure 2.4 Sex-ratio-at size (proportion of female) of sailfish caught in the southwestern and equatorial Atlantic Ocean by area.

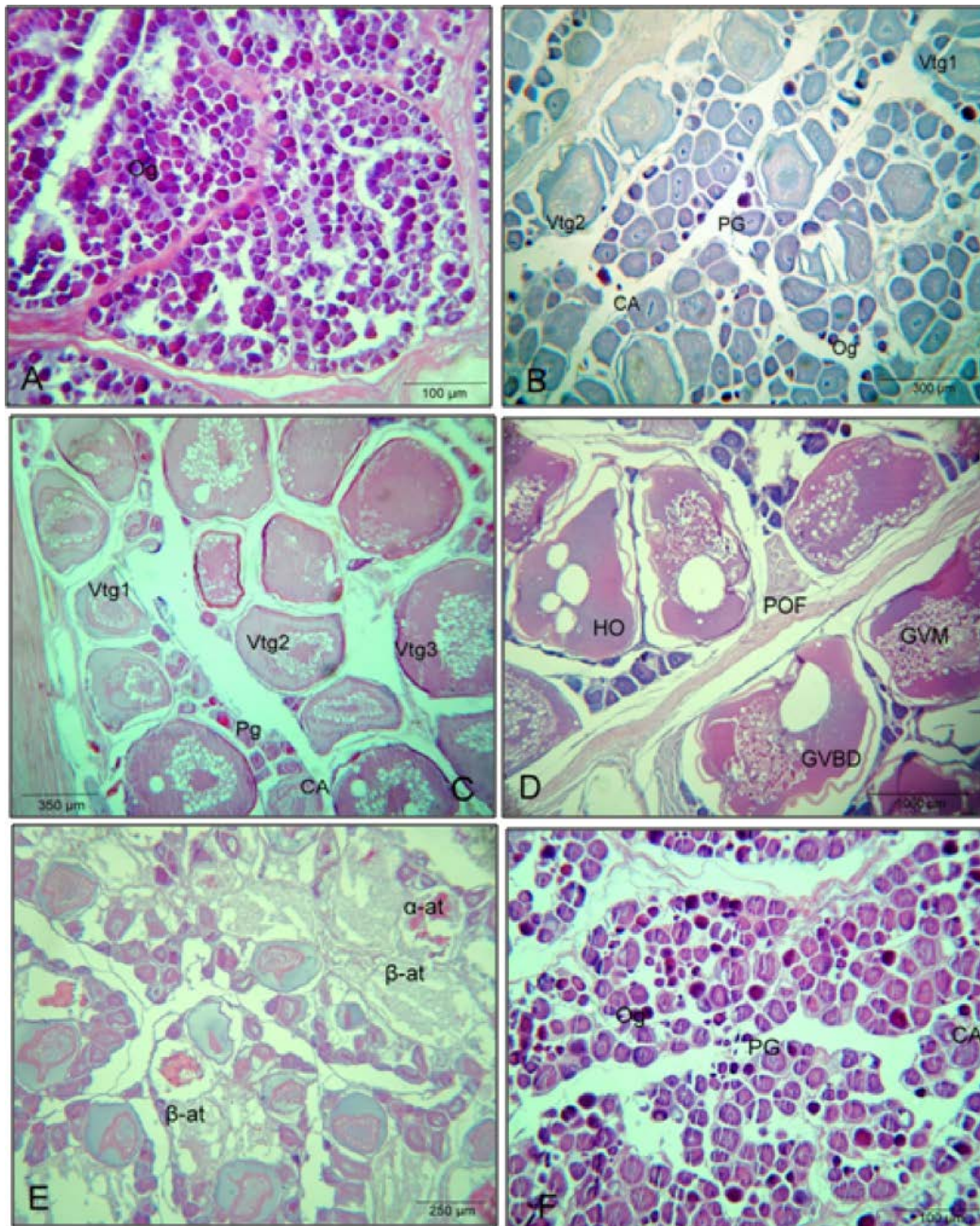


Figure 2.5 - Histological sections of ovaries of the Sailfish *Istiophorus platypterus* in different maturity phases. A: Immature (Scale bar = 100 μ m), B: Developing (Scale bar = 300 μ m), C: Spawning capable (Scale bar = 350 μ m), D: Actively spawning (Scale bar = 1000 μ m), E: Regressing (Scale bar = 250 μ m), F: Recovering (Scale bar = 100 μ m). The oocyte stages: Og (oogonia), PG (primary growth oocyte), primary vitellogenic oocyte (Vtg1), secondary vitellogenic oocyte (Vtg2), tertiary vitellogenic oocyte (Vtg3), germinal vesicle migration (GVM), germinal vesicle breakdown (GVBD), hydrated oocyte (HO), post-ovulatory follicle (POF), alpha atresia (α -at) and beta atresia (β -at). Staining by Hematoxylin/Eosin.

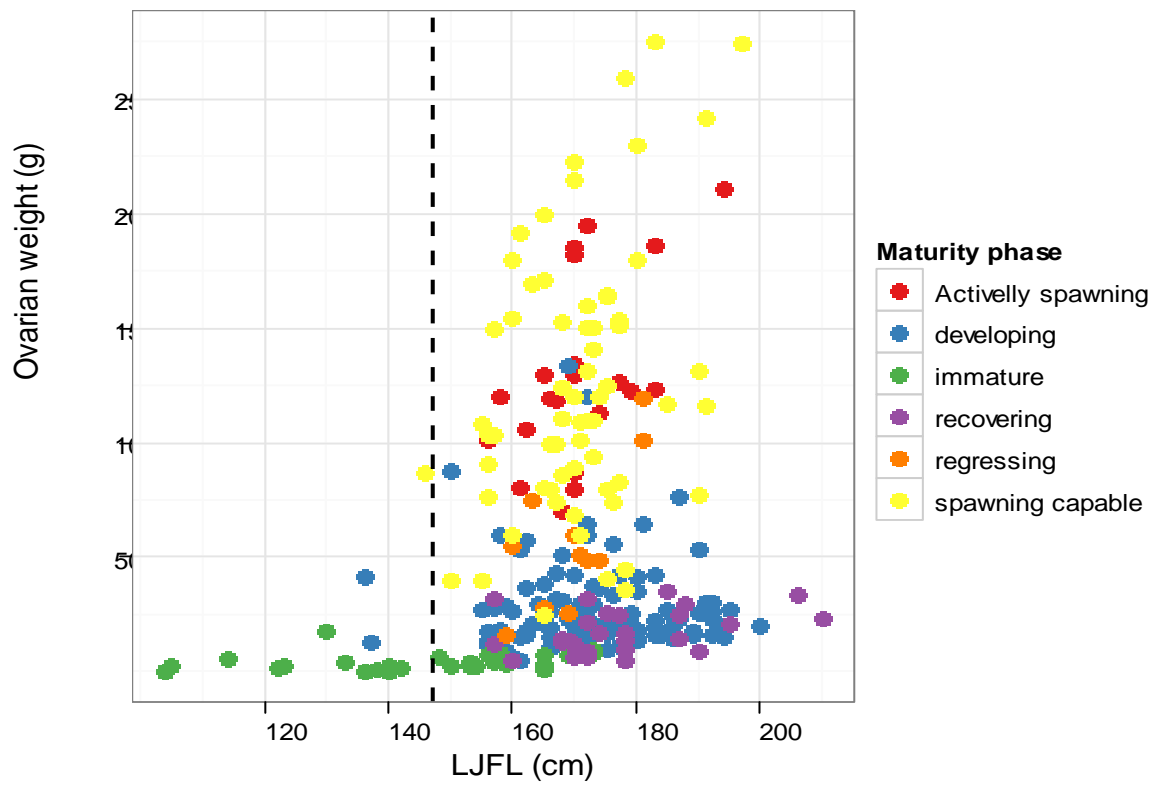


Figure 2.6 - Ovarian weight by size class and maturity stage of females of sailfish caught in the southwestern and equatorial Atlantic Ocean. The dotted line represents the length at first sexual maturity.

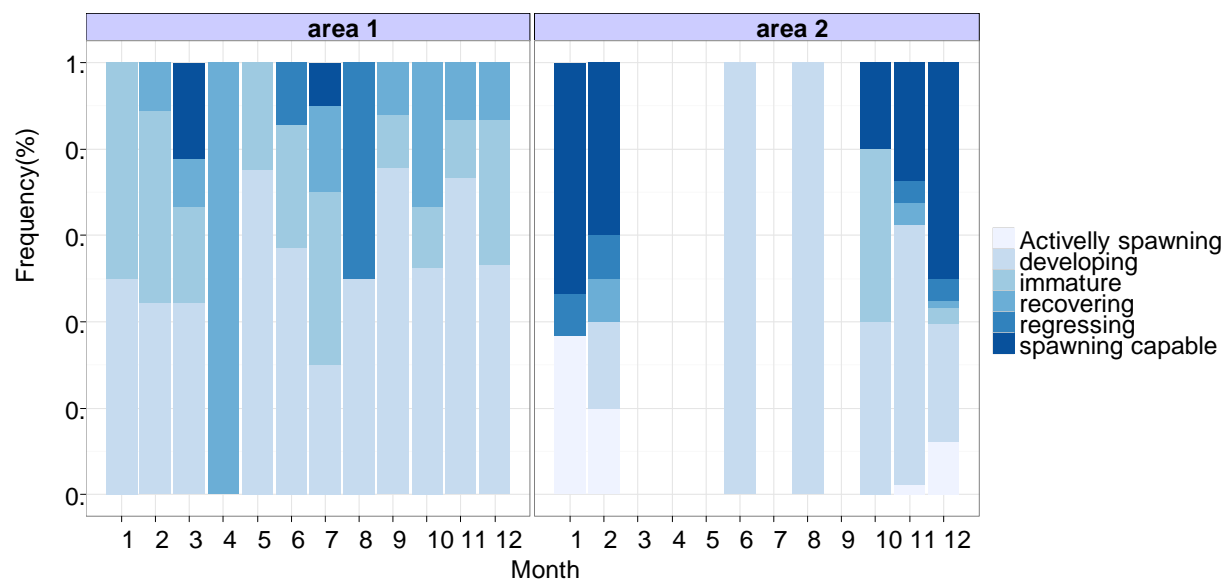


Figure 2.7 - Relative frequency of the different maturity stages of female of sailfish caught in the southwestern and equatorial Atlantic by area and month.

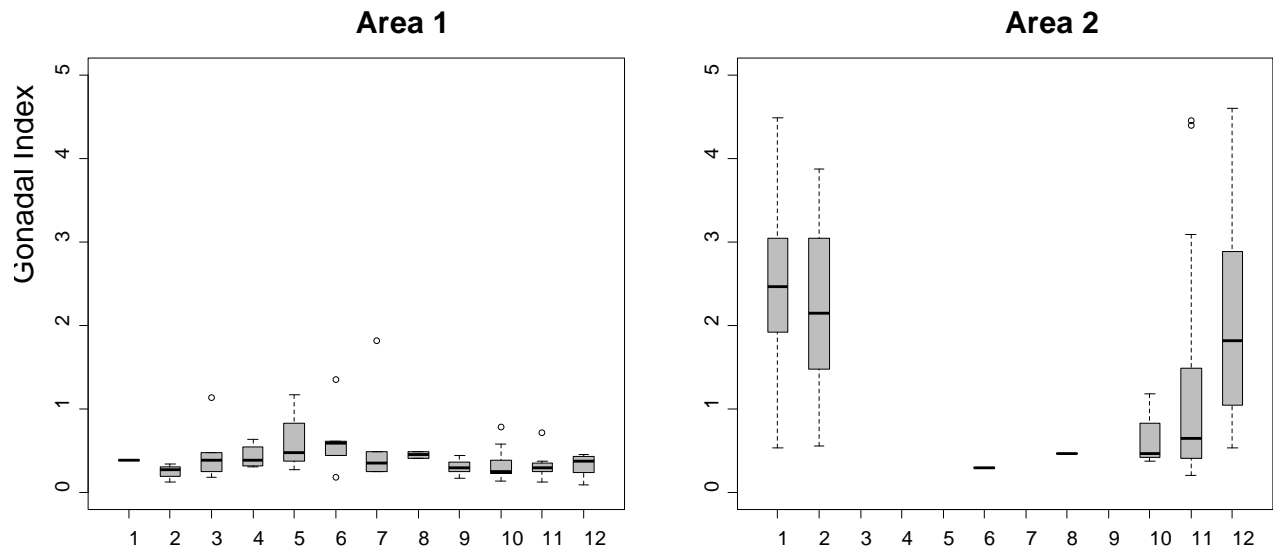


Figure 2.8 – Box-plot of the gonadal index of female of sailfish caught in the southwestern and equatorial Atlantic by area and month.

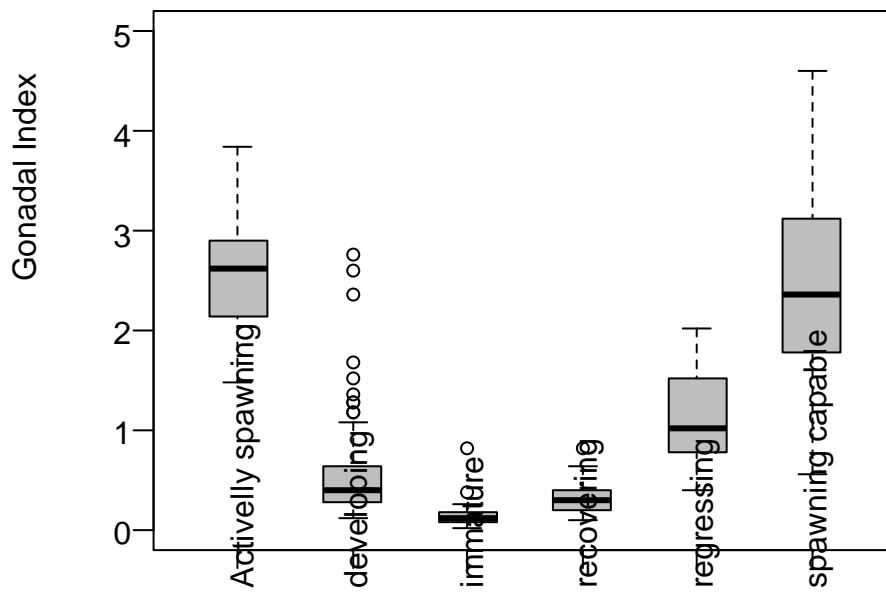


Figure 2.9 - Box-plot of the gonadal index of female of sailfish caught in the southwestern and equatorial Atlantic by maturity stage.

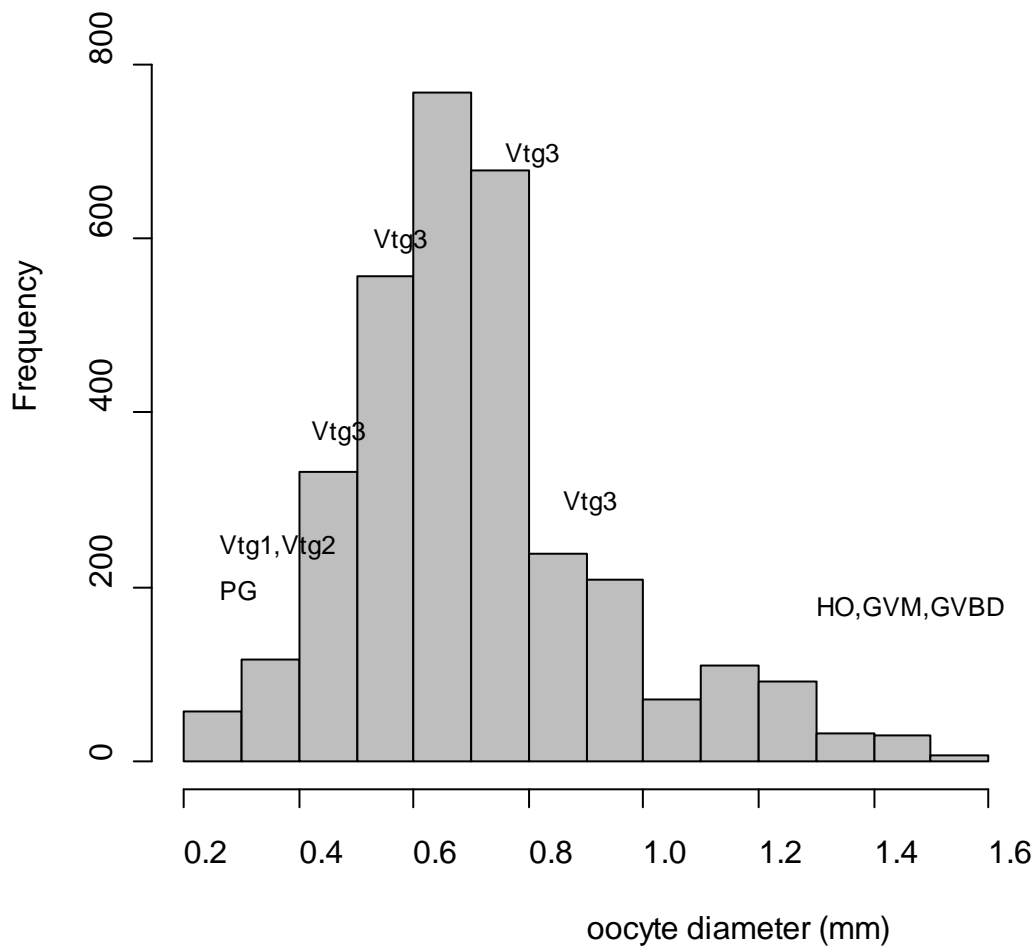


Figure 2.10 - Size frequency distribution of whole oocytes of female of sailfish caught in the southwestern and equatorial Atlantic. The oocyte stages: PG (primary growth oocyte), primary vitellogenic oocyte (Vtg1), secondary vitellogenic oocyte (Vtg2), tertiary vitellogenic oocyte (Vtg3), germinal vesicle migration (GVM), germinal vesicle breakdown (GVBD), hydrated oocyte (HO) and post-ovulatory follicle (POF).

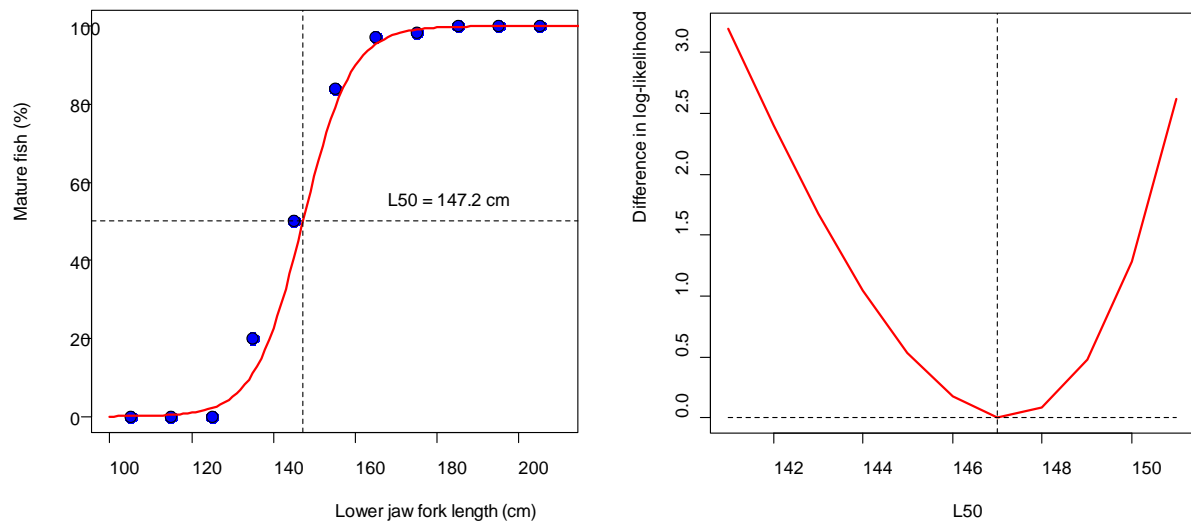


Figure 2.11 - Proportion of mature female of sailfish caught in the southwestern and equatorial Atlantic at 5 cm length intervals. *Left panel:* Fitted curve (red line) illustrate the optimal logistic curve fitted by maximum likelihood and observed values (blue points). *Right panel:* Approximate 95% confidence intervals from the likelihood profiles for parameter $LJFL_{50}$ of the proportion of maturity for sailfish.

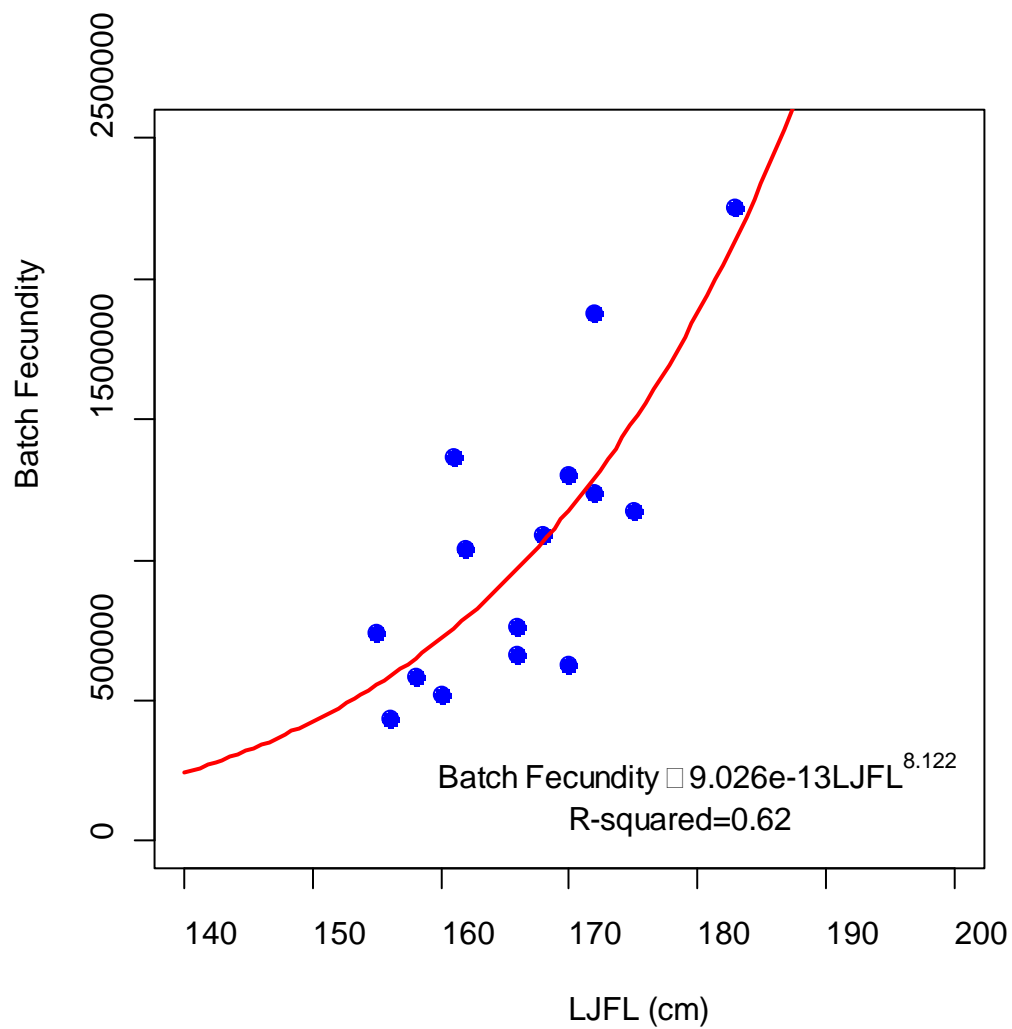


Figure 2.12 - Relationship between the batch fecundity and lower jaw fork length for females of sailfish caught in the southwestern and equatorial Atlantic

Chapter 3 - Environmental and spatial effects on the size distribution of sailfish in the Atlantic Ocean

Abstract

Generalized Regression Analysis and Spatial Prediction (GRASP) was applied to size data for sailfish (*Istiophorus platypterus*) to better describe its preferential habitats, in relation to juveniles and adults, based on environmental and spatial factors in the equatorial and southwestern Atlantic. A total of 9,954 Lower Jaw Fork Length (LJFL) size data (7,541 fish caught by longline and 2,413 by gillnet) from the International Commission for the Conservation of Atlantic Tunas (ICCAT) database, were analyzed from 1998 to 2007. Four main environmental variables were considered: sea surface temperature, depth of mixed layer, chlorophyll concentration and bathymetry. Results indicated that adults were more frequent to the east of 25°W in areas with shallow mixed layer (<30m) between 3000 and 6000 m depth with SSTs lower than 24°C. Chlorophyll concentration showed the highest proportion of adults between 0.3 and 0.8 mg/m³. High densities of adults were also observed to the west of 40°W, both at northern and southern parts of the studied area. An opposite trend was observed in relation to juveniles, which appear to be associated with waters with SSTs higher than 28°C and deep mixed layer (>50m) in the western side, particularly between 10° - 20°S and 25° - 35°W.

3.1. Introduction

Sailfish, *Istiophorus platypterus* (Shaw and Nodder, 1791), is an important commercial and recreational fisheries resource, being exploited throughout all tropical and subtropical oceans. Sailfish has been recognized by some authors as comprising Atlantic and Indo-Pacific species (Nakamura, 1985). However, genetic data are consistent with the existence of a single species (Finnerty and Block, 1995; Graves, 1998) with a worldwide distribution (Beardsley *et al.* 1975) and, therefore, the sailfish, together with the blue marlin (*Makaira nigricans*), are the only pandemic istiophorid billfishes (Nakamura, 1985). Due to its highly migratory nature, it is fished by several nations with different fishing gears. Consequently, international management is required, which in the Atlantic Ocean, comes under the jurisdiction

of the International Commission for the Conservation of Atlantic Tunas (ICCAT). Fishing impacts on Atlantic billfish stocks is currently the focus of considerable international concern. Bycatch fishing mortality in pelagic longline fisheries, targeting tunas and swordfish, represents one of the main impacts on billfish stocks in the Atlantic Ocean (Uozumi, 2003). In the eastern tropical Atlantic, a large amount of billfishes are also caught as bycatch in European purse-seine fisheries (Gaertner *et al.*, 2002), and by artisanal fisheries, such as the canoe fishery, in Ghana (ICCAT, 2009). In addition, billfishes are also a very important resource for various coastal and artisanal fisheries in the Caribbean, as well as for recreational fisheries, mainly in USA, Venezuela, Brazil and several Caribbean countries (Peel *et al.*, 2003). In the most recent sailfish assessment, using data up to 2008, results indicated a decline in biomass of the sailfish stocks, particularly for the east Atlantic. However, the analyses in this assessment were severely hampered by an acute lack of accurate data (ICCAT, 2009). One of the main requirements for a proper assessment of stock condition is an understanding of its geographic stock structure and identification of the main areas of occurrence of different size classes, as well as the influence of environmental factors on distribution.

Size frequency data from the commercial longline fishery have always been an important information for understanding the changes in the age structure of the stocks and the seasonal variability in the distribution of tunas and tuna-like species in relation to environmental and spatial factors. A number of methods have been applied to investigate the fishery oceanography of pelagic species. These include generalized linear models (GLM), habitat based models, generalized additive models (GAM), regression tree models and Geographic Information Systems (GIS) (Swartzman *et al.*, 1992, Hinton and Nakano, 1996, Zheng *et al.*, 2004, Valavanis *et al.*, 2004, Venables and Ditchmond, 2004, Maunder and Punt, 2004, Valavanis *et al.*, 2008). Another approach is the employment of spatial prediction techniques based on interpolation algorithms (*e.g.* kriging), which are generally highly data intensive, requiring large amounts of well distributed data. This requirement is rarely attainable by fisheries data, especially when the studied species is not the main target of the fishery, such as it is commonly the case for billfishes (Ortiz and Arocha, 2004).

Recently, a new method based on statistical models for spatial prediction has been developed, called GRASP (*Generalized Regression Analysis and Spatial Prediction*). This

method uses statistical relationships between response (i.e. species distribution) and environmental variables to model spatial prediction by means of prediction maps (Lehmann *et al.* 2002).

In the GRASP approach, GAM models are used to fit the response variables to the environmental explanatory variables using a non-parametric smoothing function (Hastie and Tibshirani, 1990). The GRASP approach has been proved to be suitable for fisheries resources. It was initially applied in the South Atlantic Ocean to model the spatial distribution of swordfish (*Xiphias gladius*), using data from Brazilian commercial longline fisheries (Hazin and Erzini, 2008). In the present paper, GRASP was applied to size data of sailfish caught by longline and gillnet fisheries obtained from ICCAT *data record* to better understand the relationship between size distribution and spatial and environmental factors.

3.2. Material and methods

3.2.1. Size data

Data on length frequency distribution (Lower Jaw Fork Length (LJFL) in cm) were obtained from the ICCAT *Data Record* on fish caught by longline and gillnet fisheries operating in the equatorial and southwestern Atlantic. The data were grouped in 5°x5° stratum considering the initial position of the fishing operation, by month, year, latitude and longitude, from 1998 to 2007. A total of 9,954 LJFL data were utilized, of which 7,541 were from catches of longline fleets based in Brazil, Venezuela and Spain, and 2,413 were from catches of gillnet fisheries based in Côte D' Ivoire, Ghana and Venezuela. The spatial distribution and density of these data are show in Figure 3.1. To evaluate the spatial distribution by length, two LJFL size classes were established following procedures described by Jolley (1977) and Mourato *et al.*, (2009a) as follows: (a) <155 cm, immature individuals (or juveniles), (b) >155 cm, mature individuals (or adults). These data were transformed into proportion of juveniles and adults, by 5° square, assuming a binomial distribution.

3.2.2. Environmental data

A time-series of sea surface temperature (SST) and mixed layer depth (DML) were obtained from the Physical Oceanography Distributed Active Archive Center (PODAAC) -

Jet Propulsion Laboratory/NASA (1998–2007). The bathymetry (BATH) at the location of the fishing sets (BATH) was obtained from the National Geophysical Data Center (ETOPO5 - Earth Topography 5 min). Chlorophyll- α concentration (CHO) were obtained from SeaWiFS images, provided by “SeaWiFS Project” from Goddard Space Flight Center/NASA. These images were turned into numerical data (in mg/m^3) with the GDRA2XYZ program provided by the Phoenix Training Consultants. These data, with an original resolution of 0.5° (except Chlorophyll- α concentration, which had a initial resolution of 9 km resolution), were used to construct a database of $5^\circ \times 5^\circ$ resolution, by month, year, latitude and longitude. These data were then matched with the length frequency data.

3.2.3. Modeling

The spatial prediction of the proportion of adult individuals (PR) as a function of environmental and spatial variables was modeled using GRASP v3.2 (Lehmann *et al.*, 2002). In the GRASP approach, the spatial predictions are obtained by the relationships between a response variable (proportion of individuals at adult stage) and selected predictor variables (environmental and spatial variables) by the fitting of a GAM model. The general formulation of the GAM is expressed in the following manner:

$$\text{PR} = a + s_1(x_1) + s_j(x_j) \dots + e$$

where PR is the proportion of adults, a is a constant, s_1 is the effect of the smoothing function for the independent variable x_1 and e is the random error of the function. The non-linear effects of the model were adjusted by smoothing “Spline” functions (*natural cubic*) with four degrees of freedom. The choice of the degrees of freedom was based on visual inspection and exploratory analysis. Such approach allows the detection of major effects and reduces spurious patterns that can arise from overfitting (Maravelias *et al.*, 2000). The binomial distribution was used with a logit link function. Due to a spatial distribution discontinuity of the LJFL classes, the analysis was restricted to the delimited area shown in the Figure 3.1. This is necessary due to the decreased predictive capacity of the models in areas with low density of data.

The consistency of the final model was evaluated using: 1) linear regression between randomly chosen observed values of proportion of adults and those generated by the

model using the included independent variables as input (simple validation) and 2) a cross-validation method which assessed the goodness of fit of the model. The correlation between the observed and predicted values was estimated by the Pearson correlation coefficient, whereas the Receiver Operating Characteristic (ROC) test was used for the binomial model. ROC indicates model performance, independently of the apparently arbitrary probability threshold required in the proportion models, at which the presence of a target feature is accepted (Fielding and Bell, 1997). A total of 5,000 lengths were randomly chosen from the length frequency data set (besides the 9,954 measurements used in the model). These were used for the exclusive purpose of cross validation, and therefore were not included in the model. Predictors were selected using a forward and backward stepwise procedure, going in both directions from a full model and removing predictors according to an *F*-test ($\alpha = 0.05$). The relative effect of each x_j variable over the dependent variable (here the proportion of adults) was evaluated using the distribution of partial residuals.

3.3. Results

The final model explained 52.8% of the total variance, including latitude, longitude, sea surface temperature, chlorophyll- α concentration, depth of mixed layer and bathymetry as continuous variables and month as a factor. The relative contribution for each variable in the total explained variance (52.8%) for the selected model shows that longitude effect was the most significant factor in the analysis. Among the environmental variables, the depth of mixed layer was the most important, followed by chlorophyll- α concentration, sea surface temperature and bathymetry (Figure 3.2). The results of the simple and cross-validations of the final model are also shown in the table 1. The ROC values (validation and cross-validation, 0.78, 0.81, respectively) indicate that predictions were reasonably fitted and matched well with the data.

There was an increase in the proportion of adults to 0.3 mg/m³ of chlorophyll- α concentration, then rather stable at higher concentrations (Figure 3.3). The effect of bathymetry indicated that adult sailfish were more abundant than juveniles when depths exceeded 4,000 m. Adult sailfish were also more abundant in areas when depth of the mixed layer was less than 20 m and in waters with SST was <24°C (Figure 3.3). The proportion of adults was highest in March and September (Figure 3.3).

Spatial prediction (Figure 3.4) shows that adult sailfish were more frequent to the west of 40°W, both at northern and southern parts of the studied area, as well as to the east of 25°W. Along the Brazilian coast, from 25°W to 40°W, the proportion of adults was very low in particular from 10°S to 25°S (Figure 3.4).

3.4. Discussion

A proper understanding of essential fish habitats has been considered crucial to the development of fishery management strategies based on an ecosystem approach (Valavanis *et al.*, 2004). In this study, the GRASP tool was used to describe the preferential habitats of sailfish, in relation to juveniles and adults, based on size distribution, environmental and spatial data. There have been many applications of GRASP, including use with terrestrial animals (Fraser *et al.*, 2005), plants (Lehmann *et al.*, 2002; Zerger *et al.*, 2009), seagrass (Bekkby *et al.*, 2008) and coral reefs (Garza-Pérez *et al.*, 2004).

Although the spatial factor longitude provided the highest explanatory ability on the proportion of adults of sailfish, the environmental effects were also significant. The inclusion of environmental variables in the analysis often resulted in low levels of explanation, because fishing and environmental data were generally not obtained simultaneously (Brill and Lutcavage, 2001) and relationships are not well described on scales of 5°- month data. Conversely, many species, in particular the highly migratory, have a life cycle strictly related to environmental conditions that affect their availability and vulnerability (Fréon and Misund, 1999). Thus, the inclusion of environmental variables in the model is relevant for an appropriate understanding of the distribution of sailfish in the South Atlantic Ocean.

The much higher proportion of adults east of 25°W, agrees with Beardsley (1980) and Prince and Goodyear (2006), who also indicated that the largest sailfish are located on the eastern side of the Atlantic. Data on size distribution of sailfish from the Pacific Ocean also shows a similar trend to the South Atlantic with the largest fish being concentrated in the eastern side of that ocean (Kume and Joseph, 1969; Wares and Sakagawa, 1974; Prince and Goodyear, 2006). The difference in size distribution of sailfish in both sides of the South Atlantic is likely linked to life cycle and migratory movements, which, in turn, is probably related to the diverse oceanographic conditions affecting habitat preferences of juveniles and adults in a different manner. Prince and Goodyear (2006), however, attribute the larger size of eastern Atlantic and

eastern Pacific sailfish as a likely consequence of hypoxia based habitat compression which increases ambush opportunities for sailfish which are compressed in a shallow surface layer along with their prey. The eastern tropical Atlantic Ocean is characterized by intense nutrient upwelling with a consequently very shallow thermocline (~25 m) and high surface chlorophyll concentration. Upwelling off the coasts of Ghana, Cote d'Ivoire and Nigeria occurs seasonally, with a weak upwelling from January to March, and intense upwelling from July to September (Longhurst, 1962; Picaut, 1983; Ibe and Ajayi, 1985). Conversely, the western Atlantic has a warm surface layer, a deep thermocline (~75 m) and much lower surface chlorophyll concentration (Hazin, 1993; Becker, 2001). Juveniles appear to be associated with waters with SSTs higher than 28°C in the western side, particularly between 10° - 20°S and 25° - 35°W. Besides, the higher concentration of juveniles in the western side can also be a result of their proximity to the spawning area, dispersing later from this location as they grow (Mourato *et al.*, 2009a). Adult sailfish, in turn, seem to be more common in the eastern side of the Atlantic with large concentrations occurring close to the African coast and the Gulf of Guinea, an area very rich in nutrient content, consequently, increasing the amount of potential sailfish prey, such as small cupleids, like *Engraulis* sp. and *Sardinella* sp. (Ibe and Ajayi, 1985; Ovichinikov, 1971). Sailfish have an opportunistic feeding behavior and it is, thus, commonly attracted to regions with high concentrations of prey (Beardsley *et al.*, 1975; Nakamura, 1985).

The model used in the current analyses considered four main environmental variables: SST, mixed layer depth, chlorophyll concentration and bathymetry, all of which have been linked to billfish abundance (Ueyanagi *et al.*, 1970; Ovichinikov, 1971; Nakamura, 1985; Brill and Lutcavage, 2001; Prince and Goodyear, 2006). Sailfish spend most of the time in the mixed layer and prefer waters with temperatures between 25° and 30° C, as shown by other studies based on PSAT tags and ultrasonic telemetry (Hoolihan, 2004; Prince and Goodyear, 2006; Hoolihan and Luo, 2007; Mourato *et al.*, 2010). The preference for near surface and warmer waters was also reported for other Istiophoridae fishes in the Atlantic Ocean (white marlin, *Tetrapturus albidus*: Horodysky and Graves, 2005; Horodysky *et al.*, 2007; blue marlin, *Makaira nigricans*: Graves *et al.*, 2002; Goodyear *et al.*, 2008). Therefore, sailfish and others Istiophorids, the depth of mixed layer which marks the top of the thermocline is an important feature that might directly affect vulnerability, catchability and local abundance. Prince and Goodyear (2006) pointed out that the depth distribution of sailfish in areas with intense

upwelling processes may be restricted to the thin layer as shallow as 25 m at the surface ocean by the compression of the acceptable physical habitat due to the lower concentration of dissolved oxygen below the thermocline, turning them more vulnerable to the surface fishing gears (i.e. longline and gillnet).

In the Eastern tropical Atlantic, sailfish abundance varies seasonally, linked to the cooling of surface water by the seasonal intensification of the upwelling process. Sailfish move along the African coast from south to north, in spring, and apparently back again, from north to south, in autumn, following the warmer isotherms (Ovchinikov, 1971; Diouf, 1994; Bard *et al.*, 2002).

Similarly, several studies have shown that sailfish abundance is highly seasonal in the southwestern Atlantic Ocean, as well (Arfelli and Amorim, 1981; Hazin *et al.*, 1994; Mourato *et al.*, 2009a and b). Mourato *et al.* (2009a) stated that the sailfish start its reproductive migration from the Brazilian northeast coast to southeast, in mid-September, arriving in the southeast Brazilian coast in November/December. Spawning takes place mainly during January/February, with the species remaining near the southeast coast until early March. As it has been shown to occur with white and blue marlin, this southward migratory movement is probably related to the seasonal change of SST, reflected in the displacement of surface isotherms. Several authors have reported that the sailfish migratory pattern is restricted to the 28°C surface isotherm in several parts of the world (Ovchinnikov, 1971; Ueyanagi *et al.*, 1970; Nakamura, 1985), a SST that occurs only during the 1st and 4th quarters of the year along the southeast coast of Brazil (Matsuura, 1986).

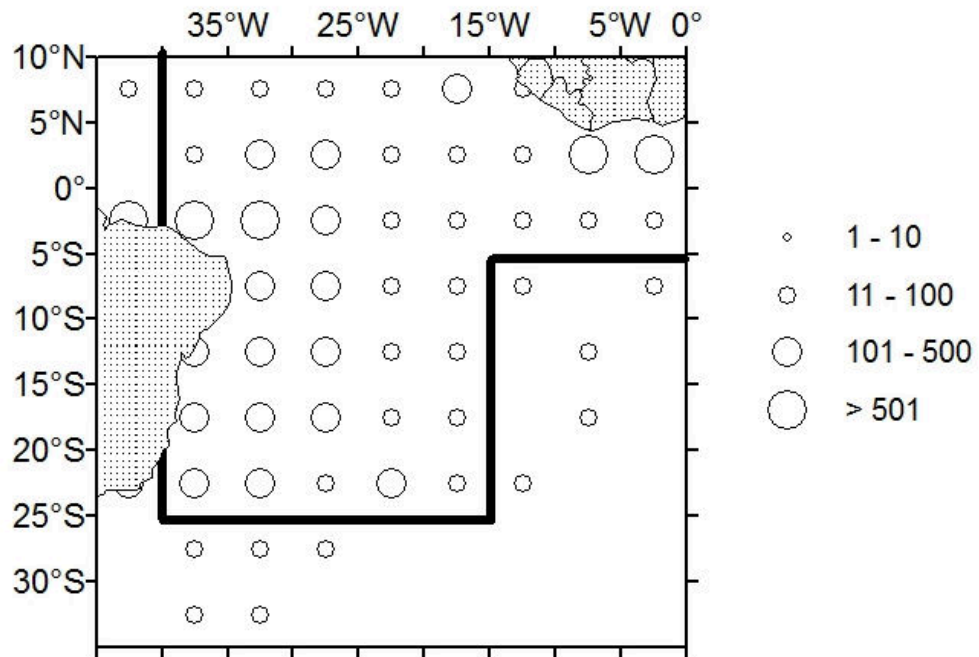


Figure 3.1 - Spatial Distribution of length frequency (LJFL) data obtained through the ICCAT *Data Record* from 1998 to 2007. The legend represents the number of fishes measured.

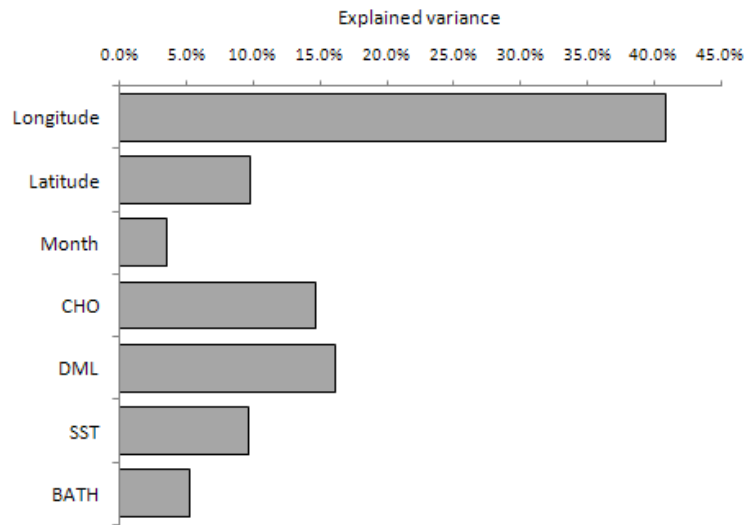


Figure 3.2 - Contribution of each variable added on the final model (model contribution). SST, sea surface temperature, CHO, chlorophyll- α concentration, DML, deep mixed layer and bathymetry, BATH in explanation of total variance.

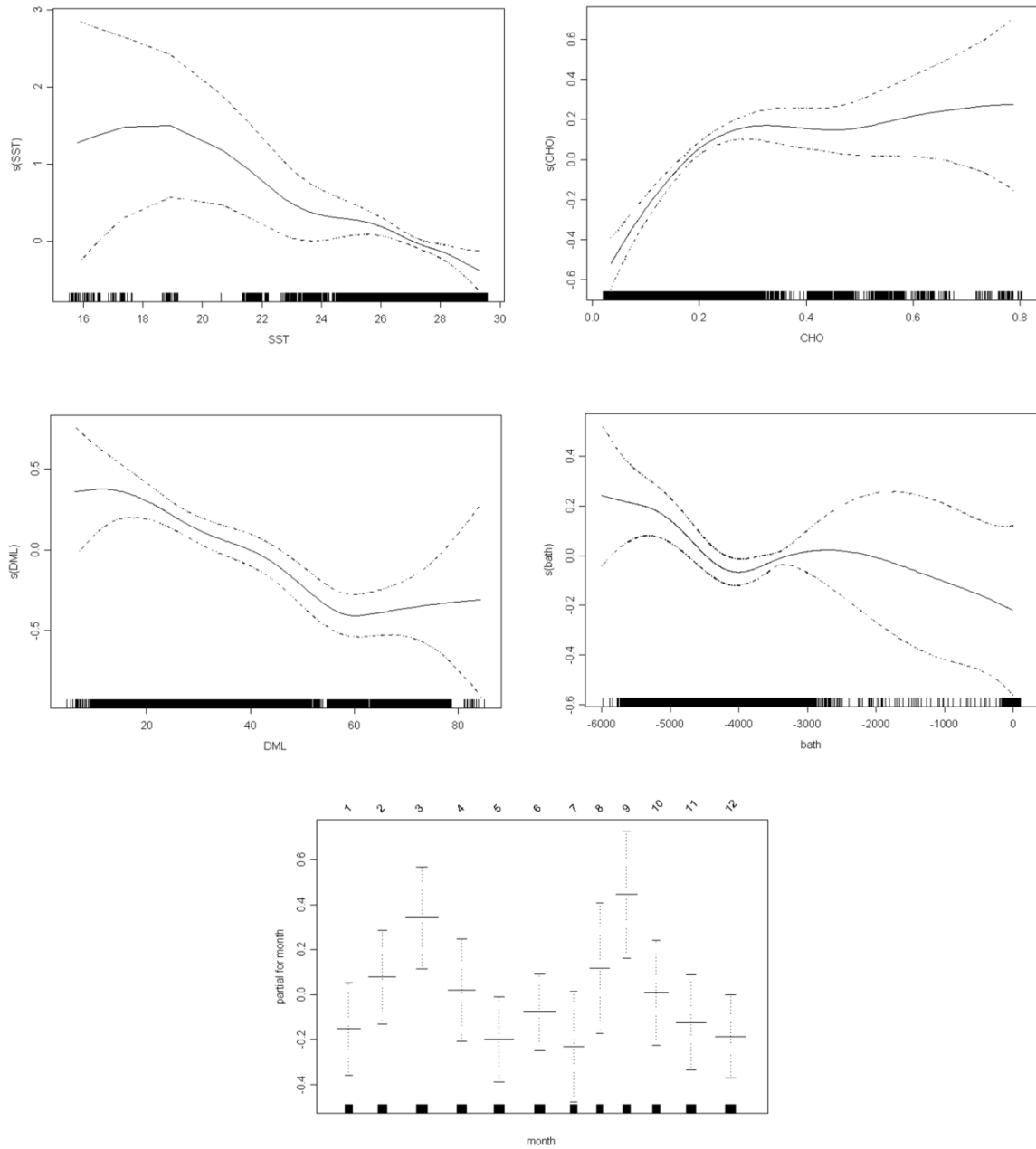


Figure 3.3 - Partial response curves showing the effects of the predictor variables added on the size model of adult sailfish in the South Atlantic from 1998 to 2007. SST, sea surface temperature, CHO, chlorophyll- α concentration, DML, deep mixed layer and BATH, bathymetry. Dashed lines represent the 95% confidence interval limits.

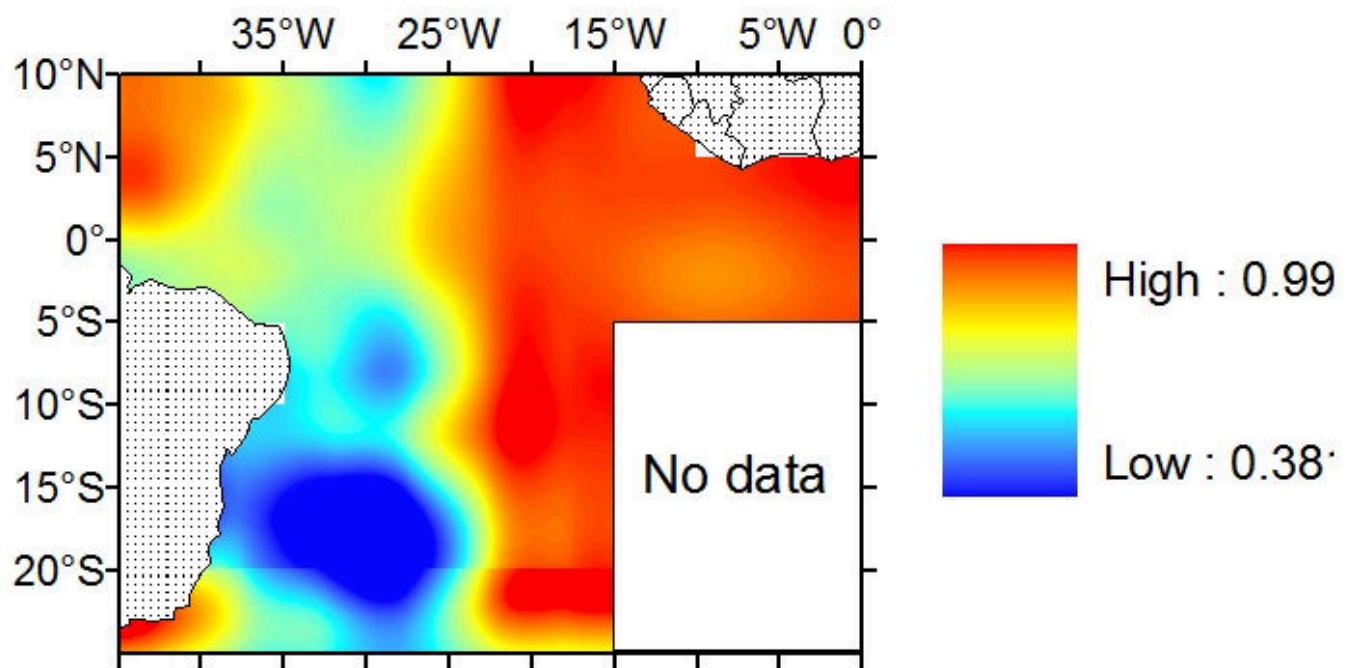


Figure 3.4 - Spatial prediction for the proportion of adult sailfish, using data from ICCAT data record from 1998 to 2007.

Chapter 4 - Spatio-temporal trends of sailfish catch rates in relation to spawning season and environmental factors in the equatorial and southwestern Atlantic Ocean

Abstract

Spatial and temporal trends of sailfish catch rates in the southwestern and equatorial Atlantic Ocean in relation to environmental variables were investigated with generalized additive models (GAMs) using fishery dependent data that were contemporaneously collected with biological information. Two GAMs were fit: (1) “spatio-temporal” including only latitude, longitude, month, and year and (2) “oceanographic” including sea surface temperature (SST), chlorophyll-a concentration, wind velocity, bottom depth, depth of mixed layer and year. The spatio-temporal model explained more (average, ~30%) of the variation in catch rates than the oceanographic model (average, ~18%). Catch rate predictions revealed a seasonally high aggregation of sailfish off the southeast Brazilian coast during peak spawning (November to February) while the mid-west Atlantic to the south of ~15°S as well as the Brazilian north coast may represent important winter feeding grounds. The oceanographic model revealed that SST and wind velocity were the most important variables describing catch rate variation. The results presented herein may help to understand sailfish movements in the Atlantic Ocean and to improve catch rate standardization.

4.1. Introduction

Sailfish, *Istiophorus platypterus*, is a circumtropical epipelagic species mainly distributed in subtropical and tropical oceanic waters. In the Atlantic Ocean, sailfish are distributed from 40°N to 40°S in the west and from 50°N to about 40°S in the east (Beardsley *et al.*, 1975; Nakamura, 1985). Important sport and artisanal (e.g. drift net) fisheries target these species in Atlantic waters (Brison *et al.*, 2006; ICCAT, 2009), but sailfish are considered bycatch in most commercial longline fisheries targeting tunas (*Thunnus* spp.) and swordfish (*Xiphias gladius*) throughout the Atlantic Ocean (Restrepo *et al.*, 2003). In Brazil, sailfish are caught primarily by pelagic longline fisheries as incidental bycatch, although some are also caught by

drift gill nets. Off the Brazilian coast, sailfish are abundant throughout the year mainly in tropical areas with the peak abundance from October to February in the southeast Brazilian coast. From 1991 to 2006, annual landings of sailfish in Brazil have fluctuated from 90 t in 1991, to 598 t in 2000 and then decreased to 140 t in 2006.

Atlantic sailfish populations have been managed by the International Commission for the Conservation of Atlantic Tunas (ICCAT) since 1966. Based on distribution of catch, tagging information, and morphological data, ICCAT has traditionally considered this species to comprise two different stocks in the Atlantic Ocean with western and eastern stocks separated arbitrarily by the meridians associated with the mid-Atlantic Ridge, at 40°W in the north Atlantic and 20°W in the south Atlantic). Limited tag-recapture data has indicated no trans-Atlantic or trans-equatorial movements (Ortiz *et al.*, 2003; Orbesen *et al.*, 2008). Furthermore, analysis of the distribution of catch-at-length data indicated that at least part of the sailfish population in the Atlantic was structured longitudinally by ontogenetic stages, as reflected by by environmental preferences of adults and juveniles or sub-adults (Mourato *et al.*, 2010a). This two-stock hypothesis, however, requires further investigation because genetic analyses suggest Atlantic sailfish comprise a single, highly mobile, pan-Atlantic stock (Graves 1998, Graves and McDowell 2003).

For highly migratory fishes, one of the essential requirements for understanding population dynamics is the delineation of the spatial variability of the stock during important biological processes. Migration to spawning grounds is believed to be the dominant behavioral aspect of fish aggregation (Laevastu and Hayes, 1981). Therefore, understanding migratory corridors and cues are essential for ecosystem-based management and conservation. Earlier studies have highlighted the southwestern Atlantic Ocean as an important spawning ground for sailfish (Arfelli and Amorim, 1981; Mourato *et al.*, 2009a). Limited tagging data prevent a characterization of the mechanisms affecting sailfish distribution, including the possible influence of environmental factors during important life-cycle events. Based on catch-effort statistics, SST it thought to significantly affect the horizontal distribution patterns of sailfish (Ueyanagi *et al.*, 1970; Ovchinnikov, 1971). In addition, vertical movements may be limited by the concentration of dissolved oxygen, depth of the mixed-layer, or by an 8°C change in water temperature (Brill and Lutcavage, 2001). For example, limited dissolved oxygen may act as a

barrier to constrain vertical movements in the eastern Atlantic Ocean (Prince and Goodyear, 2006; Prince *et al.*, 2010).

Population dynamics models that incorporate spatial heterogeneity in vital biological parameters are needed to understand species distribution and impacts of commercial exploitation on stocks (Cadrin and Secor, 2009). Due to significant gaps in the knowledge about sailfish biology and catch rates in the Atlantic, a study was undertaken to describe the spatio-temporal pattern of sailfish abundance in the equatorial and southwestern Atlantic Ocean. Moreover, key environmental variables were evaluated to determine the possible affect(s) on the distribution and catchability of sailfish during important life-cycle events. These analyses allowed us to address various aspects of the ecology of sailfish, particularly with inferences about the kinds of variables that influence sailfish distribution during spawning.

4.2. Material and Methods

4.2.1. *Catch and effort data*

Data on catch and nominal fishing effort were obtained from logbooks of the Brazilian pelagic tuna longline fleet (national and chartered vessels) which were completed by fishing captains during trips from 2004 to 2008. The logbooks contain vessel identification, date, location of fishing ground (latitude and longitude), time of the longline set and retrieval, fishing effort in number of hooks and the number of fish caught by species.

In order to have a homogenous data set, the analyses were limited to shallow (< 120 m), nighttime longline sets that targeted swordfish (n=18,395 sets). Deep daytime (>200 m) sets that targeted tunas (n=1,936) were deleted. Longline sets were distributed throughout a wide area of the equatorial and southwestern Atlantic Ocean, ranging from 7°N to 40°S and 50°W to 0° (Figure 4.1). However, due to the low fishing effort and no sailfish catches below 35°S (33 sets), the analysis was constrained to a narrower area, ranging from 7°N to 35°S and 50°W to 10°W (18,362 sets) (Figure 4.1).

4.2.2. *Environmental data*

Time-series of SST (°C), depth (m) of the mixed layer (DML) and zonal and meridional wind components were obtained from the Physical Oceanography Distributed Active

Archive Center (PODAAC) - Jet Propulsion Laboratory/ NASA (2004-2008). Wind velocity (m/s) estimates were obtained for each fishing location from wind velocity = $\sqrt{(\text{meridional wind}^2 + \text{zonal wind}^2)}$. The bottom depth (m) at the deployment location was obtained from the National Geophysical Data Center (ETOPO5- Earth Topography 5 min) and data on chlorophyll-*a* concentrations (Chla) were obtained from SeaWiFS images, provided by the Goddard Space Flight Center/ NASA and converted to $\text{mg} \cdot \text{m}^3$. These data, with an original resolution of $0.5^\circ \times 0.5^\circ$ (except Chla with initial resolution of $9 \text{ km} \times 9 \text{ km}$ resolution), were used to construct a database of $1^\circ \times 1^\circ$ resolution assembled by day, month, year, latitude and longitude. These data were then matched to the fisheries catch and effort data on the same temporal and spatial scale.

4.2.3. Generalized additive model fitting procedures

Generalized additive models (GAMs) using penalized regression splines (estimated by penalized iterative least squares, Wood, 2006) were applied to predict areas with high catch rates. Data were separated into two distinct periods: (a) spawning (November to February) and; (b) non-spawning (March to October). The spawning period was determined based on the spatial differences of monthly mean gonadal index values and the non-spawning period was assumed to commence immediately after spawning within the study area (Figure 4.1) (Mourato *et al.*, 2009). Since there was high correlation between SST and latitude ($r = 0.83$) and between bottom depth and longitude ($r = 0.63$), two kinds of models were used to avoid confounding issues with multiple collinearity (Maunder and Punt, 2004; Zuur *et al.*, 2010): (1) “spatio-temporal”, included the factors year, month, latitude and longitude; and (2) “oceanographic” which included several environmental variables, as well as year, to account for inter-annual variability. Formulations of these models were:

- *Spatio-temporal model:*

$$\text{catch} \sim \text{year} + \text{month} + \text{s}(\text{longitude}, \text{latitude}) + \text{offset}(\log[\text{fishing effort}]) + e$$

- *Oceanographic model:*

$$\text{catch} \sim \text{year} + \text{s}(\text{wind}) + \text{s}(\text{bathymetry}) + \text{s}(\text{SST}) + \text{s}(\text{Chla}) + \text{s}(\text{DML}) + \text{offset}(\log[\text{fishing effort}]) + e;$$

where catch is the number of sailfish caught per set, s (longitude, latitude) represents the effect of the spatial location as an isotropic bivariate function (Wood and Augustin, 2002), fishing effort is an offset term, and e is an error term from any distribution from the exponential family. Two main parametric predictors (*i.e.* factors) were considered: year ($n = 5$ levels, 2004 thru 2008), and month ($n = 4$ levels, November thru February for the spawning period and; $n = 8$ levels, March thru October, for the non-spawning period). Models were fit using the *mgcv* package in R 2.12.0 (R Development Core Team, 2010) with the optimum degree of smoothing being estimated by the generalized cross-validation (GCV) criterion (Wood, 2006).

Due the high percentage of zeros in the catch data (~60%, sets with no sailfish catches), three statistical probability distributions were initially considered: Poisson, negative binomial and Tweedie. A Poisson distribution is a common approach to model spatio-temporal distributions of count data (Augustin *et al.*, 1998) and the negative binomial GAMs were implemented using automatic selection of a scale parameter θ available in package *mgcv* (Wood, 2006). For the Tweedie distribution, the estimation of the power-parameter was obtained by maximizing the likelihood for each value candidate (Dunn and Smith, 2005). The final estimation of this parameter was approximately 1.3 (compound Poisson-gamma distribution), which was considered appropriate for the analysis (Shono, 2008).

The selection of predictors and the decision on their entry or exclusion was based on the GCV score, Akaike Information Criterion (AIC) (Akaike, 1978) and the total deviance explained. However, in *mgcv*, fitting algorithms using GCV scores for negative binomial is not appropriate (Wood, 2006). Thus, for negative binomial models the selection of predictors was evaluated by AIC and the total deviance explained. Chi-square tests were also computed to determine whether predictors yielded significant ($p < 0.05$) reductions in the residual deviance upon entry into the GAM. Lastly, selection of the best statistical probability distribution for the oceanographic and spatio-temporal models for each period (*i.e.* spawning or non-spawning) was based on distribution of residuals, lowest values of AIC and Bayesian Information Criterion (BIC) (Schwarz, 1978) and the total deviance explained.

4.3. Results

Of 18,362 sets analyzed, 6,492 sets corresponded to the spawning period and 11,870 sets to the non-spawning period and the proportion of positive catches (sets with at least

one sailfish caught) was 42% and 35% for the spawning and non-spawning periods, respectively. However, the proportion of positive catches varied over time with the highest proportions occurring in 2005 for the spawning period (53%), and 2004 for the non-spawning period (38%). The distribution of sailfish catch per set showed a highly skewed distribution, with high numbers of zeros and few observations of greater than five sailfish captured per set (Figure 4.2).

4.3.1. Modeling

For both the spawning and non-spawning periods, the results of the spatio-temporal models indicated that the negative binomial distribution provided the best fit (Table 4.1). The oceanographic model, using data from the spawning period, exhibited the lowest AIC and BIC scores (Table 4.1). However, during the non-spawning period, the best fit for the oceanographic model was provided by the Tweedie distribution. For all models, the traditional Poisson distribution had the highest AIC and BIC scores, in comparison with negative binomial and Tweedie models (Table 4.1). Though there were only small AIC and BIC differences between the negative binomial and the Tweedie models, the negative binomial oceanographic model explained a higher proportion of the deviance (18.0% vs 16.5%). Residuals from the negative binomial distribution (Figure 4.3 and Figure 4.4) showed a better fit in comparison with Tweedie and Poisson models and suggests no evidence of heteroscedacity. Based on these criteria, all analyses were consequently based on the negative binomial distribution.

4.3.2. Selection and significance of variables in the models

All terms added to the spatio-temporal models for both the spawning period and the non-spawning period were highly statically significant ($p < 2.20^{-16}$) and resulted in a decrease in AIC value (Table 4.2). The isotropic bivariate $s(\text{longitude, latitude})$ term was the most important for both periods. For the spawning period, the effect of geographic location accounted for 31.6% of the explained deviance, while for the non-spawning period this contribution was 26%. Other variables (month and year) were also significant, however with much lower explanatory power (Table 4.2). All terms added to the analysis of deviance for the oceanographic models were statistically significant ($p < 2.20^{-16}$) and resulted in greater resolving power (i.e. lower AIC value) (Table 4.3). For the spawning period; based on percentage deviance explained, wind velocity and ocean depth were the most important terms, followed by year, SST, Chla and

DML (Table 4.3). By contrast, during the non-spawning period, SST was the most important factor. The inclusion of other oceanographic parameters in this model also resulted in a decrease of residual deviance with wind velocity being the most important factor, followed by Chla, bathymetry, year and DML (Table 4.3).

4.3.3. *Spatiotemporal trends of catch rates*

The spatial prediction (Figure 4.5) of sailfish catch rates for spawning and non-spawning periods show spatio-temporal variation of sailfish densities in the South Atlantic. During the spawning period, three distinct areas of high densities were evident: (1) the largest area was in a oceanic region, between 5°S and 15°S and 20°W and 30°W; (2) the second area was situated close to the southeastern coast of Brazil, between 15°S and 25°S and 39°W and 50°W; and (3) the third area was from 0° to 5°S and from 39°W to 45°W (Figure 4.5). During the non-spawning period, the most prominent feature was the disappearance of sailfish from southeastern Brazil and the notable increase in catch in the more oceanic region of the South Atlantic, extending from 5°S to 20°S and from 18°W to 35°W (Figure 4.5). The high catch area close to the northern coast of Brazil was present in both periods with a slight north-west displacement during the non-spawning period.

Standardized catch rates for all models and periods were very similar, except for the strong peak in 2005 in the spatio-temporal model during spawning. A moderate decline of standardized catch rates is evident for all models throughout the time period analysed in this study (Figure 4.6). The standard deviations of the year effects are provided in the Table 4.4. Monthly patterns show that sailfish abundance is expected to be high during the spawning period (November to January), followed by a strong decline in February (Figure 4.7). During the non-spawning, sailfish abundance is highest during the months before and after the spawning season which coincides with warmer water temperatures (Figure 4.7).

4.3.4. *Environmental effects on catch rate*

Figure 4.8 and Figure 4.9 depict the smoothed terms from the oceanographic model during the spawning and non-spawning periods, respectively. During spawning, sailfish catch rates are expected to be highest when the wind velocity is higher than 4 m/s with the most pronounced peak ≈ 9 m/s (Figure 4.8) and a similar trend was also observed during the non-

spawning period with higher catch rates associated with higher wind velocities (Figure 4.9). As expected, the influence of bottom depth on sailfish catch rate was different between spawning and non-spawning periods. During spawning, higher catch rates were associated with coastal areas (< 2000 m, Figure 4.8), especially off southeastern of Brazil (Figure 4.5). However, high catch rates were also noted in waters greater than 5000 m deep (Figure 4.8), which may be associated with a different water mass, between 5°S and 15°S (Figure 4.5). In the non-spawning period, the effect of variability in bottom depth indicated sailfish were more concentrated in waters greater than 3500 m deep (Figure 4.9) as shown by the distribution maps (Figure 4.5).

The influence of SST on sailfish abundance was similar for the two periods, with the highest catch rates occurring when SST was $>26^{\circ}\text{C}$ (Figure 4.8 and Figure 4.9). Of all factors examined, however, SST was the most important variable to explain distribution of sailfish catch rates for non-spawning activities, while during spawning, wind velocity was the most prominent variable (Table 4.3). Sailfish catch rate were similar between spawning and non-spawning periods regarding chlprophyll a concentrations with the highest values in the range between 0.6 and $1.0 \text{ mg}\cdot\text{m}^{-3}$, followed by a decline thereafter (Figure 4.8 and Figure 4.9).

4.4. Discussion

In an effort to understand variability in sailfish catch rates in the western and south Atlantic, various GAMs were investigated to analyze the spatio-temporal trends in catch with spawning seasonality and environmental factors incorporated into models. Moreover, also linked to models was a spatially explicit gonadal index value (to assess reproductive activity) (Mourato *et al.*, 2009a). By matching catch statistics with biological and environmental factors on the same scale, our analysis suggested a new insight about the spatio-temporal catch variability of sailfish in southwestern Atlantic and the factors that influence catchability and availability of sailfish associated with pelagic longline fishery.

4.4.1. Modeling approach

The negative binomial distribution appeared to be the most appropriate distribution to analyze sailfish catch rates caught by the Brazilian longline fleet based on distribution of residuals, AIC, and percentage of deviance explained. Due to high correlation between SST and latitude and between bottom depth and longitude, we fitted models with spatial

and environmental predictors separately to avoid problems with collinearity. When SST and bottom depth were fit in a single model, the results were non-intuitive as higher sailfish catch rates were associated with lower SST ($<18^{\circ}\text{C}$), but this species has been described by several authors to prefer warmer waters ranging from 24° to 30°C (Ovchinnikov, 1971; Beardsley *et al.*, 1975; Nakamura, 1985). The unrealistic effect of SST, however, is probably related to problems of concurvity, a common problem in GAM modeling. Concurvity is the non-parametric analogue of colinearity where the effect of one of the predictors (e.g. SST) can be approximated by a linear combination of the effects of other predictors (i.e. latitude) (Ramsay *et al.*, 2003; Figueiras *et al.*, 2003; Walsh *et al.*, 2006). For these reasons, the separate treatment of environmental parameters from the spatial parameters was crucial to better assess the effects of environmental effects on the spatio-temporal distribution of sailfish catch rates, as well as to avoid bias caused by over parameterization.

4.4.2. *Spatiotemporal trends of catch rates*

Previous authors have reported that the southeast Brazilian coast is an important spawning area for sailfish from December to February (Arfelli and Amorim, 1981; Mourato *et al.*, 2009). The observations in our study also provide evidence of a major spawning ground in the south Atlantic. Moreover, based on relatively high densities and low gonadal index values throughout the year (Mourato *et al.*, 2009a), the mid-west Atlantic (i.e. south of 15°S), as well as the north coast of Brazil may represent important winter feeding grounds areas. Additionally, our findings are also supported by Mourato *et al.* (2010a) which showed that the proportion of adults on the three hotspots identified in the present study is much higher than juveniles or sub-adults proportion and the average size of the specimens caught by the Brazilian pelagic longline fishery on these aforementioned areas is higher than the length of sexual maturity estimated for sailfish in the southwestern Atlantic. Hence we may consider that the specimens caught in these areas are able to reproduce.

Based on the reproductive data and catch rate analyses, it can be hypothesized that starting in October, mature sailfish migrate from the western central tropical Atlantic towards the southeast Brazilian coast to spawn and remain in the area from about February to March. After spawning, sailfish probably migrate in a north-east direction perhaps following the south Atlantic gyre (Peterson and Stramma, 1991), to return to the tropical western central tropical Atlantic to

forage. Pop-up satellite archival tagging of two sailfish indicated that fish may remain off southeastern coast of Brazil during the spawning season for periods up to one month (Mourato *et al.*, 2010b).

4.4.3. Impact of environmental factors

The spatio-temporal models had better explanatory ability to explain variability of sailfish catch rates than oceanographic models. A lower explanatory ability and a larger residual deviance of the oceanographic models were, however, not unexpected, since the inclusion of environmental variables in the modeling of species distribution can be problematic (Brill and Lutcavage, 2001) when remotely sensed predictor variables represent averages over time and space. The relationship between environmental variables and sailfish relative abundance, however, may help explain habitat preferences during spawning.

Results showed that sailfish were caught over a large SST range (16 – 29°C) and higher densities were associated with warmer waters (>26°C) during both spawning and non-spawning periods. It is thought that during September to October, sailfish migrate southward prior to spawning, and afterwards they migrate to the north-east. Changes in catch and sailfish distribution were probably related to seasonal changes in SST, and in particular, the displacement of 28°C surface isotherm during these movements. Temperature strongly influences fish metabolism and during spawning, may accelerate the process of gonadal development (Freon and Misund 1999). Several authors described that sailfish migration was probably restricted to the 28°C surface isotherm in several parts of the world (Ovchinnikov, 1971; Ueyanagi *et al.*, 1970; Nakamura 1985). Furthermore, information from satellite tagging also suggested the preference of sailfish for warm waters of the uniform surface mixed-layer (Prince and Goodyear, 2006; Mourato *et al.*, 2010b).

The appearance of sailfish on spawning grounds and in fisheries off southeast Brazil may be related to the oceanographic conditions that prevail during warm periods. The intrusion of South Atlantic Central Water (SACW) during summer over the continental shelf and slope may be related to sailfish reproduction in the southwestern Atlantic. The SACW is characterized by temperatures lower than 18°C, salinity ranging between 34.4 and 36 ppt and a high concentration of nutrients (Matsuura, 1986). The seasonal expansion of the SACW

promotes an influx of deep nutrients to the shallow parts of water column and consequently may accumulate large concentrations of potential prey items for sailfish larvae, juveniles and adults. On the other hand, there is currently no evidence of a fishery oceanographic relationship that could help explain the high sailfish densities observed in more oceanic areas between 5°S and 15°S and in the area close to the northern coast of Brazil.

Despite the preference of sailfish for warmer waters, which are usually more oligotrophic, the higher band of chlorophyll concentration ($>0.9 \text{ mg} \cdot \text{m}^{-3}$) had a negative effect on the catch rate. This might be explained by the time needed for the chlorophyll bloom to mature into forage for sailfish, such as squid and small pelagic fish. Similar patterns were also observed for blue shark in the southwest Atlantic (Mourato *et al.*, 2008) and albacore in the northwest Pacific (Laurs, 1983). For example, Lehodey *et al.* (1998) suggest it takes about 3 months for a chlorophyll bloom to mature into forage for skipjack tuna in the equatorial Pacific.

Wind velocity may also affect the availability and vulnerability of sailfish, as well as the behavior of the longline. The higher sailfish catch rates associated with high wind velocities may be an indirect result of other operational variables related to the behavior of the fishing gear in the water column. For example, higher wind stress may induce greater vertical hook movements, which would increase sailfish vulnerability to the baited hooks. Higher wind velocities associated with higher current velocities, for instance, may shoal and therefore reduce the fishing depth of the pelagic longline gear by $\approx 50\%$ (Bigelow *et al.*, 2006). Similar longline shoaling may occur in the western equatorial Atlantic (B.L. Mourato, *unpublished data*), thus increasing sailfish vulnerability given the reported shallow vertical distribution based on free-ranging animals (Prince and Goodyear, 2006; Hoolihan and Luo, 2007; Mourato *et al.*, 2010b). Identification of spawning areas in the southwestern Atlantic Ocean will be useful for delineating stock structure of sailfish in the Atlantic. Furthermore, areas of high catch rates could be included in models that may prove valuable for catch rate standardizations which in turn could provide information on catchability.

The inclusion of oceanographic variables in catch rate standardization, however, had a small statistical benefit since the standardized catch rates were very similar to spatial-temporal models. On the other hand, the oceanographic models provided a better understanding of fishery oceanographic relationships, the physiological ecology of sailfish and the possible

relationship between the fishing gear behavior and catchability (*e.g.*, wind velocity effect). New applications incorporating other oceanographic variables (*e.g.*, dissolved oxygen) are still required to improve the understanding of the environmental effects on sailfish catches. Finally, the fishery oceanographic relationships presented herein should also be tested and developed in other areas with sailfish fisheries in order to better evaluate the benefits of the inclusion of environmental factors on catch rate standardization.

Table 4.1 – Summary of model diagnostics used to select the error distribution of the spatiotemporal and oceanographic models for sailfish caught by Brazilian longline fleet in the southwestern Atlantic Ocean from 2004 to 2008. Deviance explained (%): Explained deviance by each model; AIC: Akaike Information Criterion and; BIC: Bayesian Information Criterion.

	Poisson	Tweedie	Neg. Binomial
Spatiotemporal model (Spawning period)			
Deviance explained (%)	30.5	30.2	31.6
AIC	25469	19068	18896
BIC	25717	19315	19144
Spatiotemporal model (Non-spawning period)			
Deviance explained (%)	24.6	24.6	26.0
AIC	37254	29000	28907
BIC	37550	29297	29205
Oceanographic model (Spawning period)			
Deviance explained (%)	21.2	20.5	21.1
AIC	27819	20033	19983
BIC	28117	20328	20282
Oceanographic model (Non-spawning period)			
Deviance explained (%)	16.2	16.4	17.7
AIC	40148	30104	30290
BIC	40489	30449	30639

Table 4.2 - Deviance analysis in the spatiotemporal models of sailfish caught by Brazilian longline fleet in the southwestern Atlantic Ocean from 2004 to 2008. Resid. df: residual degrees of freedom; df: degrees of freedom; Resid. Dev.: Residual deviance; P(>|Chi|): Chi-square test p value; Dev.expl. (%): Explained deviance by each model and; AIC: Akaike Information Criterion.

Predictor	Resid.df	df	Resid.Dev	Deviance	P(> Chi)	Dev. expl. (%)	AIC
<i>Spatiotemporal model (Spawning period) - Negative Binomial</i>							
Null model	6492		10211				22052
Month	6489	3	9860	351.38	2.20E-16	3.44	21707
+Year	6485	4	9543	317.10	2.20E-16	6.55	21397
+s(longitude,latitude)	6456	28	6984	2558.81	2.20E-16	31.60	18896
<i>Spatiotemporal model (Non-spawning period) - Negative Binomial</i>							
Null model	11870		16369				33088
Month	11863	7	16150	218.30	2.20E-16	1.33	32884
+Year	11859	4	16009	140.90	2.20E-16	2.19	32751
+s(longitude,latitude)	11831	28	12108	3901.10	2.20E-16	26.00	28907

Table 4.3 - Deviance analysis in the oceanographic models of sailfish caught by Brazilian longline fleet in the southwestern Atlantic Ocean from 2004 to 2008. Resid. df: residual degrees of freedom; df: degrees of freedom; Resid. Dev.: Residual deviance; P(>|Chi|): Chi-square test p value; Dev.expl. (%): Explained deviance by each model and; AIC: Akaike Information Criterion.

Predictor	Resid.df	df	Resid.Dev	Deviance	P(> Chi)	Dev. expl. (%)	AIC
<i>Oceanographic model (Spawning period) - Negative binomial</i>							
Null model	6492		10211				22052
Year	6488	4	9941	270.39	2.20E-16	2.7	21790
+s(wind)	6480	7.3	9201	739.73	2.20E-16	9.9	21065
+s(Bottom depth)	6472	7.8	8620	580.88	2.20E-16	15.6	20499
+s(SST)	6463	8.9	8353	266.57	2.20E-16	18.2	20251
+s(Chlorophyll)	6456	7.7	8165	188.86	2.20E-16	20	20077
+s(Depth of mixed layer)	6448	7.3	8055	109.18	2.20E-16	21.1	19983
<i>Oceanographic model (Non-spawning period) - Negative binomial</i>							
Null model	11870		16369				33088
Year	11866	4	16202	166.78	2.20E-16	1	32929
+s(SST)	11857	8.6	14919	1282.66	2.20E-16	8.9	31664
+s(wind)	11850	6.8	14405	514.43	2.20E-16	12	31163
+s(Chlorophyll)	11841	9.5	13922	482.57	2.20E-16	14.9	30700
+s(Bottom depth)	11832	8.5	13607	315.12	2.20E-16	16.9	30402
+s(Depth of mixed layer)	11824	8.6	13478	129.02	2.20E-16	17.7	30290

Table 4.4 - Standardized sailfish catch rates and standard deviations (in parenthesis) associated of spatiotemporal and oceanographic models for spawning and non-spawning periods.

	Spawning period		Non-spawning period	
	<i>Spatiotemporal model</i>	<i>Oceanographic model</i>	<i>Spatiotemporal model</i>	<i>Oceanographic model</i>
2004	0.90 (± 0.12)	1.08 (± 0.08)	1.04 (± 0.13)	1.28 (± 0.06)
2005	1.49 (± 0.10)	1.23 (± 0.10)	1.21 (± 0.08)	1.07 (± 0.08)
2006	0.87 (± 0.13)	0.89 (± 0.12)	0.82 (± 0.09)	0.76 (± 0.10)
2007	0.86 (± 0.13)	1.09 (± 0.11)	0.98 (± 0.09)	1.01 (± 0.10)
2008	0.88 (± 0.18)	0.71 (± 0.17)	0.94 (± 0.12)	0.88 (± 0.12)

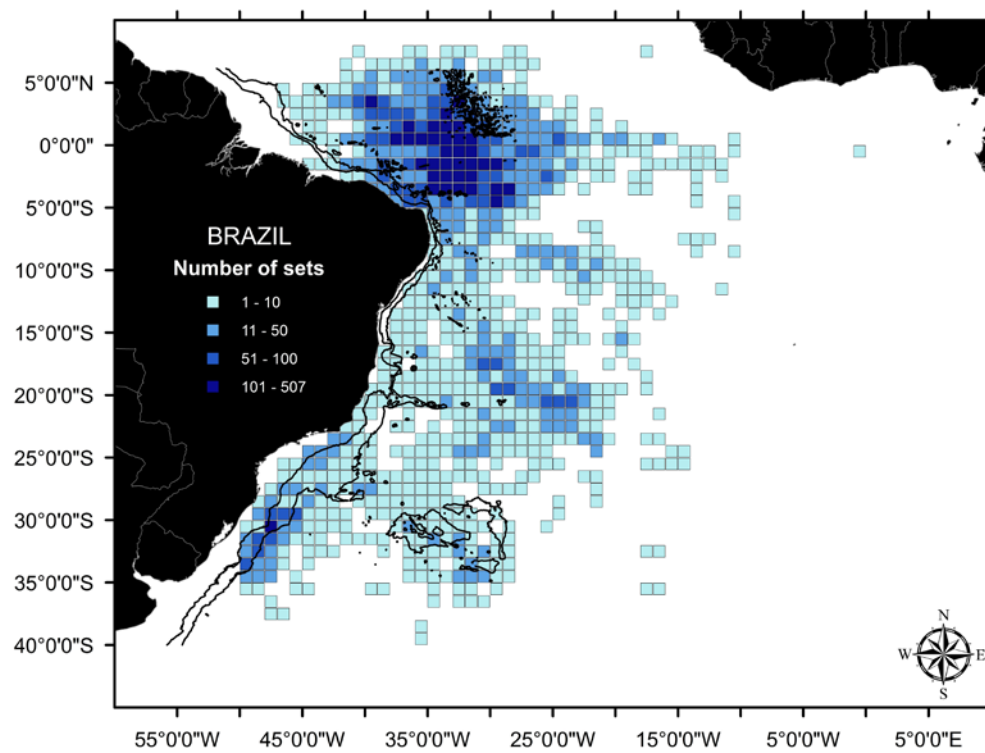


Figure 4.1 - Distribution of the Brazilian fishery longline sets in the Atlantic Ocean, from 2004 to 2008.

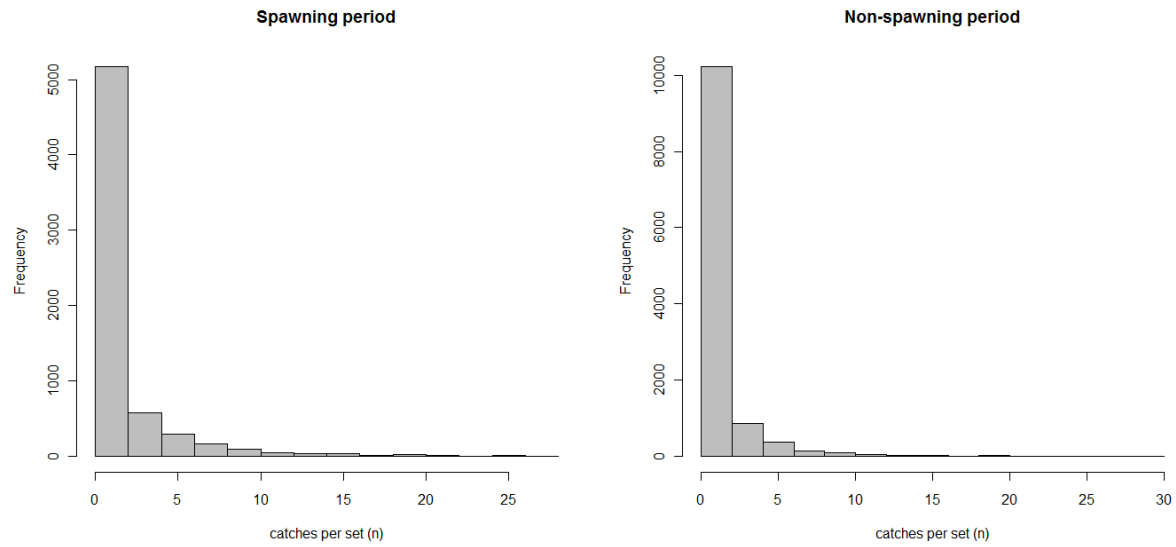


Figure 4.2 - Sailfish catch per set for the Brazilian longline fishery in the Atlantic Ocean from 2004 to 2008. Spawning period (left panel) and non-spawning period (right panel).

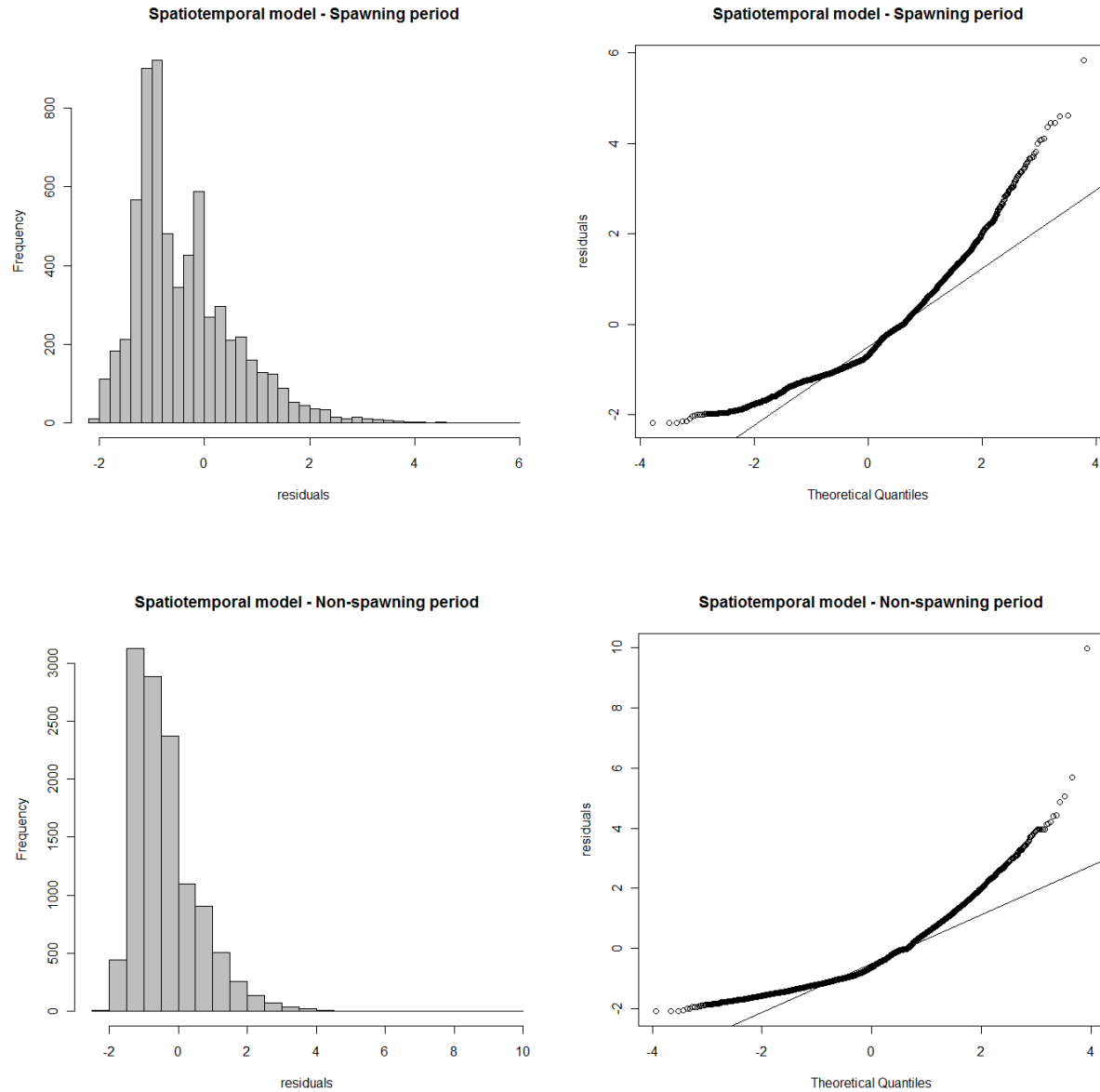


Figure 4.3 - Histogram of standard residuals (left panels) and quantile–quantile (QQ) plots of the deviance residuals (right panels) of the spatio-temporal models fitting sailfish catches using negative binomial error distribution.

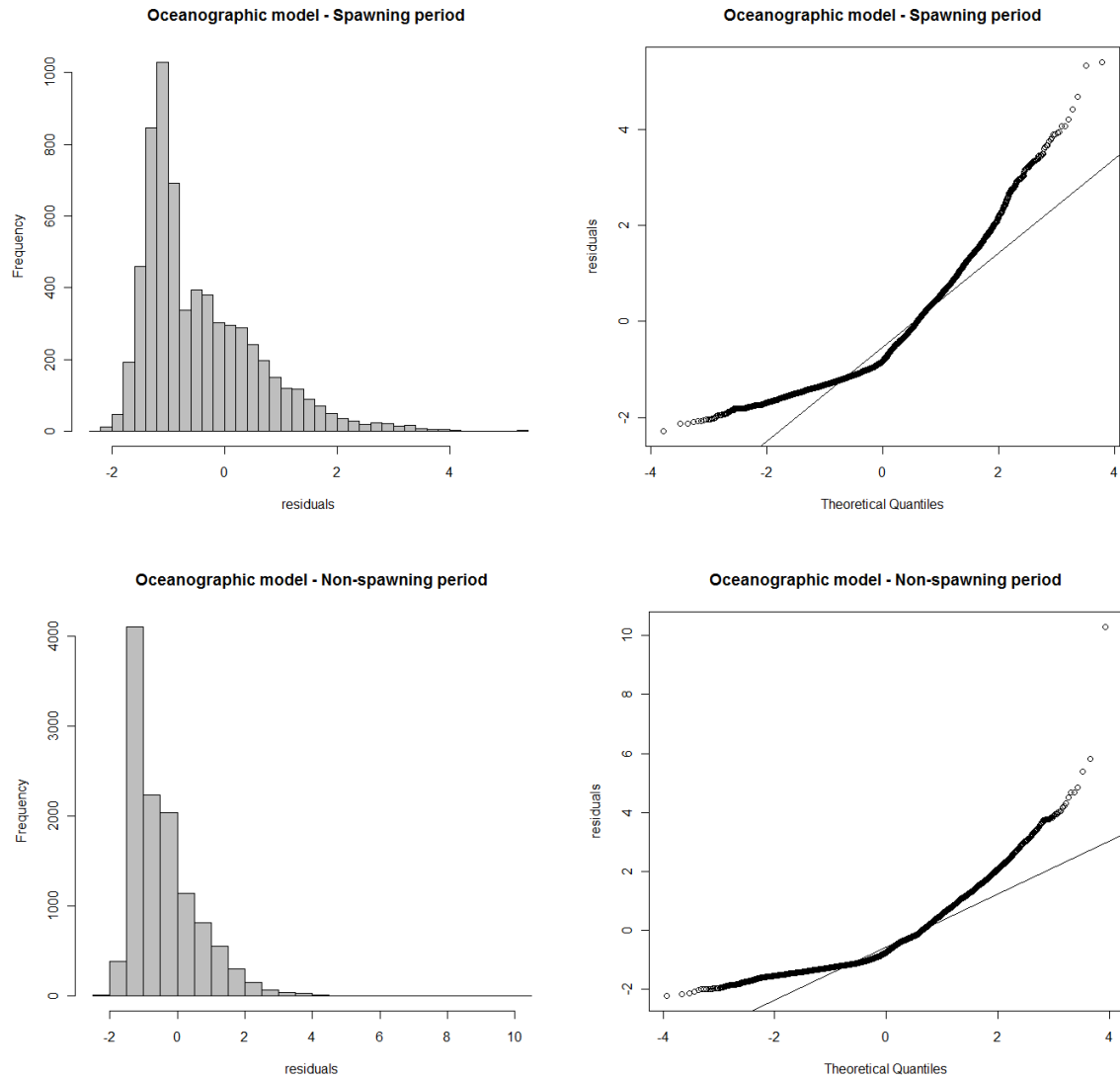


Figure 4.4 - Histogram of standard residuals (left panels) and quantile–quantile (QQ) plots of the deviance residuals (right panels) of the oceanographic models fitting sailfish catches using negative binomial error distribution.

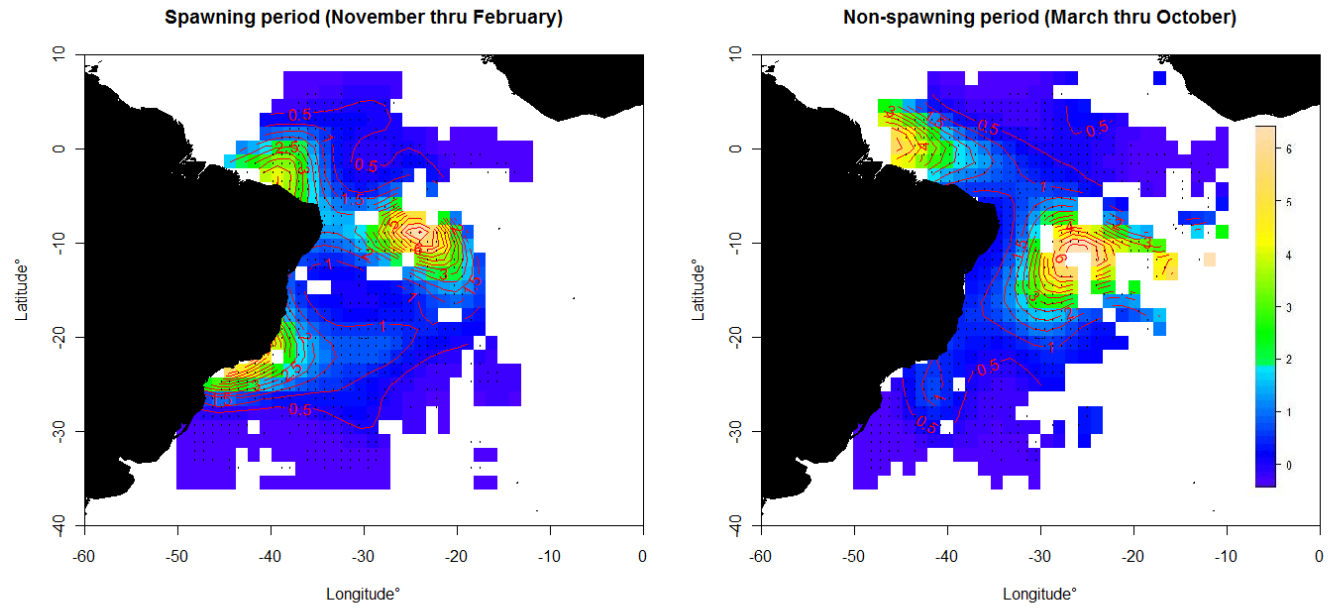


Figure 4.5 - Spatial predictions of catch rate for sailfish in the Brazilian longline fishery based on negative binomial spatio-temporal models (2004–2008). Spawning period (left panel) and non-spawning period (right panel). The color scale and contour lines represent the magnitude of the model predictions.

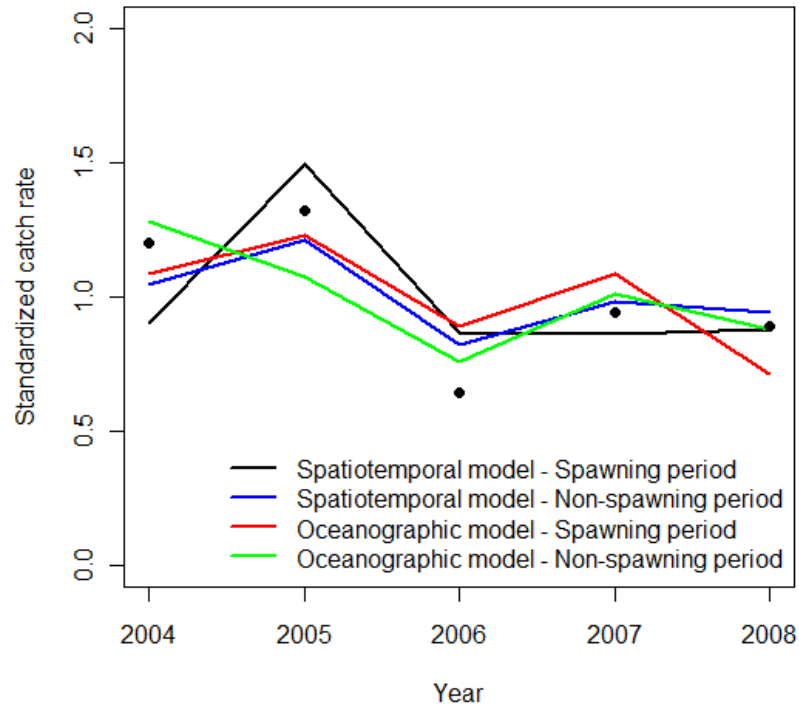


Figure 4.6 - Standardized catch rate using a negative binomial error distribution of sailfish caught by the Brazilian longline fleet from 2004 to 2008. Black points represent the annual nominal catch rates.

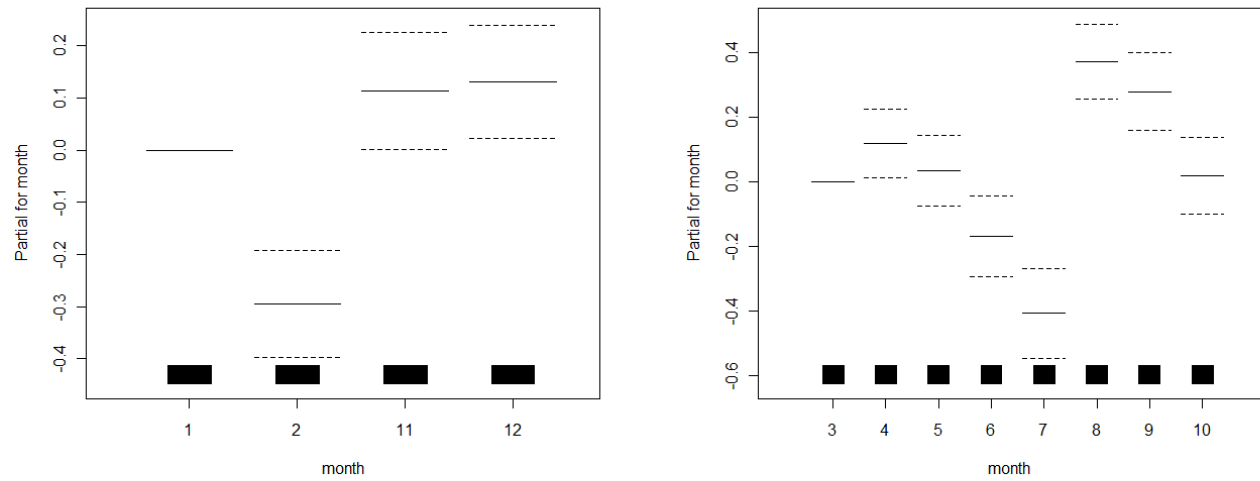


Figure 4.7 – Partial residuals showing the effect of month on catch rate of sailfish caught by the Brazilian longline fleet from 2004 to 2008. Spawning period (left panel) and non-spawning period (right panel)

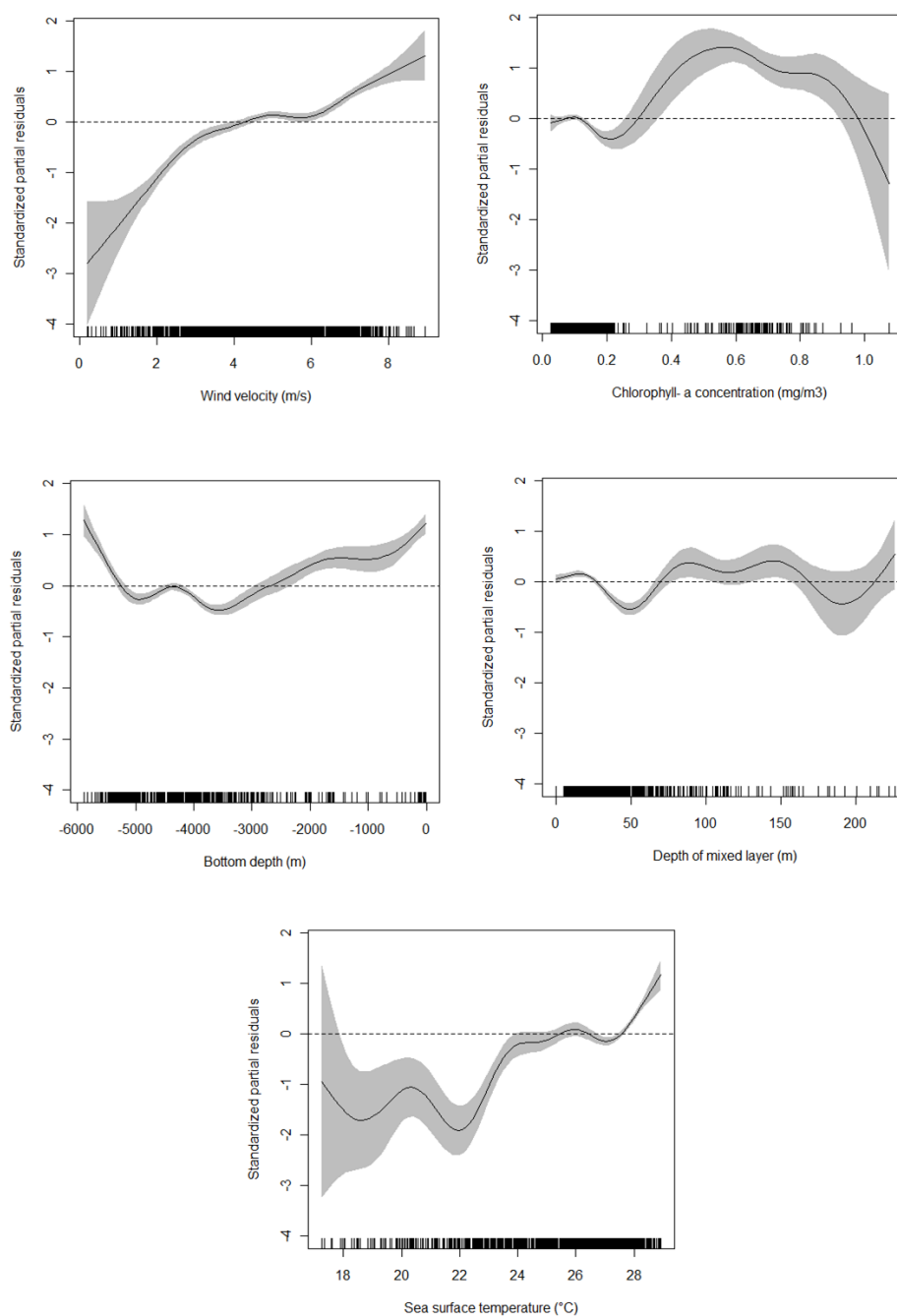


Figure 4.8 - Partial response curves showing the effects of the oceanographic variables on catch rate of sailfish caught by the Brazilian longline fleet from 2004 to 2008 for the spawning period. Shaded area represents the 95% confidence interval limits and the dotted line displayed on the plots indicates the mean catch rate estimated by the model.

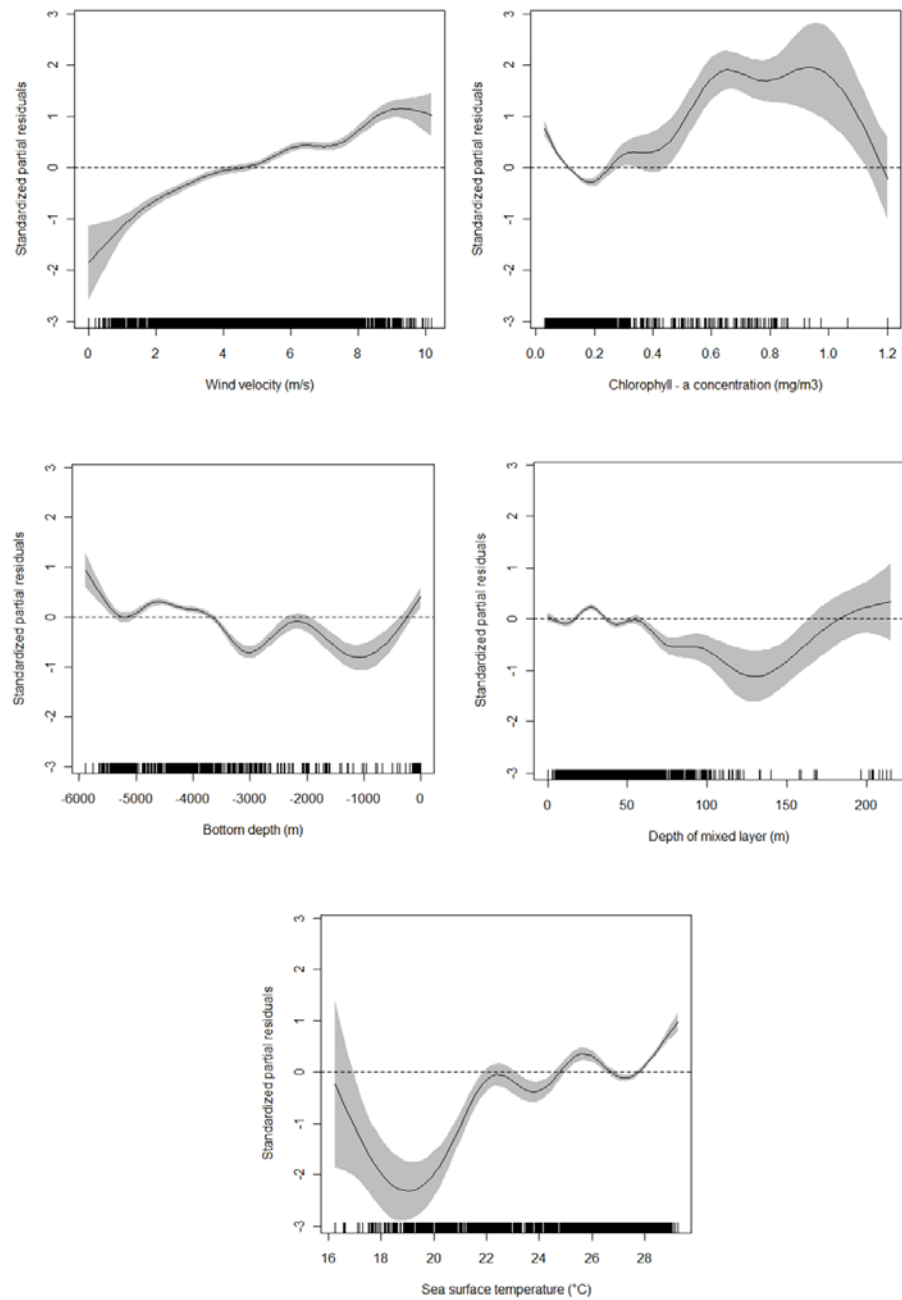


Figure 4.9 - Partial response curves showing the effects of the oceanographic variables on catch rate of sailfish caught by the Brazilian longline fleet from 2004 to 2008 for the non-spawning period. Shaded area represents the 95% confidence interval limits and the dotted line displayed on the plots indicates the mean catch rate estimated by the model. The dotted line displayed on the plots indicates the mean catch rate estimated by the model

Chapter 5 - Movements and habitat utilization of Atlantic sailfish off Southeast Brazil, determined by pop-up satellite tagging

Abstract

Information about habitat selection and migration pattern of highly migratory species like tunas and billfishes are of primary interest in stock assessment and management, since that they are key factors in the identification of stock units. PSATs were deployed on four sailfish in the coastal waters of Rio de Janeiro State located in Southeast Brazilian coast during January and February of 2009 (for the tags sailfish I and sailfish II) and between November 2010 and January 2011 (for the tags sailfish III and sailfish IV). Wildlife Computers Inc MK10 PAT model were the tags used. The total number of days monitored (such as the time that the tags remained attached) were 12 (sailfish I), 51 (sailfish II), 16 (sailfish III) and 43 days (sailfish IV). In brief, the results indicate a clear pattern of vertical habitat utilization of sailfish, with the majority of the time spent being predominantly concentrated near the sea surface with a relatively narrow temperature range preference. Despite the preference for surface waters the tagged sailfish demonstrated vertical movements into deeper waters (around 50 m depth) regularly within 3 to 6 hour interval. In brief, the “most probable tracks” suggest that tagged sailfish did not move significantly away from the tagging site. Sailfish I moved southeastward away from the Brazilian coast until the 7th day of liberty, presenting, after that, a westward movement towards the Brazilian coast, until the pop-up event, very close of the tagging site. Sailfish II moved towards southeast farther away from the Brazilian coast with the position of the first transmission of tag relatively not too far from the tagging site. Sailfish III showed relatively meandering moving behavior however with the position of the first transmission of tag being relatively close to the coast. Sailfish IV moved initially southward, presenting subsequently an eastward movement farther away from the Brazilian coast, but returning towards the continent, until the pop-up event.

5.1. Introduction

Information about habitat selection and migration of highly migratory species, like tunas and billfishes, is of primary interest for stock assessment and management, since they are key factors in the identification of stock units. The distribution and time variability at different scales (*i.e.* circadian, seasonal, interannual) of fish stocks help to delineate how many fisheries are exploiting a given stock and conversely how many stocks a given fishery is exploiting (Fréon and Misund, 1999). Furthermore, the habitat utilization and movements also govern the availability of fish in both the horizontal and vertical dimensions, thus directly affecting the catchability coefficient and consequently the catch rates (Fréon and Misund, 1999, Bigelow and Maunder 2007). Therefore, it is indispensable that these factors be taken into account in the development of abundance indices for stock assessments purposes and related management advice.

However, the gathering of information on migration and habitat selection of large pelagic fish has always presented several challenging obstacles. Traditionally, information on spatiotemporal variability of fish stocks has been obtained by analysis of catch-per-unit-effort (CPUE) from commercial fisheries. However, the use of nominal CPUE to estimate abundance has been criticized for a long time (Garstang, 1900; Baranov, 1918; Ricker, 1940; Mar, 1953), since the basic assumptions (e.g., fish and fishing effort are randomly distributed) are rarely met (Hilborn and Walters, 1992).

On the other hand, the practice of fish tagging has provided valuable information about fish movements and distribution, particularly because of its “fisheries-independent” nature. The first tagging experiments on billfishes took place in the early 50s, through a cooperative tagging program operating out of Woods Hole Oceanographic Institute, in Massachusetts (USA). During this program, between 1954 and 1960, 1,305 sailfish and 1,500 white marlins were tagged (Mather, 1963). Few years later, by 1965, around 6,793 sailfish had already been tagged. In the other side of the USA, in the Pacific Ocean, extensive billfish tagging were also happening. During the first International Billfish Symposium held in Kailua-Kona, Hawaii (USA), in 1972, the results of 15,540 billfish tagged in that ocean were also reported. An extensive literature review on the application of conventional tagging in large teleosts, including tuna and tuna-like fishes is available in Bayliff (1993, 1996) and Ortiz *et al.* (2003).

Despite of its great utility for the understanding of fish longevity and movements, conventional tagging studies are rather limited, since they provide only fish positions at release and recapture. The actual track taken by the fish between these two points, as well as its daily vertical movements, are therefore impossible to infer. Besides, conventional tagging depends directly on fishing to recover the tagged fish. In the mid-1950s, however, the underwater telemetry in form of acoustic tags began to allow fishery biologists to actually follow individual fish over several days, making it possible to describe their behavior and simultaneously to collect data about the surrounding physical environment (Arnold and Dewar 2001).

The first experiment of acoustic telemetry on sailfish was conducted by Jolley and Irby (1979) off the east coast of Florida (USA), aiming at the assessment of the post-release mortality of eight tagged sailfish. Since then, technological advances, such as the reduction in size and weight of the acoustic tags, as well as the increase of battery life and signal strength (Reine, 2005), have allowed the application of telemetry studies in several billfishes, including striped marlin (Holts and Bedford, 1990; Brill *et al.*, 1993), blue marlin (Holland *et al.*, 1990; Block *et al.* 1992a and b), black marlin (Pepperell and Davis, 1999), and swordfish (Carey and Robison, 1981; Carey, 1990). More recently Hoolihan (2004) utilized acoustic telemetry to investigate the small scale movements of sailfish in the Arabian Gulf, showing that the depth distribution of this specie is predominantly superficial with more than 84.3% of its time being spent in the first 10m.

Despite the importance of acoustic telemetry to the advance on the knowledge of vertical and horizontal movements of fish, this technique still has some limitations, since it requires the active following of the tagged animal. The length of observation on active acoustic telemetry is therefore usually restricted to relatively short periods of time (few days), restrained by vessel autonomy, crew fatigue and tag battery life. The advent of the automatic pop-up tags in the late 1990s, however, gave a new impulse to the research on the migratory movements of marine animals.

The pop-up tags record data on ambient light levels, which can be analyzed with daily geolocations algorithms to determine the geographic position during the track period, depth and water temperature. Basically, the pop-up tags continuously record data for a predetermined period and set intervals, automatically detaching itself from the fish when this period is attained.

It then floats to the sea surface and transmit all stored data by satellite through the ARGOS System (Worldwide Tracking and Environmental Monitoring by Satellite). The most beneficial feature of this innovative technology in comparison to the acoustic telemetry is the possibility of a long-term monitoring (months to years) of marine animals (Arnold and Dewar, 2001). Moreover, the pop-up tags are “fisheries independent” which means that the recapture of the animal is not necessary. This is a very important characteristic since that the recapture rates in some remote locations might be very low. Furthermore, this technology also allows the tracking of species, such as marine mammals and turtles, which are not targeted by fishery operations.

The first studies on scombrid fish using pop-up tag were done on the Atlantic bluefin tuna (*Thunnus thynnus*) (Block *et al.*, 1998, Lutcavage *et al.*, 2000). The first study with pop-up tags in billfishes were conducted by Graves *et al.* (2000) to understand the mechanisms that affect the post-release survival of Atlantic blue marlin after capture with recreational fishing gears. The first experiment with pop-up tags in a sailfish, was conducted by Hoolihan (2004) in the Gulf of Arabia. Prince and Goodyear (2006) also deployed pop-up tags in sailfish and blue marlins in the Northwestern Atlantic and in the Eastern Central Pacific to assess and compare the vertical distribution of these species in these two oceans. Few years later, Hoolihan and Luo (2007) provided detailed information of 18 sailfish tagged with pop-up tags to assess the summer residence of the species the in the Gulf of Arabia. Studies of post-release mortality estimates for sailfish with pop-up tags were later conducted Kerstetter and Graves (2008) based on pelagic longline fishing in the Gulf of Mexico. More recently, Hoolihan *et al.* (2009) also provided detailed information about vertical movements of sailfish in the western North Atlantic, based on two recovered pop-up tags.

In this context, in the present chapter the satellite telemetry technology was utilized in order to better understand and determine the summer presence, residence time and movements of sailfish during and after spawning season in southeast Brazilian coast.

5.2. Material and Methods

5.2.1. Field Operation and PSAT tag programming

PSATs were deployed on four sailfish in the coastal waters of Rio de Janeiro State located in Southeast Brazil during January and February of 2009 (for tagged sailfish I and

sailfish II) and between November 2010 and January 2011 (for tagged sailfish III and sailfish IV). Wildlife Computers Inc (Redmond, WA, USA) MK10 PAT tags were used. The tags were programmed to record depth, temperature and light intensity every second. The depth and temperature records were compiled into histograms at 3-hour intervals (for sailfish I and sailfish II) and at 6-hour intervals (for sailfish III and sailfish IV), with sampling every 60 s. The minimum and maximum temperature bins were programmed for temperatures $\geq 12^{\circ}\text{C}$ and $\leq 30^{\circ}\text{C}$, while the depth bins were programmed to sample the minimum depth of ≤ 1 m (or 0) and maximum depth of 300 m. These bins were chosen based on the vertical movement behavior of sailfish in other areas (Hoolihan, 2004, Prince and Goodyear, 2006). The data collected included the minimum and maximum temperature and depth, and amount of time spent in each of 13 specified depth and temperature bins for each sampled interval (Table 5.1).

The pop-up tags were programmed for a deployment period of 60 days (sailfish I and sailfish II) and 140 days (sailfish III and sailfish IV). A pressure-activated mechanical detachment device was also used, to prevent data loss in the event of fish mortality, remaining at constant depth or going over 1000m. Release locations were obtained from global positioning systems onboard the tagging vessel and pop-up locations were obtained directly from the ARGOS transmissions. The tags were prepared with a tether made of nylon monofilament with \approx 16-20 cm of length. To alleviate torque forces, a swivel was placed halfway along the tether (Figure 5.1).

Deployment of pop-up tags was conducted from recreational fishing vessels using standard trolling gear with natural bait and titanium circle hooks in order to increase the chances of survival of tagged fish. Once fish were hooked and brought to leader and reeled close to the boat, the tag was deployed. The tagging target area was a little below the base of the dorsal fin, between the interneural and neural spines (Musyl and Naughton, 2007, Figure 5.2). The PSAT tags were anchored by a harpoon equipped with a stainless steel tag applicator modified to be driven 5-7 cm into the dorsal musculature. Prior to release, individual weights and lengths were estimated.

5.2.2. Horizontal distribution

Light intensity records were pre-processed using the global positioning software WC-GPE (Wildlife Computers, Redmond, WA, USA) to get the daily raw geo-locations (i.e. unfiltered and uncorrected estimates) of tagged fish for each day at liberty. Then, the Kalman Filter State-Space Model (KFTRACK) (Sibert *et al.*, 2003) was applied to predict the most probable track of the tagged fish. The KFTRACK model was fitted using the “KFTRACK package” (<http://www.nielsensweb.org/ukfsst/>).

5.2.3. Vertical distribution

After running the KFTRACK algorithm, the daily geographical position of the tagged fish was used to estimate the times of sunrise, sunset, and local noon using standard astronomical formulae (Duffett-Smith, 1988). Then the local sunrise and sunset at estimated longitudes were used to assign three distinct periods (day, night and transition) to the data. Although most works on satellite telemetry have used only day and night periods, the transition period was necessary in the present study since the tags were programmed to compile data into histograms at 3-hour intervals (e.g. for sailfish I and II, from 5AM to 8AM and from 5PM to 8PM). For sailfish III and IV, however, this procedure was not needed since the tags were programmed to compile data into histograms at 6-hour intervals, requiring the assignment of only night and day periods.

After assigning the period of the day to the data, a chi-square goodness-of-fit test (*G-test*) was applied to evaluate the independence between the temperature and depth distributions within and among tags. All statistical tests were performed at the $p = 0.05$ level of significance. Furthermore in order to look for similarities between periods and tags, the frequency distributions of the proportion of time at depth and temperature were formatted into an input matrix to apply a non-hierarchical cluster analysis (based on euclidean distances and “ward” method).

The proportions of records within successively deeper layers of temperature, relative to the temperature of the surface mixed layer (termed Delta T; Goodyear *et al.*, 2008) by each 3 h (sailfish I e II) or 6 h (sailfish III e IV) intervals were also calculated for the period that could be clearly identified as day, night or transition time. Average daily surface temperature

was calculated by extracting the temperatures from PDT data where depth was ≤ 10 m. Delta T values were then calculated by subtracting the mean temperature of each PDT observation from the generated average daily temperature values and tabulating the proportion of time spent at temperatures using 1°C bin resolution.

5.3. Results

5.3.1. Tag deployments and performance

The estimated sizes and weights of the tagged fish ranged from 135 to 165 cm (Eye-Fork length - EFL) and from 20 to 30 kg. Fish were hooked in the mouth and appeared in good condition when released. However, all sailfish lost their PSAT prematurely and began transmitting data before the expected dates (60 or 140 days after deployment). The total number of days monitored (*i.e.* the period of time the tags remained attached) were 12 (sailfish I), 51 (sailfish II), 16 (sailfish III) and 43 days (sailfish IV). However, the total percentage of data successfully transmitted through the ARGOS satellite system was 82%, 75%, 46% and 12.5% of the total archived data for the tags I, II, III and IV, respectively. The geographical positions (raw geolocations) were obtained for only 63 days (sailfish I: 12 days; sailfish II: 21 days; sailfish III: 18 days; and sailfish IV: 12 days).

5.3.2. Vertical habitat use and temperature preference

The results indicate a clear pattern of vertical habitat utilization of sailfish, with the majority of the time being spent near the sea surface with a relatively narrow temperature range preference. Sailfish I spent 67%, 90% and 81% between 0 and 10 m, during day, night and transition periods, respectively, while sailfish II spent 72%, 69% and 66%, in the same depth stratum and periods (Figure 5.3). Sailfish III spent 73% and 64% between 0 and 10 m during day and night periods, respectively, while sailfish IV spent 72% and 54% in the same depth stratum and periods (Figure 5.3).

Sailfish I remained in waters with temperatures between 25° and 28°C for 90% of day time, 87% of night time and 77% of transition time (Figure 5.4), while sailfish II remained between 25° and 28°C, for 77%, 73% and 74% of day, night and transition periods, respectively (Figure 5.4). Sailfish III spent more time in a bit cooler waters, with temperature ranging from

24° to 27°C for 89% and 82% during day and night time respectively (Figure 5.4). Sailfish IV, in turn, had a similar behavior of sailfish I and II, remaining in waters with temperatures between 25° and 28°C for 90% of day time and 69% of night time (Figure 5.4).

The cumulative depth and temperature frequencies plots are also similar for the tagged specimens indicating the species preference for surface layers, with temperatures ranging from 24° to 28°C (Figure 5.5). Delta T frequency distributions showed that all sailfish spent the vast majority of their time in the uniform temperature surface layer, being exposed to a maximum temperature change of ~8-10° C (Figure 5.6).

None of the heterogeneity chi-square analyses using the *G-test* for the time at depth distributions (44 total tests) provided significantly different results among periods for each fish, as well as for the data combined (data of all fishes). Likewise, none of the results of G-test for time at temperature distributions (44 total tests) were significantly different among periods for each fish, or for the data combined. Additionally, the resultant clustering dendrogram for depth and temperature distribution showed some similarities between the analyzed specimens and periods (Figure 5.6 and Figure 5.7).

The depth readings by 3-hour (sailfish I e II) or 6-hour (sailfish III e IV) intervals during the monitored time for all tagged sailfish (Figure 5.8; Table 5.2) show that, despite their preference for surface waters, all sailfish performed vertical movement into deeper waters (around 50 m depth) regularly within 3 or 6 hour interval (Figure 5.8). However, in general, sailfish I and III made shallower dives (around 50 m depth), when compared to sailfish II and IV, which frequently visited deeper depths, around 100 m. Furthermore, the two deepest dives made by sailfish I (120 m) were observed immediately after release (Figure 5.8, Table 5.2). For sailfish II the deepest observed dives reached 376 m, while sailfish III made its deepest dive at 112 m. Sailfish IV presented, however, a much deeper dive, going down to 560 m (Figure 5.8, Table 5.2). The depth records by period suggest that the average depths for all tagged sailfish were close (approximately between 20 and 30 m depth), although sailfish IV had an average depth of 46 m during night time (Figure 5.9, Table 5.2).

The minimum and maximum daily temperature and depth experienced by the tracked sailfish (Figure 5.10, Figure 5.11 and Figure 5.12) (except for sailfish IV) show that sailfish I spent most of the time in waters above 20°C (average depth of 40m) with only two

dives on February 2th to waters with temperature of 16°C (120m, Figure 5.8 and Figure 5.10, Table 5.2). On the other hand, sailfish II experienced temperatures and depths much cooler and deeper than sailfish I, with a minimum temperature value of 11.1°C during its deepest dive (376m) on February 25th (Figure 5.8 and Figure 5.11, Table 5.2). Sailfish III, in turn, had a similar behavior of sailfish I, spending most of the time in waters above 23°C (average depth of 40m), with two dives on November 25th to waters with temperature of 20°C (120m, Figure 5.8 and Figure 5.12, Table 5.2). Due to significant gaps on data transmission of the tag from sailfish IV this analysis could not be done for this specimen. However, it experienced the lowest temperature of 12.40°C during its deepest dive at 560 m (Table 5.2).

After February 24th, and more specifically between February 25th and March 10th, sailfish II presented minimum daily temperatures notably much cooler than the rest of the tracked period (Figure 5.11). This may indicate that the fish moved into a different and cooler water mass. Depth-temperature profiles also provide indications that the sailfish II swam at least in two different water masses (Figure 5.13). The first water mass occupied by the sailfish II, prior to 25th February, was warmer and had a deeper mixed layer, while from 25th February to 10th March the fish occupied a cooler water mass with a shallower mixed layer (Figure 5.13). The other 3 fishes, however, were associated to only warmer water masses during their whole track with apparently the same depth of mixed layer (Figure 5.13).

In order to check if the depth behavior of sailfish II was different between the two water masses, the depth distribution data were split into two distinct periods. The first one related to the time the fish was associated to the warmer water mass and the second one related to the cooler water mass. While in the warmer water mass, the fish spent 72%, 65% and 62% of the day, night and transition time, respectively, in the upper 10 m, in the cooler water mass, the fish spent 77%, 75%, 75% of the day, night and transition time in the same depth layer (Figure 5.14). Moreover, while in the warmer water mass sailfish II spent 20% of the time (three periods combined) between 30 and 100 m depth, in the cooler water mass this percentage was only 7% (Figure 5.14). Furthermore, the maximum daily depths when the fish moved into the cooler water mass were notably smaller (around 50 m depth) in comparison to the rest of tracked period (around 100m depth) (Figure 5.11). Nevertheless, the depth distribution of sailfish II in the two water masses were not significantly different (*G-test*, $p > 0.05$).

5.3.3. *Horizontal movements*

The estimated parameters of KFTRACK model for all sailfish (Table 5.3), as well as the geolocation estimates (Figure 5.15 to Figure 5.18) indicate that the KFTRACK model was able to estimate a more reliable fish track than the manufacturer geolocation. The model corrected the raw values of longitude and latitude, especially for latitude since some positions fell completely outside of the confidence area (*i.e.* 95% confidence interval estimated by the model) (Figure 5.15 to Figure 5.18). In the case of sailfish II, an extreme raw geolocation latitude position (around 40° N) was recorded, corresponding to the equinox (when the latitude error is maximal) (Figure 5.16). Regarding the longitudes estimates, with a few exceptions, the raw geolocations were placed outside of the confidence interval of the KFTRACK model (Figure 5.16).

For sailfish III all positions were completely outside of the expected since the raw geolocations were positioned over the continent (Figure 5.17). The raw latitudes estimates were all outside of the confidence area while the longitude estimates lied reasonably inside it. This problem was solved fixing the release and pop-up positions (Figure 5.17). For sailfish IV, despite the light levels readings were not satisfactorily added to the model, due to the significant gaps in data transmission, the KFTRACK model seems to have reasonably estimated the most probable track (Figure 5.18). The confidence area for longitude estimates was very narrow while for latitude estimates the model fit much better, correcting, for example, an extreme raw latitude position on the 30th day of liberty (Figure 5.18).

The “most probable tracks” suggest that all tagged sailfish did not move significantly away from the tagging site. Sailfish I moved southeastward away from the Brazilian coast until the 7th day of liberty, presenting, after that, a westward movement towards Brazilian coast until the pop-up event very close of the tagging site (Figure 5.15). Sailfish II moved towards southeast farther away from Brazilian coast with the position of the first transmission also relatively not too far from the tagging site (Figure 5.16). Sailfish III showed a kind of meandering movement, with the position of the first transmission, however, being relatively close to the coast (Figure 5.17). Sailfish IV moved first towards south, presenting, then, an eastward movement farther away from the Brazilian coast, but returning towards the continent until the pop-up event (Figure 5.18).

5.4. Discussion

5.4.1. Tag performance

In the present study all sailfish lost their tags prematurely, on average, at around 30% of the programmed attachment time. The results suggest that the pop-up event occurred while the fish were alive and not as a result of death followed by sinking. Besides, all tagged specimens were large enough to carry a pop-up tag and were released in good condition, with the hooks being removed before release. The hypothesis of death due to the trauma resulting from the interaction with the fishing gear is therefore unlikely. Moreover, estimates of post release survival also indicate that sailfish have a high survival rate after capture by pelagic longline fishing gears (Kerstetter and Graves, 2008), which is probably even more traumatic than the recreational fishing gear used in the present case. According to Musyl et al (2011), probable causes of tag failure and premature release include battery failure, antennae damage, increased drag as a result of biofouling, infections and tissue necrosis around the tagging site and interference on the frequency reserved to the ARGOS satellite system.

Although the exact reasons for the premature releases observed in this study are not clear, the kind of the tagheads used and the site of tagging may have been a contributing factor. The regular nylon tagheads, used in the present work, have a low retention rate (Musyl and Naughton, 2007). Besides, according to the same authors, in order to maximize the retention time of the tags, the surface area of the tagheads should be increased and placed between adjacent interneural and neural spines (see Figure 5.2), near to the basis of the dorsal fin. All sailfish in this study, therefore, may have been tagged a little lower than the proper target area (see Figure 5.1).

5.4.2. Vertical distribution

The present results showed a marked preference of the tagged sailfish for the upper 10m of the water column during any time of the day. This pattern is consistent with previous studies with acoustic and pop-up tags on sailfish in other parts of world (Hoolihan, 2004; Hoolihan and Luo, 2007; Prince and Goodyear, 2006; Kerstetter and Graves, 2008; Chiang *et al.*, 2010).

The tagged sailfish also seemed to have a rather narrow temperature distribution. Delta T results showed a marked preference of sailfish for the warmer waters of the mixed layer, with all sailfish having spent less than 3% of their time in waters colder than 8°C relative to the change in water temperature in relation to the surface temperature. Other studies have also shown a restricted temperature range for the species, in the Pacific and Atlantic Oceans (Prince and Goodyear, 2006; Hoolihan *et al.*, 2011).

The clear sailfish preference for near-surface warm waters is shared by other istiophorid billfish as well, including the black marlin in the Coral Sea (Pepperell and Davis, 1999; Gunn *et al.*, 2003), Atlantic blue marlin (Graves *et al.*, 2002; Kerstetter *et al.*, 2003; Prince and Goodyear, 2006; Goodyear *et al.*, 2008), Pacific blue marlin (Holland *et al.*, 1990; Block *et al.*, 1992), and striped marlin (Holts and Bedford, 1990; Brill *et al.*, 1993).

The present results also showed that the tagged sailfish did not exhibit much depth variability in habitat use, although some variation was noticeable among individuals, as indicated by the cluster analysis. This pattern is consistent with the results reported for sailfish in Gulf of Arabia by Hoolihan and Luo (2007). On the other hand, Goodyear *et al.* (2008), analyzing a large database of 51 pop-up tags deployed in Atlantic blue marlin, found a complex behavior of vertical habitat use for this species. Musyl *et al.* (2003) also reported a complex habitat utilization for bigeye tuna in the north Pacific ocean with a clear difference in its behavior between night and day.

Although the majority of the time spent by sailfish was restricted to warmer waters near the surface, the data showed that this species is also capable of making frequent deep dives, exceeding depths between 50 and 100 m, with the deepest one having exceeded 500 m. The depth and temperature histograms of time spent combined with the 3 or 6 hourly of maximum depth and minimum temperature suggests that the movement between the surface and deeper layers was relatively rapid.

Vertical movement patterns in large pelagic fish has been reported as very complex reflecting behaviors such as foraging, thermoregulation or predator avoidance (Brill and Lutcavage, 2001). The sailfish dives observed in the present study may be related to an opportunistic feeding behavior. Although the pop-up tags technology does not allow the study of feeding events, two particularities of the sailfish biology seem to support this hypothesis. The

first one, of physiological and anatomical nature, is related to the fact that sailfish, like other istiophorids, have a specialized eye/ brain heater organ, allowing these deeper dives (Block, 1986). The second one is related to stomach content analyses done in the same region, which show the presence of some mesopelagic species in their diet (Vaske-Júnior *et al.*, 2004; Vaske-Júnior, 2005). However, since the summarized pop-up data are not particularly useful for discriminating between different behaviors, these results need to be interpreted with caution. Analysis of high resolution data are still needed in order to allow a better understanding of the vertical movements of the species in a finer scale (i.e. at each minute or even though at each second).

The results of the present study also suggest that the ambient temperature might be the dominant factor controlling the vertical distribution of the species. Sailfish II moved between two water masses with distinct thermal profiles and mixed layer depths, but after entering into the cooler water mass, the fish modified its depth behavior, reducing its average and maximum daily depth, the depth and frequency of dives and the time spent in deeper waters. Therefore, the depth of the mixed layer may be an important feature that might directly affect the depth behavior of sailfish. However, other oceanographic features have also been shown to affect the depth behavior of pelagic fishes. Prince and Goodyear (2006), for example, demonstrated that the vertical distribution of sailfish and blue marlin is directly related to the amount of dissolved oxygen, which may act as a physical barrier to their vertical movement, at least in the eastern side of the Atlantic. Considering, however, the much higher concentrations of dissolved oxygen in the western side of this ocean, such influence is unlikely in the present case.

Some inferences regarding changes in catchability can be drawn from the vertical distributions of sailfish. Based on present results, this species tends to spend more time in shallow waters. The average depth of the shallow-set longline used by the Brazilian longline fishery targeting swordfish is ~50 m. Thus, it is very likely that sailfish vertical distribution is overlapping with the longline gear off the southeastern Brazilian coast. However, it is difficult to predict catchability from electronic tagging data since no information exists regarding how behavior may be altered by the presence of fishing gear.

5.4.3. *Horizontal movements*

In general, sailfish has been recognized to be one of the istiophorid species that presents the most restricted movements in the Atlantic Ocean, as revealed by the release-recovery vector of tagged recaptured fish, with no trans-Atlantic, trans-equatorial or intercontinental movements (Ortiz *et al.*, 2003). However, significant movements were observed between the Straits of Florida and adjacent waters, and the Gulf of Mexico and the area near Cape Hatteras (35°N) (Ortiz *et al.*, 2003; Obersen *et al.*, 2008). One of the main objectives of this study was to determine the summer residence and migratory route of sailfish during and after the spawning season off southeast Brazil. Unfortunately, the low number of tags deployed and their premature releases have left this question still unanswered.

However, the analysis of spatiotemporal distribution of catch rates and reproduction data (see Chapter 2 and Chapter 4) have suggested a southward movement of the stock from October on, from the western central tropical Atlantic towards the southeast Brazilian coast, in order to spawn. After spawning, the sailfish is probably driven northeastward in order to return to the tropical western central tropical Atlantic. Despite of the fact that the tagged sailfish did not show this migration pattern, the rather short monitored time may have prevented that. Besides, it has been known that the capture of sailfish between April and September is atypical off southeast Brazilian coast, evidencing the species exit from this area.

On the other hand, the results of the present work showed evidences that the residence time of sailfish off southeast Brazilian during the spawning season might be extended until at least mid March. Information of conventional tagging also demonstrated a degree of fidelity of sailfish in southeast Brazilian coast during the spawning season peak. One sailfish with a conventional tag was recaptured in the southeast Brazilian coast, close to one year after release and during the spawning period, very close to the tagging site (Amorim *et al.*, 2011).

Despite the number of days and the amount of data obtained in the present work were rather low, this study represents the first observations of vertical and horizontal habitat utilization of sailfish in the southwestern Atlantic Ocean. As more tags are deployed additional information will be generated, helping to better describe the migratory movements of the sailfish stock and their relationship with important events of life cycle, such as spawning season in the Atlantic Ocean. In conclusion, the present results provide information into the biology of sailfish

in the southwestern Atlantic and how vertical distributions during the day and night are influenced by temperature. The diel variability of tagged individuals highlights the need for detailed spatiotemporal studies linking habitat preferences to fisheries data.

Table 5.1 - Summary of depth and temperatures bins used to program the pop-up tags in the present study.

Depth (m)	Temperature (°C)
0- 10	12- 15
10- 15	15- 18
15- 20	18- 20
20- 30	20- 22
30- 40	22- 23
40- 50	23- 24
50- 75	24- 25
75- 100	25- 26
100- 150	26- 27
150- 200	27- 28
200- 250	28- 29
250- 300	29- 30
>300	>30

Table 5.2 – Mean, minimum, maximum temperatures and depths with the respective standard deviation experienced by tagged sailfish during the tracked period by fish and period.

Period	Fish	Mean temperature	Min temperature	Max temperature	Standard Deviation
Day	SAI I	25.06	16.30	27.10	1.85
Night	SAI I	25.34	20.50	27.10	1.48
Transition	SAI I	25.36	21.40	27.70	1.56
Day	SAI II	24.16	14.80	28.00	2.77
Night	SAI II	23.48	11.10	28.60	3.32
Transition	SAI II	23.82	15.00	28.60	2.90
Day	SAI III	24.08	20.10	26.80	1.15
Night	SAI III	23.93	20.20	26.40	1.17
Day	SAI IV	24.37	15.70	26.70	1.95
Night	SAI IV	23.51	12.40	26.80	3.30

Period	Fish	Mean depth	Min depth	Max depth	Standard Deviation
Day	SAI I	21.53	0	120	22.61
Night	SAI I	18.10	0	72	19.49
Transition	SAI I	19.42	0	72	19.17
Day	SAI II	23.72	0	120	21.06
Night	SAI II	29.18	0	376	30.72
Transition	SAI II	26.41	0	160	24.78
Day	SAI III	24.76	0	96	23.11
Night	SAI III	26.33	0	112	23.91
Day	SAI IV	23.33	0	112	23.63
Night	SAI IV	46.11	0	560	79.80

Table 5.3 - Movement parameter estimates for tagged sailfish determined from the Kalman Filter state-space model (KFTRACK). Blank spaces indicate models in which the parameters were set to zero, i.e. have no influence on the model, and were not estimated. u and v are advection parameters in longitude and latitude, respectively; D is all estimated diffusive parameters, bx , by , $bsst$ are the bias estimates for longitude, latitude and SST, respectively; σ_x , σ_y , σ_{sst} are the standard deviations, a_0 is the upper bound for the latitude variance, b_0 is the estimated number of days prior to the equinox (when latitude error is maximal), and $nlogL$ is the loglikelihood function. u and v are expressed in nautical mile (nm) day⁻¹, D in nm² day⁻¹, bx , by , $bsst$, σ_x , σ_y , and σ_{sst} in degrees, and a_0 and b_0 in days.

Parameter	Sailfish I	Sailfish II	Sailfish III	Sailfish IV
u	-1.532895	-0.643155	6.29397	-1.940762
v	-2.989511	-3.502927	-1.404793	-3.291199
D	151.9645	52.60412	305.4362	307.2597
bx				-0.4014846
by	-0.708863	0.397979	3.487166	-0.7284616
sx	0.417905	0.617296	0.32929	0.0245044
sy	1.300476	1.913034	0.42198	0.1475167
$radius$	200	200	200	200
a_0	4.26E-07	3.05E-10	1.07E-07	0.0026796
b_0	80	-0.550274	-80	65.92332
$nlogL$	88.965	181.681	118.746	43.3377

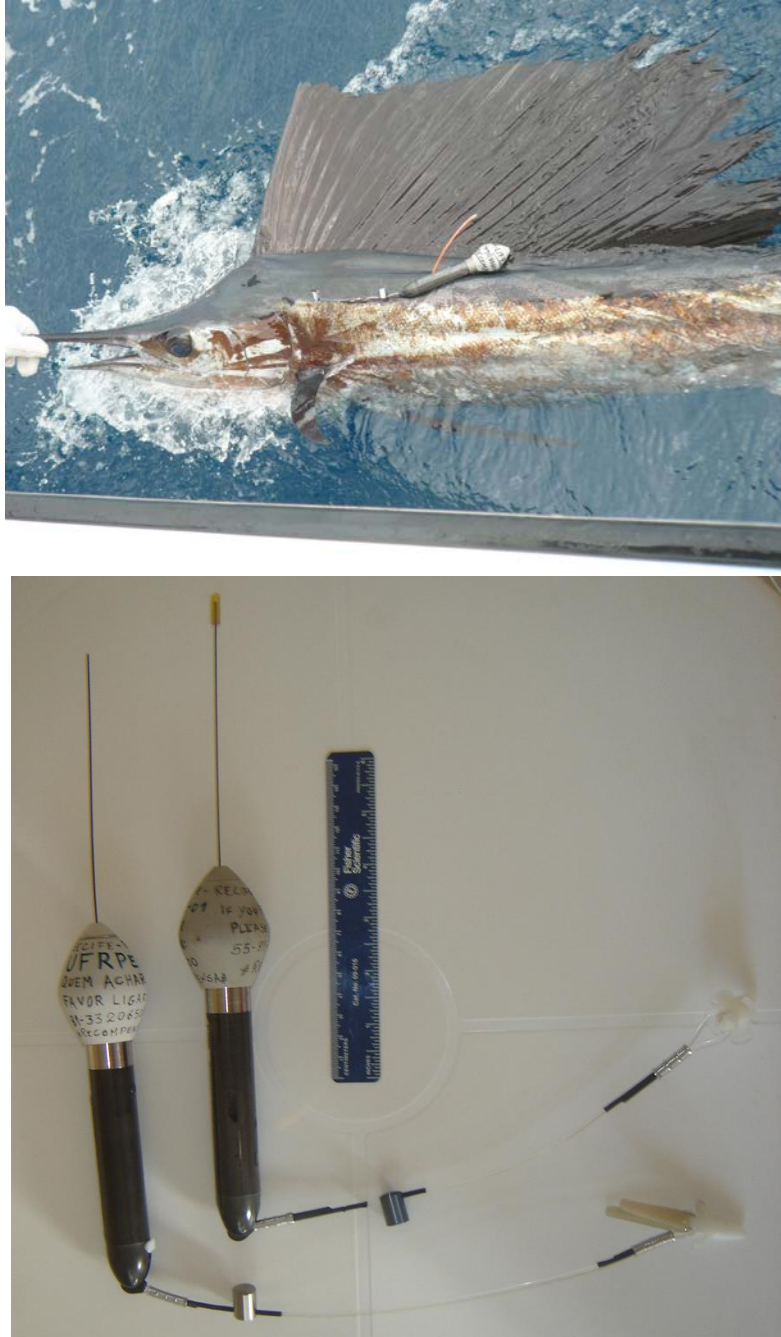


Figure 5.1 - Pop-up Satellite Archival Tag (PSAT), Wildlife Computers Inc (Redmond, WA, USA) MK10 PAT model. Lower panel shows the sailfish II in the moment of tagging.

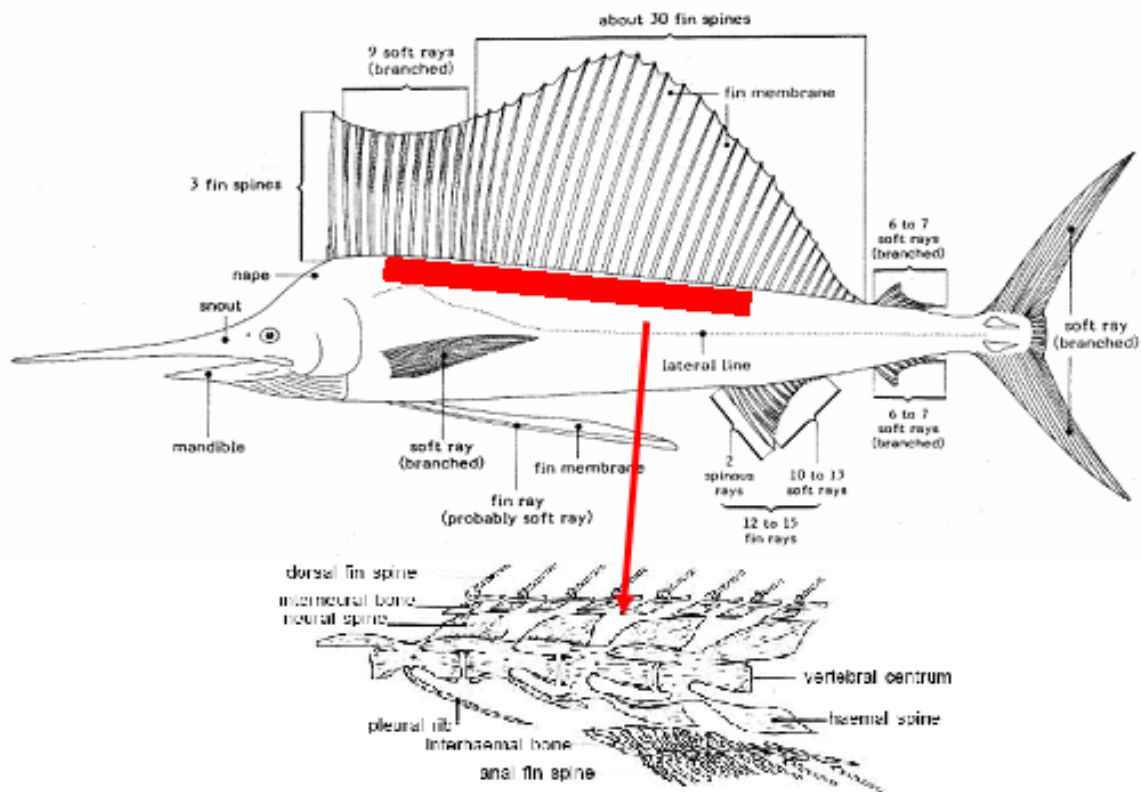


Figure 5.2 - Optimal placement of PSAT taghead in sailfish is shown in red. The area comprises the base of the dorsal fin between spaces of the interneural and neural spines

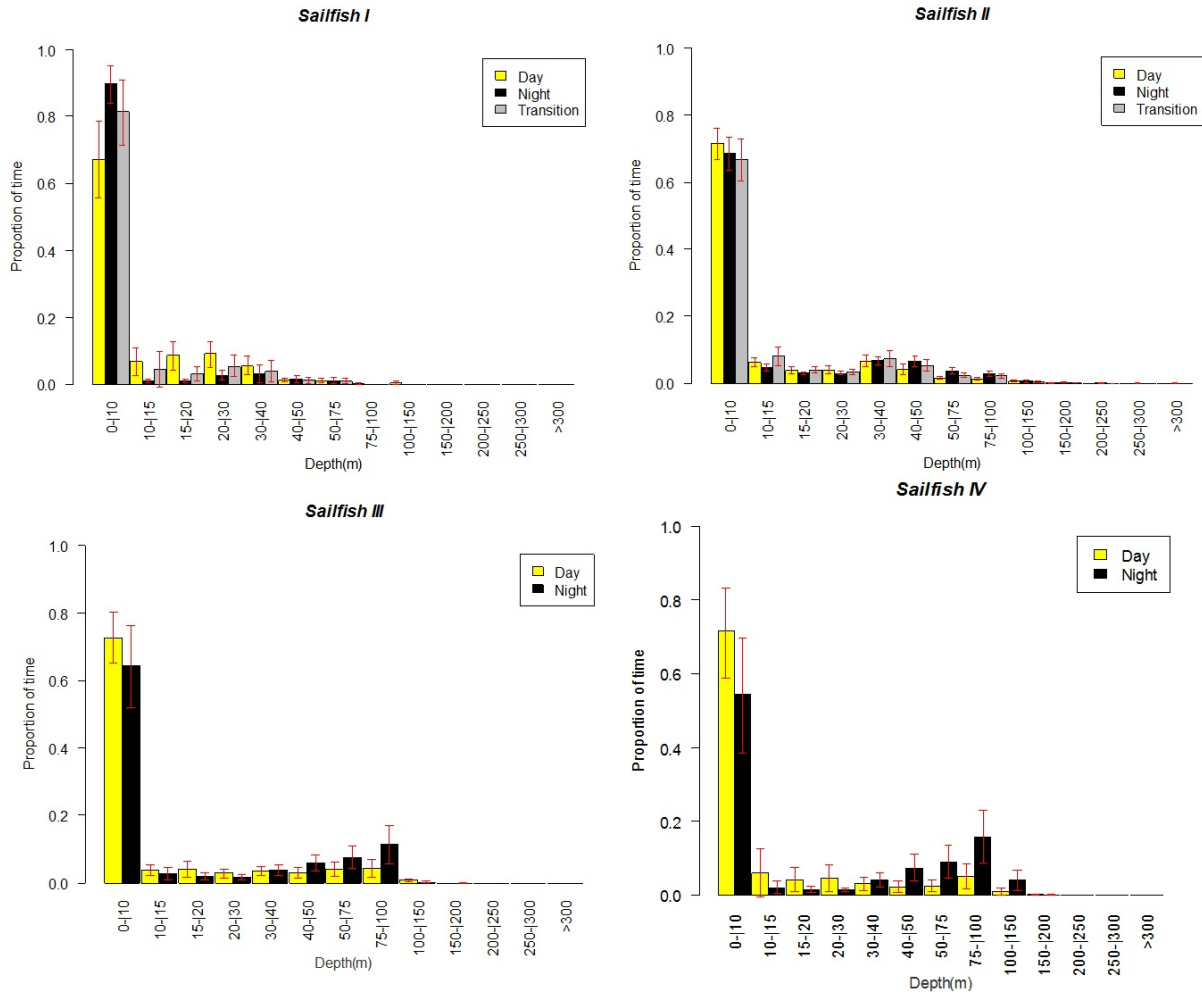


Figure 5.3 - The depth histograms, showing relative frequency of time spent that represent the entire dataset for each fish and period.

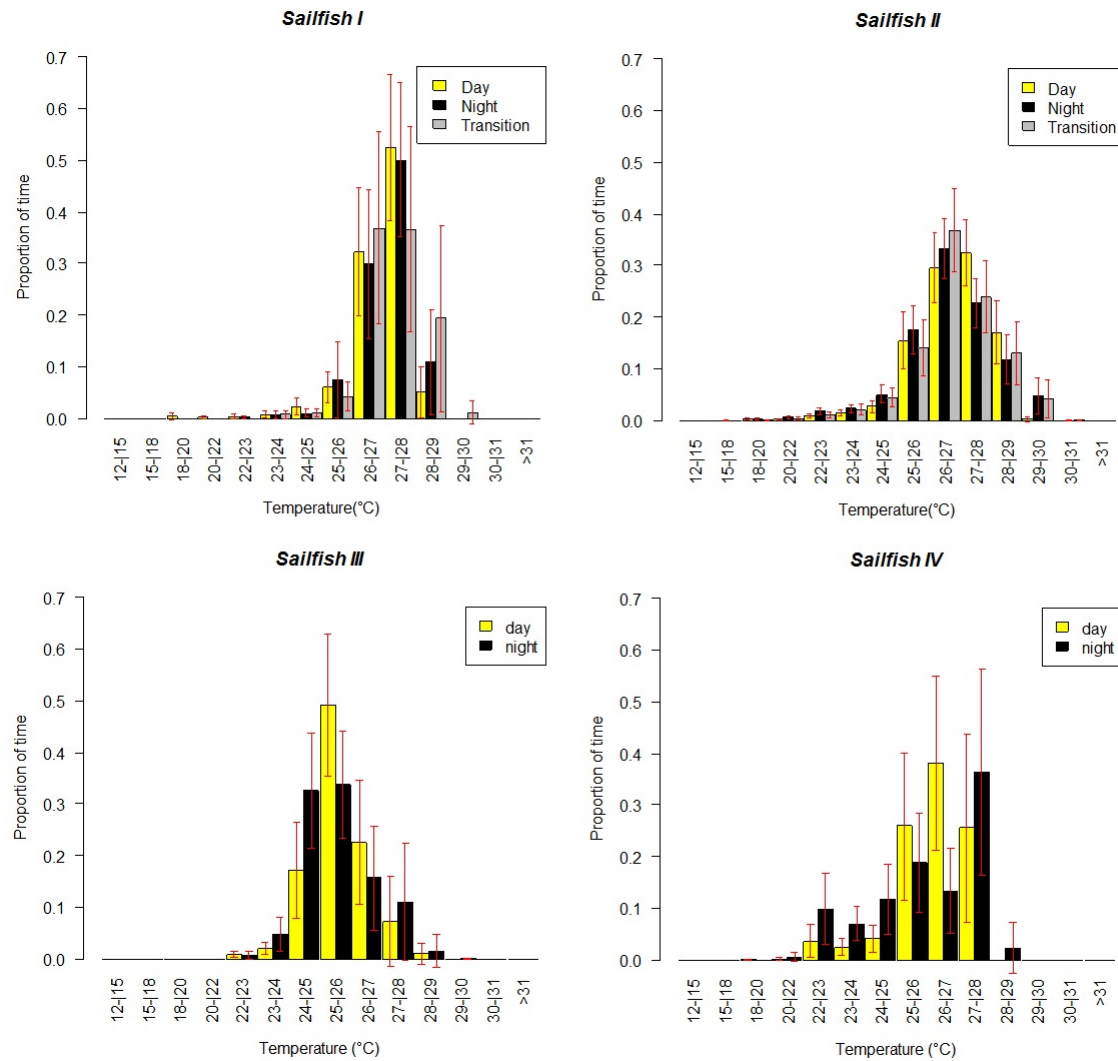


Figure 5.4 - The temperature histograms, showing relative frequency of time spent that represent the entire dataset for each fish and period.

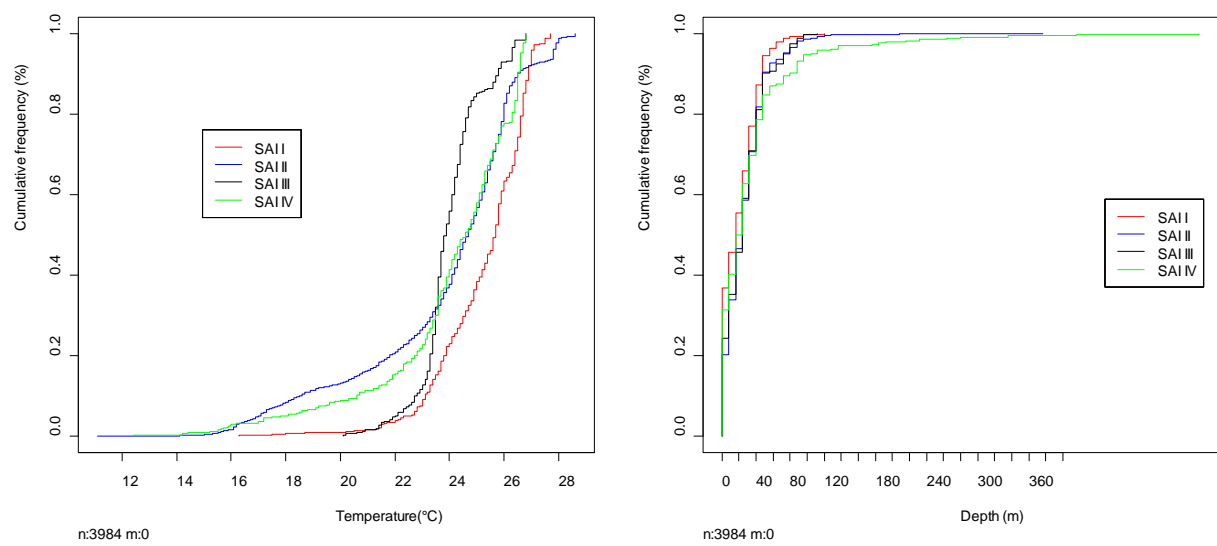


Figure 5.5 - Cumulative frequency at depth (right) and temperature (left) for each sailfish.

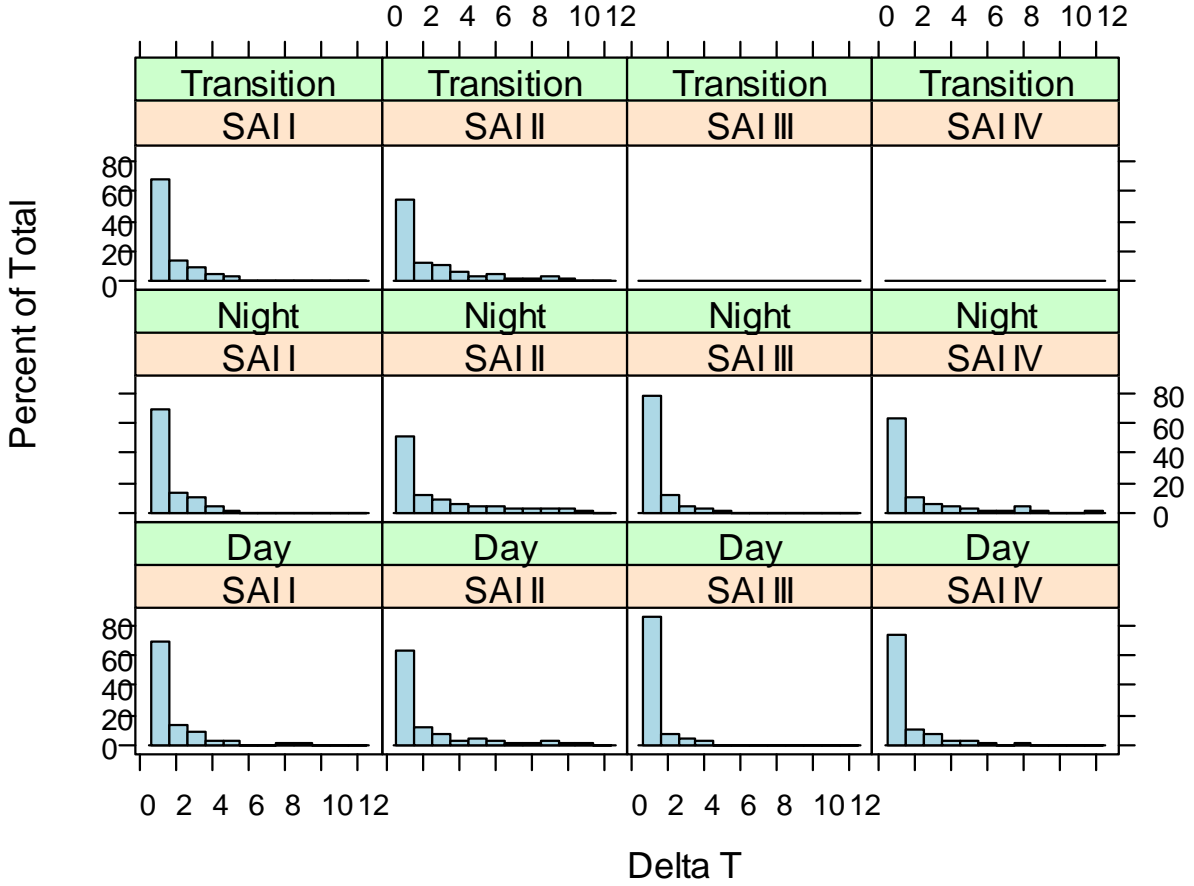


Figure 5.6 - Proportions of time spent by Delta T relative to the surface temperature for each fish and period.

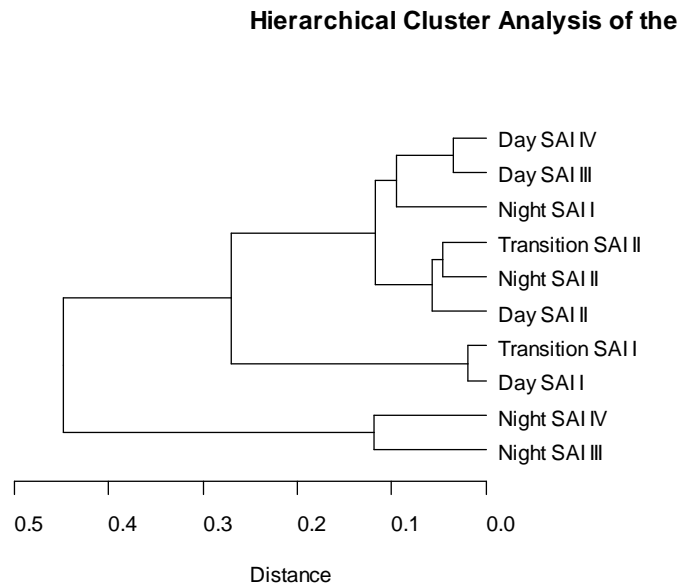
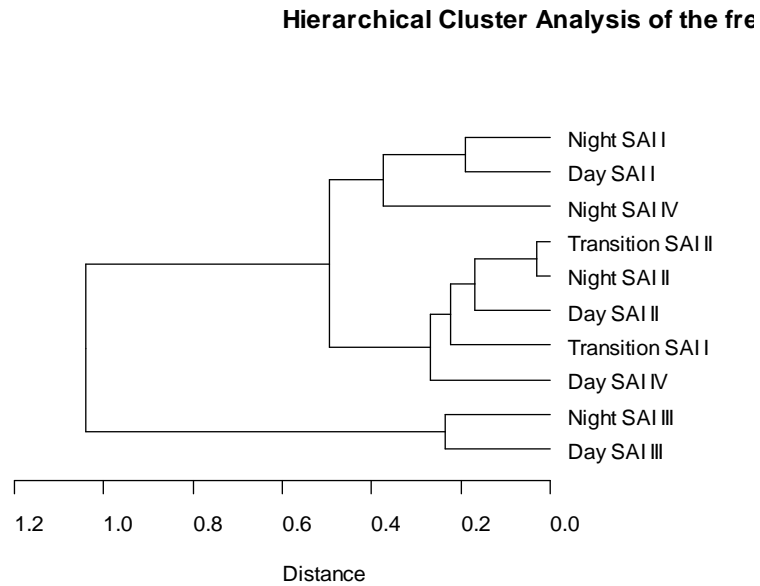


Figure 5.7 - Cluster analysis of the frequency distributions of the proportion of time at depth and temperature for each fish and period.

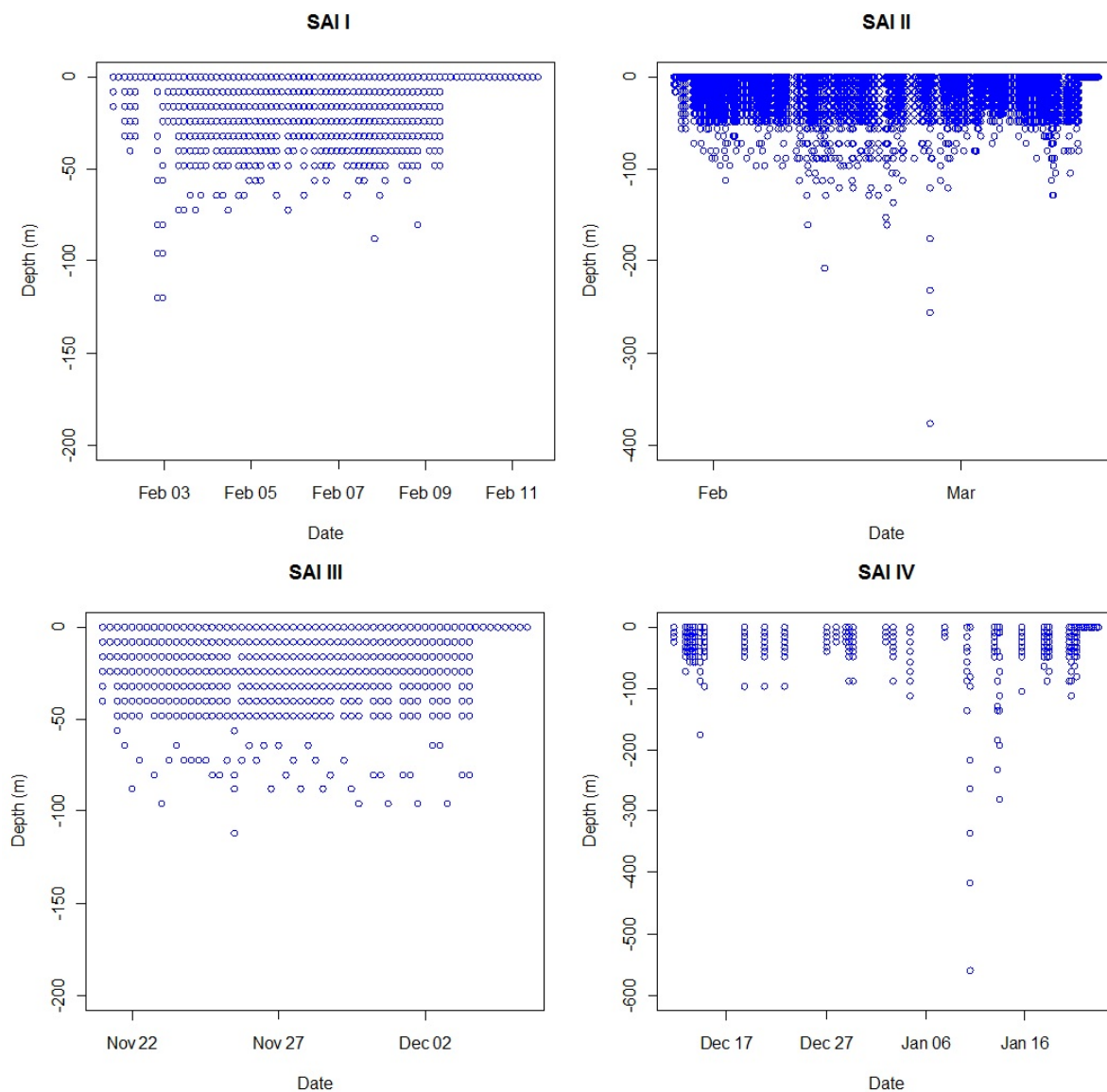


Figure 5.8 - Depth records by 3 h (sailfish I and II) and 6 h (sailfish III e IV) during the tracked period for each sailfish.

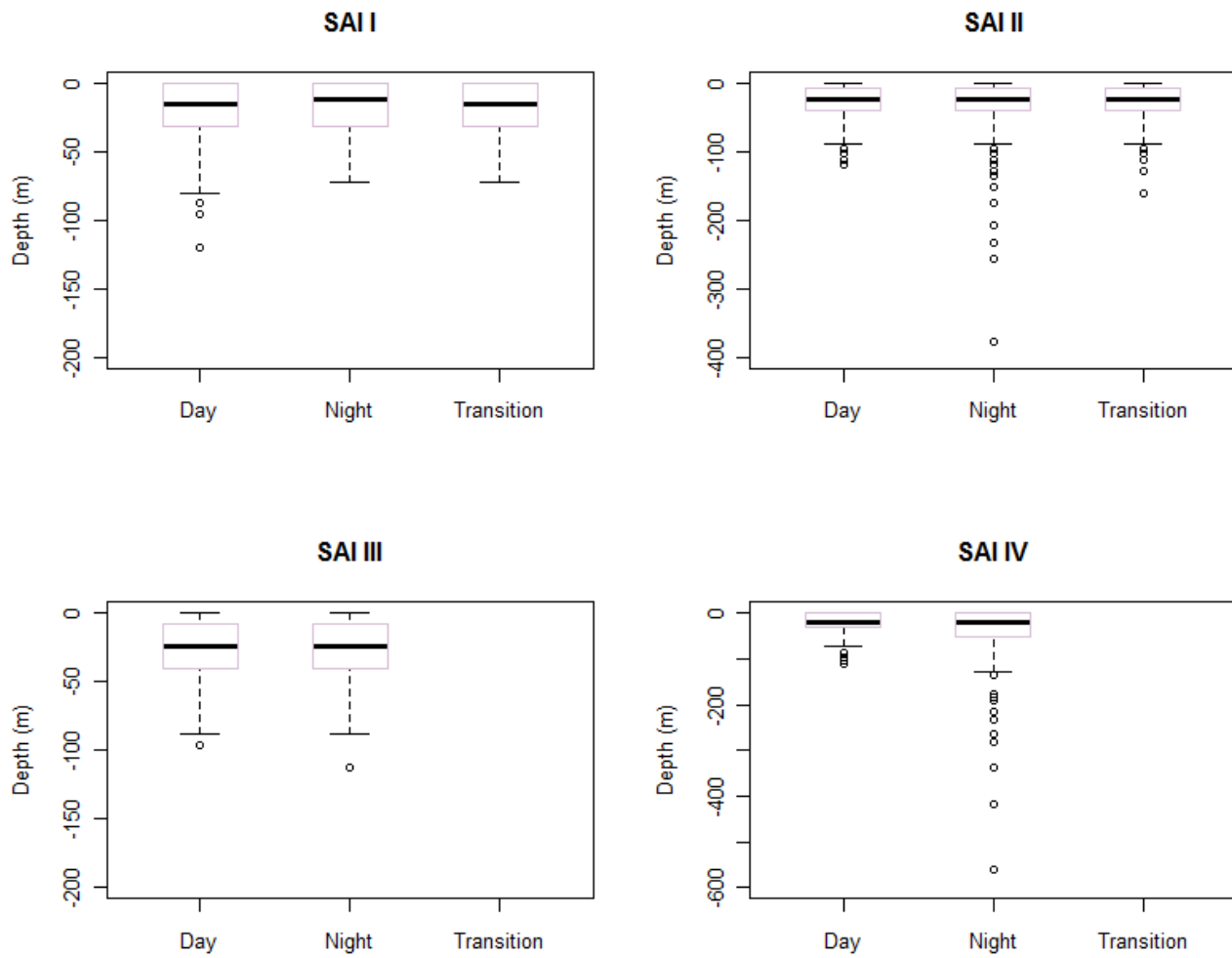


Figure 5.9 - Depth records by period during the tracked period for each sailfish.

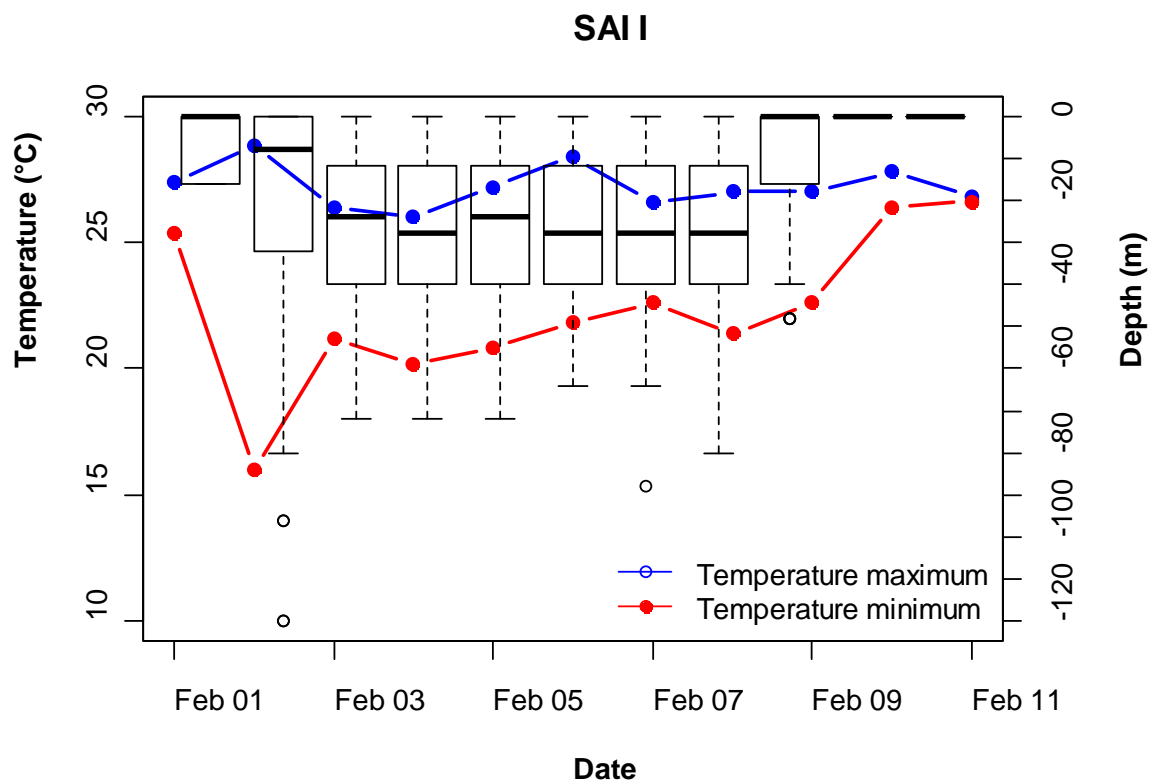


Figure 5.10 - Minimum and maximum daily temperature and depth experienced by sailfish

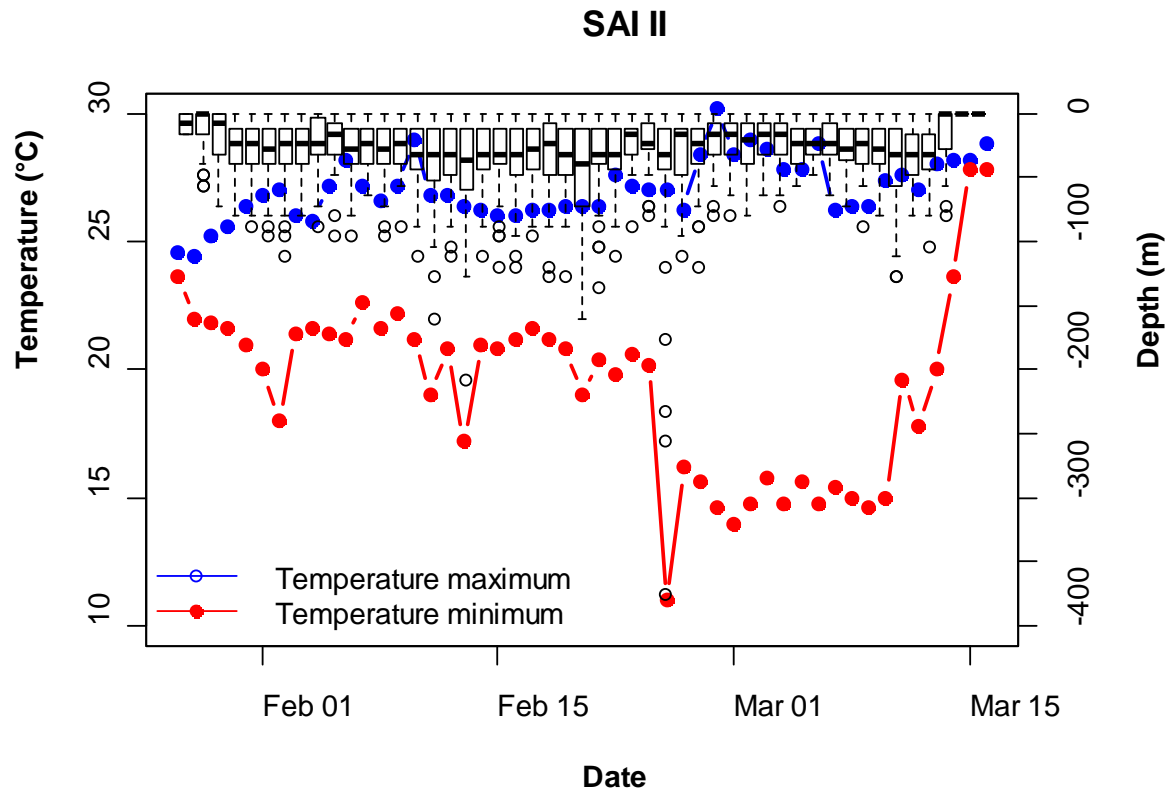


Figure 5.11 - Minimum and maximum daily temperature and depth experienced by sailfish II

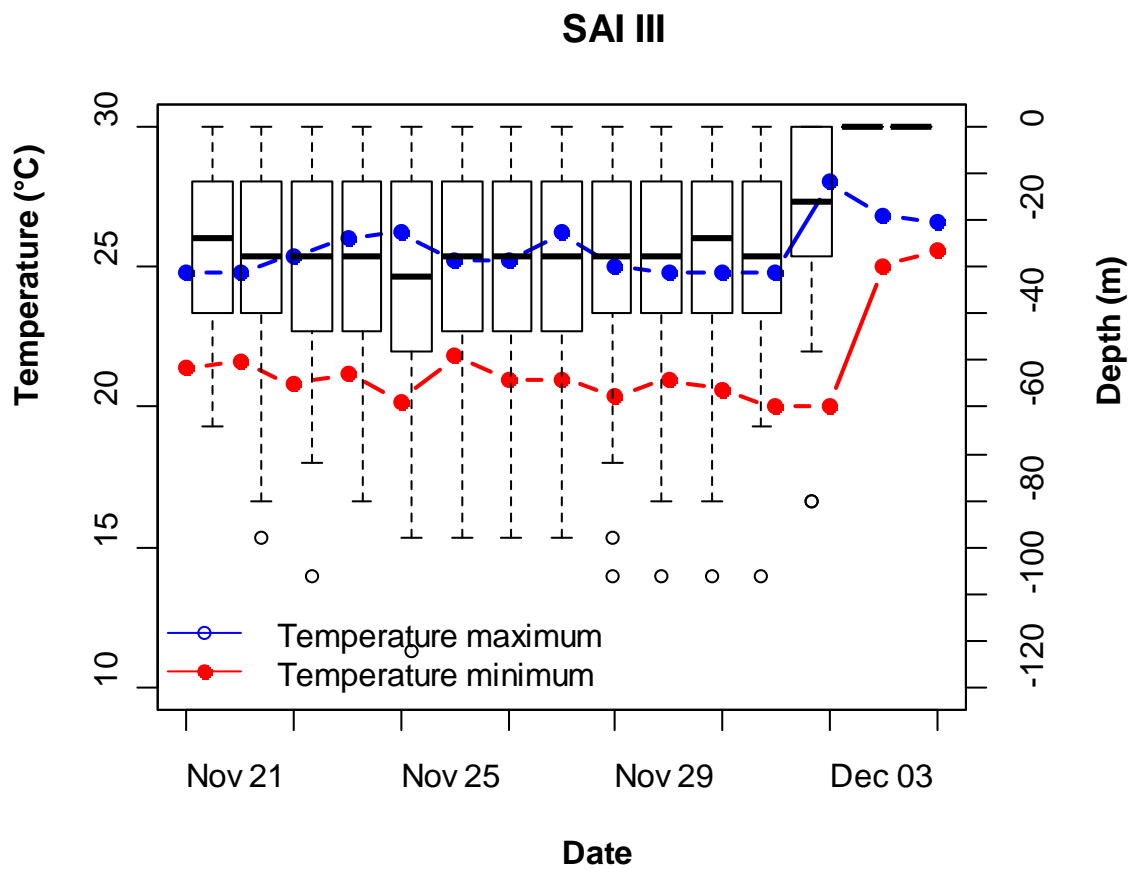


Figure 5.12 - Minimum and maximum daily temperature and depth experienced by sailfish III

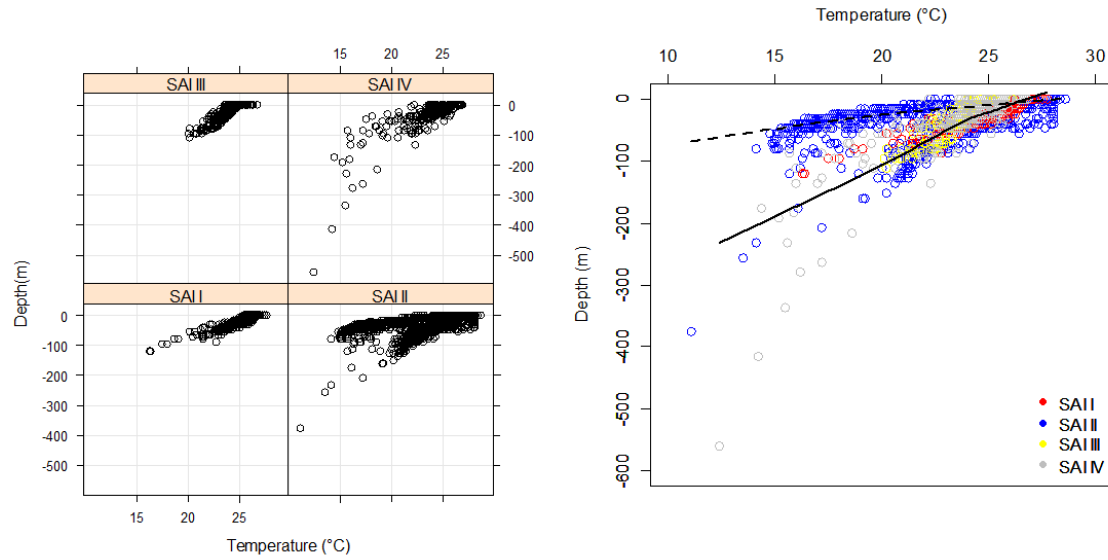


Figure 5.13 - Depth and temperature profiles experienced by tracked sailfish. Left panel shows the profiles for each fish separately and right panel shows all records pooled together.

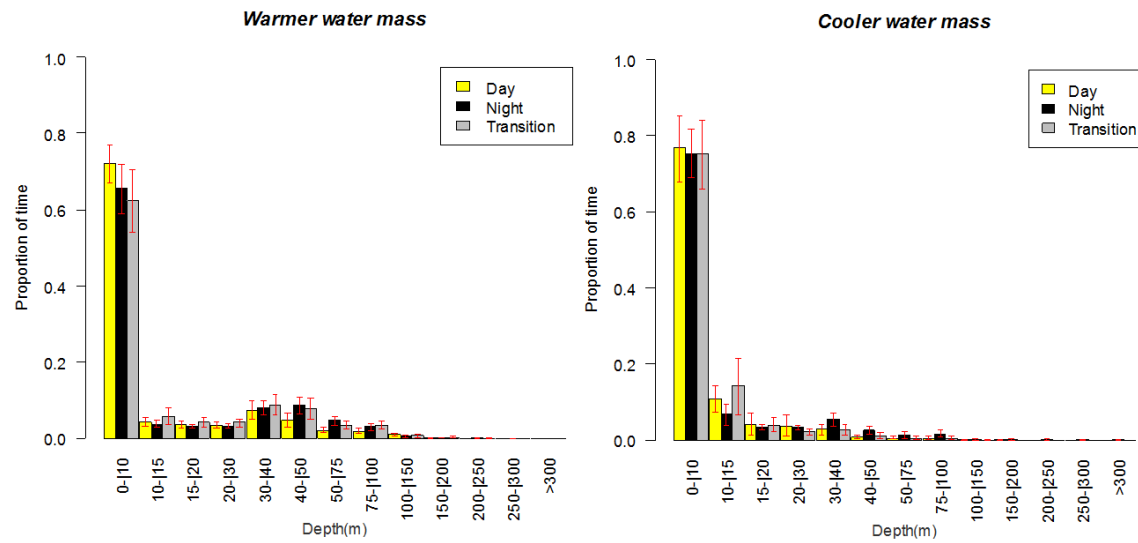


Figure 5.14 - The depth histograms, showing relative frequency of time spent that represent the entire dataset for each fish and period.

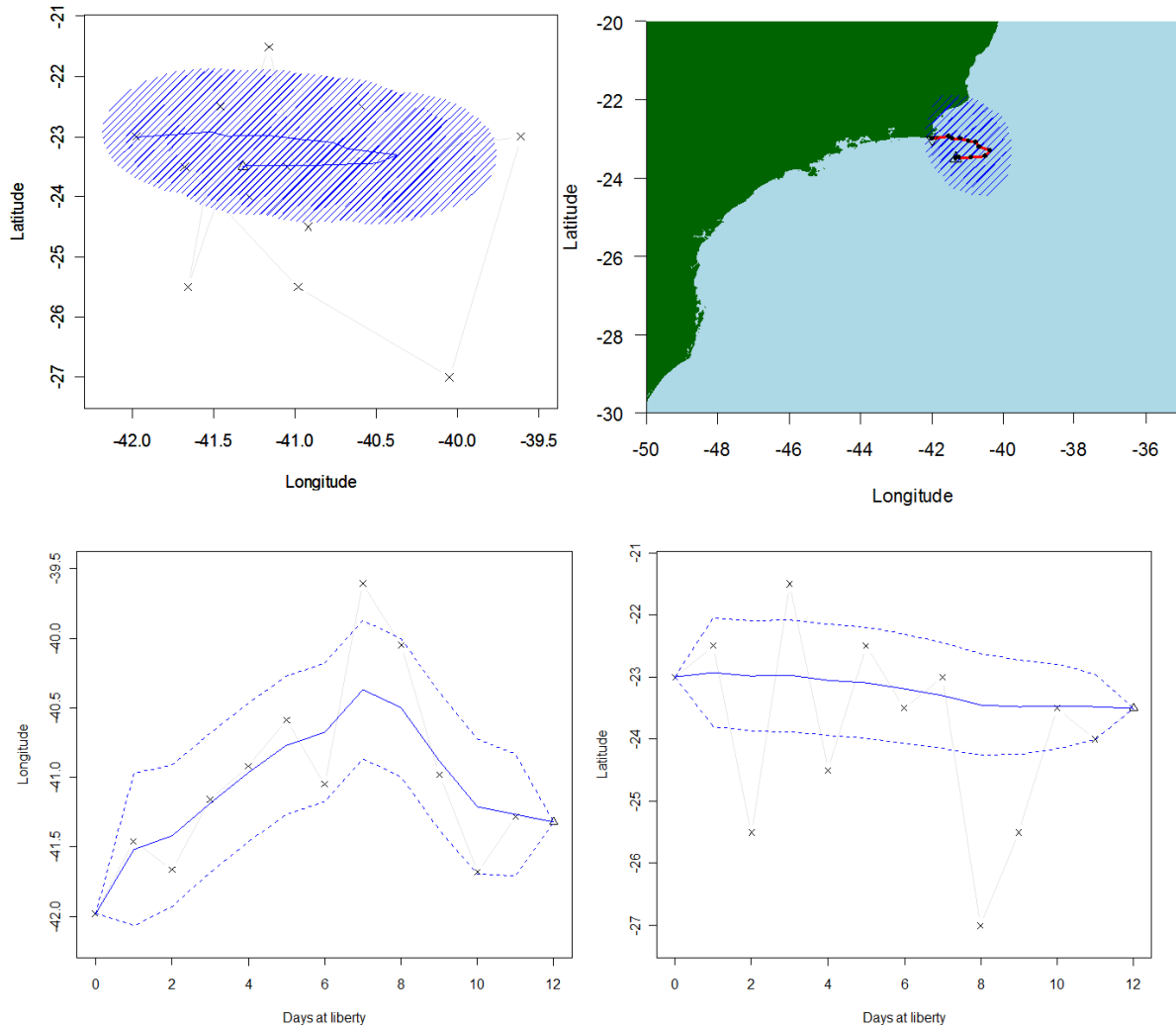


Figure 5.15 - Most-probable track for sailfish I (upper right) fitted with (red line) Kalman Filter State-Space Model. The upper left panel shows a comparison between the raw gelocation marked by crosses and fitted track. Shaded blue are represents the confidence interval of the estimates. The lower panels show how well the model fits the two different information sources (longitude-left, latitude-right). Blue and dashed line represents the fitted track and the confidence intervals, respectively. Deployment point is marked by '▲', and known recapture/pop-up position is marked by '▼'.

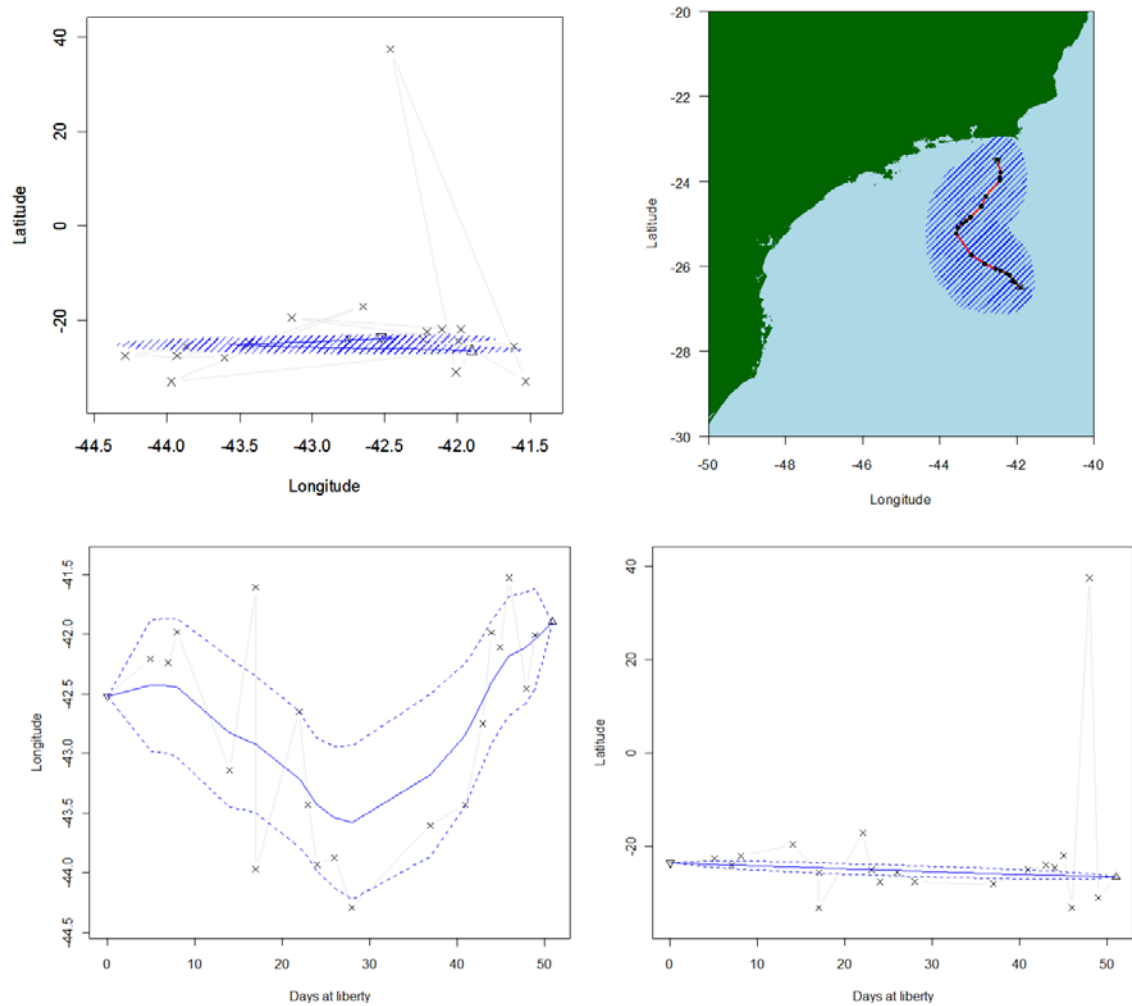


Figure 5.16 - Most-probable track for sailfish II (upper right) fitted with (red line) Kalman Filter State-Space Model. The upper left panel shows a comparison between the raw relocation marked by crosses and fitted track. Shaded blue are represents the confidence interval of the estimates. The lower panels show how well the model fits the two different information sources (longitude-left, latitude-right). Blue and dashed line represents the fitted track and the confidence intervals, respectively. Deployment point is marked by ‘▲’, and known recapture/pop-up position is marked by ‘▼’.

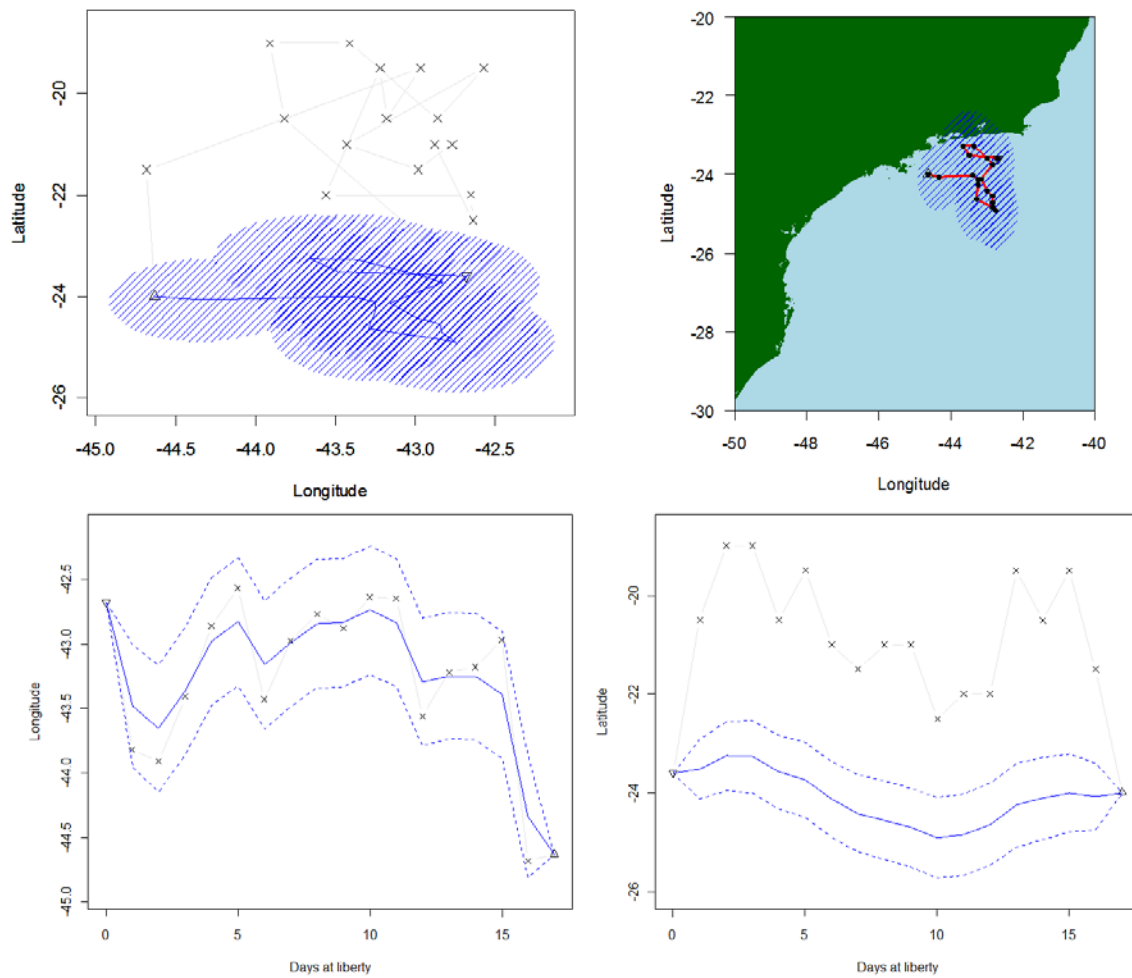


Figure 5.17 - Most-probable track for sailfish III (upper right) fitted with (red line) Kalman Filter State-Space Model. The upper left panel shows a comparison between the raw gelocation marked by crosses and fitted track. Shaded blue are represents the confidence interval of the estimates. The lower panels show how well the model fits the two different information sources (longitude-left, latitude-right). Blue and dashed line represents the fitted track and the confidence intervals, respectively. Deployment point is marked by ‘▲’, and known recapture/pop-up position is marked by ‘▼’.

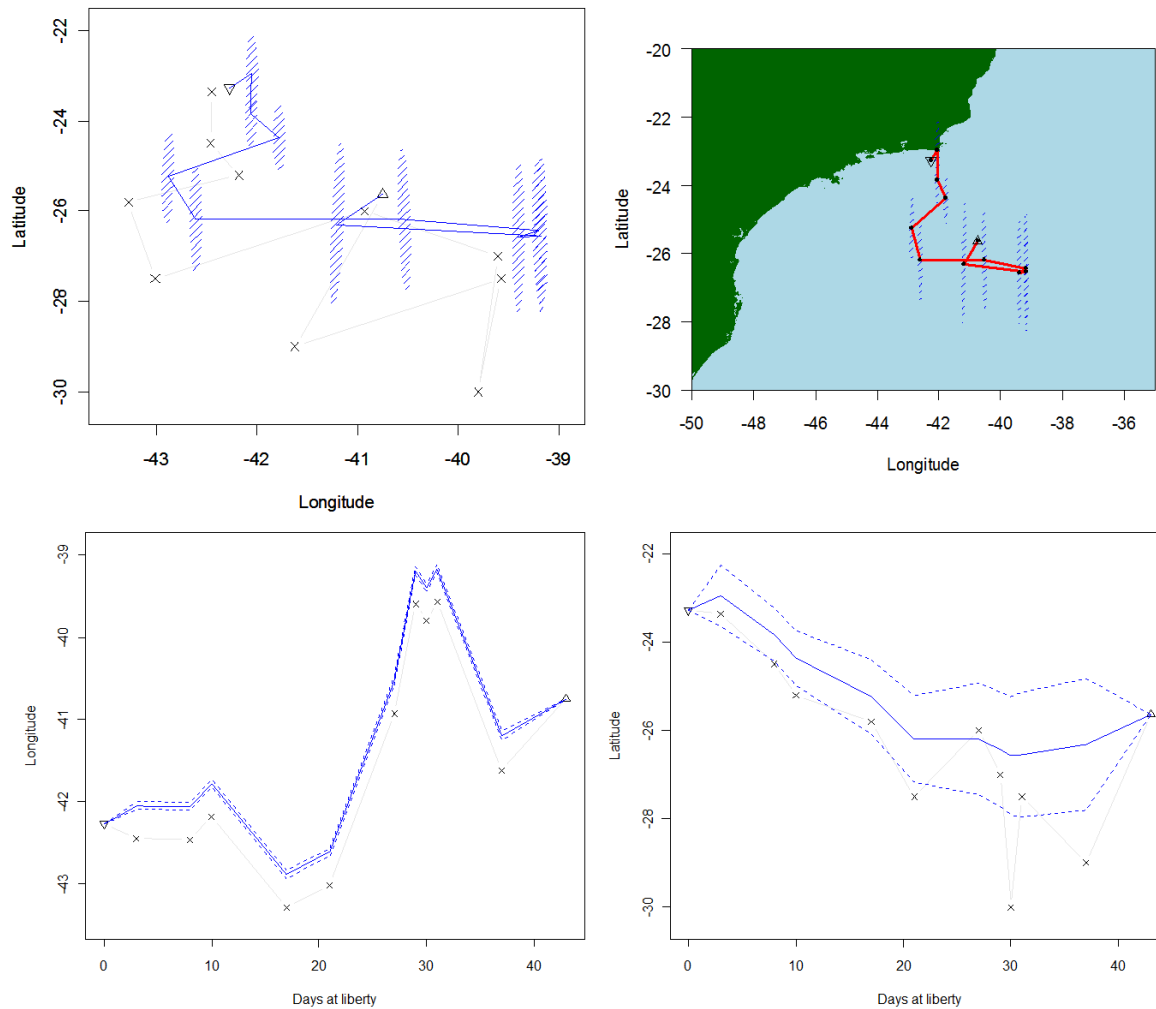


Figure 5.18 - Most-probable track for sailfish IV (upper right) fitted with (red line) Kalman Filter State-Space Model. The upper left panel shows a comparison between the raw gelocation marked by crosses and fitted track. Shaded blue are represents the confidence interval of the estimates. The lower panels show how well the model fits the two different information sources (longitude-left, latitude-right). Blue and dashed line represents the fitted track and the confidence intervals, respectively. Deployment point is marked by '▲', and known recapture/pop-up position is marked by '▼'.

Chapter 6 - Catch rates of Atlantic sailfish caught by sport fishery in southern Brazil

Abstract

In the present study, a generalized linear model (GLM), assuming a negative binomial distribution and log as link function, was used to generate a standardized CPUE series for the sailfish caught by recreational fishing boats based in São Paulo and Rio de Janeiro States, off southern Brazil, from 1996 to 2008. The response variable was the number of sailfish caught per number of boats registered in the tournament per day. The following factors were tested in the analyses: “year”, “month”, “target” and “state”, representing the main effects of the explanatory variables. Fishing effort is an *offset* term. The factor “area” was not significant and no interactions were included in the final model. The factor “month” explained the largest amount of variation, followed by “year” and “target”. The proportion of the deviance explained by the model was about 0.35 (pseudo- R^2). The diagnostic plots revealed that the model residuals are homoscedastic and model seems to be not biased. Residuals are approximately normally distributed. Discrepancies between residual and standard normal distributions are small and appear only in the tails. Therefore, both negative binomial error distribution and link functions seemed to be acceptable. The overall pattern of the standardized catch rate indicates a relatively stable trend with a slight decline throughout the whole period. Despite these results conform with previous findings, there were some discrepancies with previous standardization of sailfish catch rate in the southwestern Atlantic. This could be explained by the differences in the standardization procedures, or even because the data sets are from different fleets.

6.1. Introduction

Billfish sport fishing tournaments have a long history in Brazil. Since 1956, this activity has been promoted mainly in the States of São Paulo and Rio de Janeiro, southeast Brazil. Nowadays, however, fishing tournaments are held along the entire Brazilian coast, although they are still largely concentrated off the coast of Cabo Frio, in Rio de Janeiro, in Ilhabela, in São Paulo, and in Vitória, in Espírito Santo. The fishing season happens mainly from

October to February (spring/summer), with the blue marlin (*Makaira nigricans*), the white marlin (*Kajika albida*) and the sailfish (*Istiophorus platypterus*) being the main targeted species.

Catch and effort data from sport fisheries are an important source of information on trends of fish stocks. Time series of catch rate have been frequently used in stock assessments for large pelagic fishes, as an index of relative abundance. Such application, however, has been widely debated (Maunder and Punt, 2004), since trends in catch rate can be influenced by many factors in addition to stock abundance, including the fishing season, spatial variability of the fish stock, target species as response to changes in fishing gear, environmental conditions and fishermen's experience. Such variations may lead to significant changes in catchability, introducing serious errors in the estimation of abundance indices (Fréon and Misund, 1999). To overcome this problem, the most common approach has been to standardize the catch rate, in order to remove the effects of other factors unrelated to stock abundance (Maunder and Punt, 2004). This approach has been used widely in fisheries science, having become a crucial step for accurate stock assessments (Gulland, 1983; Maunder and Punt, 2004).

In the Brazilian sport fishery, a number of changes in fishing grounds and target species, among others, which directly affect the catch composition, have been well documented (Arfelli *et al.*, 1994; Amorim and Arfelli, 2001; Amorim and Silva, 2005). Thus, the use of nominal catch rates derived from this fishery as an index of relative abundance can lead to interpretation errors, making its utilization rather complex. Hence, in the present chapter a nominal catch rate series of sailfish caught by the sport fishery in southern Brazil (1996-2008) is presented with the corresponding standardized values, for identification of the main factors of influence.

6.2. Material and Methods

6.2.1. Catch and effort data

Radio logbook records from recreational tournaments of Yacht Clubs from São Paulo and Rio de Janeiro have been collected since 1996 by voluntary submission of the tournament organizers and by onboard observers. The data set included a total of 94 tournament days, from 1996 to 2008. Records for each tournament day included boat names, total number of operating boats per tournament day, total number of fish hooked, and their fate (i.e. lost,

released, tagged and released, or boarded), by species, as well as the size and weight of all boarded fish.

6.2.2. *Modeling*

The number of sailfish caught per number of boats recorded in the tournament per day (C) was considered as a relative index of abundance. The logarithm was used as a link function, in the following GLM model:

$$y \equiv \log(C)$$

$$\mu \sim \text{year} + \text{month} + \text{target} + \text{State} + \text{interactions} + \text{offset}(\log[\text{fishing effort}]) + \varepsilon$$

where the terms “year”, “month”, “target” and “state” represent the main effects of the explanatory variables, while “interactions” stands for the first order interaction between all main effects. Fishing effort is an offset term and ε is an independent identically distributed (i.i.d) random variable with a negative binomial distribution. Despite the relatively low zero-count (~30%, Figure 6.1), the empirical distribution of C data was still too zero-inflated and over-dispersed to fit a traditional Poisson distribution (Figure 6.2). The negative binomial distribution, however, seemed to accommodate the data well (Figure 6.3) and was, for this reason, chosen to fit the models, using statistical software R 2.12.0 (R Development Core Team, 2010).

The factor “year” included data from 1996 to 2008, while “month” included only data from October to February, since there is no tournament out of this period. The factor “target” was based in the target fish set for each tournament, including blue marlin or sailfish. The factor “State” accounted for the tournaments carried out off São Paulo or Rio de Janeiro coasts, in two different fishing areas about 90 miles from coast, as follows: A: 23° to 24°S/41° to 42°W, for Rio de Janeiro; and B: 24° to 25°S/44° to 45°W, for São Paulo (Figure 6.4).

The selection of predictors or interactions and the decision on their entry or exclusion was based on Akaike Information Criterion (AIC) (Akaike, 1978) and the total deviance explained. Chi-square tests were also computed to determine whether terms yielded significant ($p < 0.05$) reductions in the residual deviance upon entry into the GLM. Finally the residual distribution was checked in order to evaluate the goodness of fitted model. The estimates of standardized catch rate were based on the predictions obtained for each year, fixing

the level of remaining factors at the level with the highest number of observations. The standard errors of estimates were also presented.

6.3. Results

6.3.1. Exploratory analysis

The fishing effort (calculated as number of tournament days monitored) ranged from 2, in 2006 to 11 in 2003 while the total catch including all species (marlins, tunas and other teleosts) reached from 20 in 2006 to 290 in 2007 (Figure 6.5). In general, the total catch, as expected, followed the variation of fishing effort (Figure 6.5). The sailfish was the most caught species during the whole period, representing 75% of the total catch, followed by blue marlin with 18% while tunas (*Thunnus* spp.) and white marlin had a small relative participation on the total catch (7%) (Figure 6.6).

The catch composition of the main species caught in the tournaments also varied with year (Figure 6.7). The sailfish was the most caught species in almost all years, except for 1998, when the blue marlin dominated the catches (Figure 6.7). Other species were also caught in much less numbers, including the white marlin and tunas (Figure 6.6 and Figure 6.7).

The means of sailfish nominal catch rate for each level of the factors are presented in Figure 6.8. The mean nominal catch rate was much larger for 2004, 2006 and 2007, with the lowest values being observed in the rest of the years. The monthly catch rate was much higher for December and January than in other months (Figure 6.8). Expectedly, the sailfish catch rate was usually higher when it was the main target of the tournament. The catch rate in Rio de Janeiro was always higher than in São Paulo (Figure 6.8).

6.3.2. Standardization of catch rate

Table 6.1 shows the deviance analysis of the selected model. The factor “area” was not significant and no interactions were included in the final model. The factor “month” explained the largest amount of variation, followed by “year” and “target”. The proportion of the deviance explained by the model is about 0.35 (pseudo- R^2). Estimations of the coefficients are in Table 6.2. Only coefficients for the years 1998 and 2000 were positive. Most the coefficients estimated for the factor “Year” were not significant though most of standard errors were bigger

than the coefficients estimated. All estimations for “Month” were negative (except December) and most of them were significant. Residual partial plots for all main factors seem to be well distributed around zero (Figure 6.9). December and January were the most productive period for fishing sailfish. As expected, higher catch rates were observed when the sailfish was the target species of the tournament (Figure 6.9).

The diagnostic plots revealed that the model residuals are homoscedastic and approximately normally distributed (Figure 6.10). Discrepancies between residual and standard normal distributions are small and appear only in the tails (Figure 6.10). Therefore both the negative binomial error distribution and the link functions seem to conform well to the data.

The standardized catch rates and the standard error estimations (Figure 6.11) show that the standard errors of estimates were relatively small, with the great majority being smaller than the year coefficient estimations. The overall pattern of the standardized catch rate indicates a relatively stable trend with a slightly decline throughout the whole period (Figure 6.11). The nominal catch rate, in turn, showed a different trend, with an apparent increase in values after 2002, with one pronounced peak in 2004 (Figure 6.11).

6.4. Discussion

Assuming that catch rates are proportional to the actual stock abundance implies the acceptance of several assumptions related to the variation of the catchability coefficient. However, there are several limitations in this approach. Such constraints are particularly complex in the case of non-target species, such as billfishes in the pelagic longline fishery, which is characterized for high percentage of zero observations combined with few large catch values due to school aggregation, since some Istiophorid billfishes, like sailfish, often form schools in specific locations (Nakamura, 1985). Catch and effort data from sport fishery tournaments, therefore, may be a better alternative to estimate billfish catch rates.

Comparatively, the present data set had an amount of zero-valued observations much lower (30%) than the commercial longline fishing (~75%, see Chapter 4), although, it was still zero-inflated and left-skewed distribution to account with problems of overdispersion, when the ratio of the residual deviance and the degrees of freedom is much higher than 1 (Zuur *et al.*, 2009). In the previous exploratory analysis, different statistical probability distributions that are

able to accommodate a high percentage of zero observations (i.e. Poisson and Tweedie) were tested. However, the negative binomial distribution appeared to be the best option to analyze the sailfish catch rate, with no evidence of overdispersion and the most satisfactory residuals distribution.

In general, the trend of partial residuals estimated for each covariate followed the signal of nominal catch rate mean values. For the season effect (i.e. month), December and January were the most productive fishing period. In fact, sailfish catch rates are highly seasonal, since it is very likely that mature sailfish migrate from the western central tropical Atlantic towards the southeast Brazilian coast to spawn and remain in the area from about February to March. After spawning, sailfish probably depart in a north-east direction to return to the tropical western central tropical Atlantic (see Chapter 2 and Chapter 4). Regarding the target species effect, when the sailfish is the target, the yacht speed is less than when the boats are targeting blue marlins. The bait type also changes, depending on the species targeted, with a preference for dead, natural bait when the sailfish is targeted and artificial baits when the target species is the blue marlin.

The final estimations of year effect showed that most of the estimated standard errors are not larger than the coefficient estimations; hence we assumed the results are useful to evaluate the sailfish recreational fisheries status off the Brazilian coast. If the standardized catch rates are assumed to reflect well the local relative abundance of the stock, the results suggest that the biomass of sailfish caught in southwestern Atlantic have suffered a very slight decline along the studied years. Amorim *et al.* (2006) also reported catch rate indices calculated for sailfish caught by tournaments of recreational fishery carried out in São Paulo State and found a similar trend of standardized CPUE, which seemed to oscillate around a rather stable level, from 1996 to 2004. Wor *et al.* (2010) analyzed catch and effort data from Brazilian longline fleet and demonstrated a similar trend with a moderate decline between 1978 and 2008. Ortiz and Arocha (2004), in turn, reported a stable trend for sailfish caught by Venezuelan longline fleet in the Caribbean and the Gulf of Mexico.

Table 6.1 - Deviance analysis of the fitted model for the standardization of sailfish catch rate caught by the Brazilian sport fishery in the Atlantic Ocean from 1996 to 2008. Resid. df: residual degrees of freedom; df: degrees of freedom; Resid. Dev.: Residual deviance and; P(>|Chi|): Chi-square test p value.

	Df	Deviance	Resid.Df	Resid. Dev.	P(> Chi)	% of total deviance
NULL			93	159.64		
+ Month	4	42.997	89	116.65	1.04E-08	77%
+ Year	12	7.154	77	109.49	0.84730	13%
+ Target	1	5.909	76	103.58	0.01506	10%

Table 6.2 - Estimations of coefficients, standard errors (SE), t-statistic and P-value of the t-test.

	Estimate	Std. Error	z value	Pr(> z)
(Intercept)	-1.0878	0.70374	-1.546	0.12217
month2	-1.3269	0.59424	-2.233	0.02555
month10	-1.8933	0.67874	-2.789	0.00528
month11	-0.4645	0.54878	-0.846	0.39728
month12	0.78918	0.45656	1.729	0.08390
year1997	-0.1663	0.72615	-0.229	0.81889
year1998	0.04181	0.80131	0.052	0.95839
year1999	-1.408	0.83313	-1.69	0.09102
year2000	0.07085	0.69501	0.102	0.91881
year2001	-0.2702	0.72083	-0.375	0.70779
year2002	-0.4487	0.71521	-0.627	0.53044
year2003	-0.5677	0.7122	-0.797	0.42538
year2004	-0.5172	0.82359	-0.628	0.53002
year2005	-1.0861	0.84922	-1.279	0.20092
year2006	-1.083	1.11706	-0.97	0.33229
year2007	0.24061	0.76737	0.314	0.75386
year2008	-0.7378	0.83159	-0.887	0.37494
Targetsai	1.38235	0.43456	3.181	0.00147

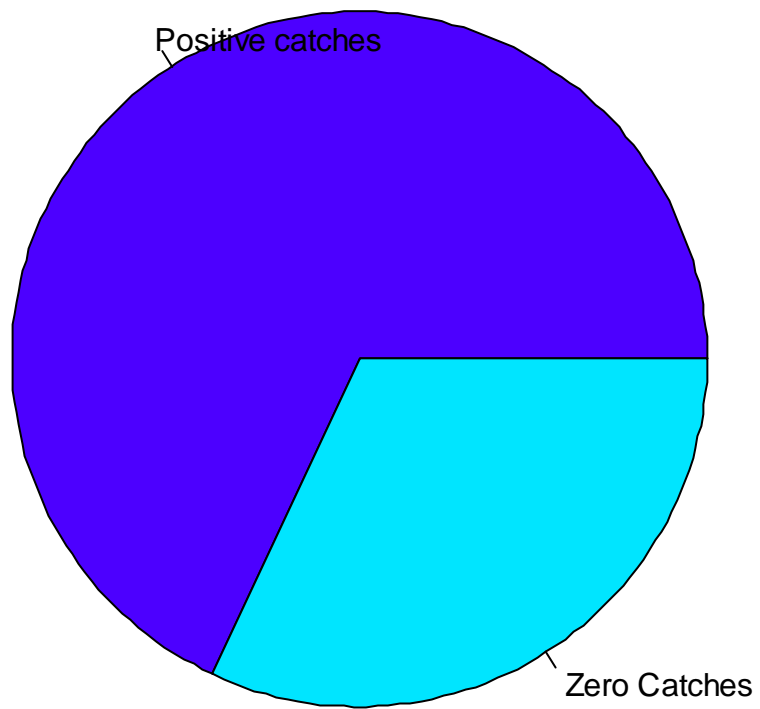


Figure 6.1 - Proportion of positive catch for sailfish in the Brazilian sport fishery in the Atlantic Ocean from 1996 to 2008.

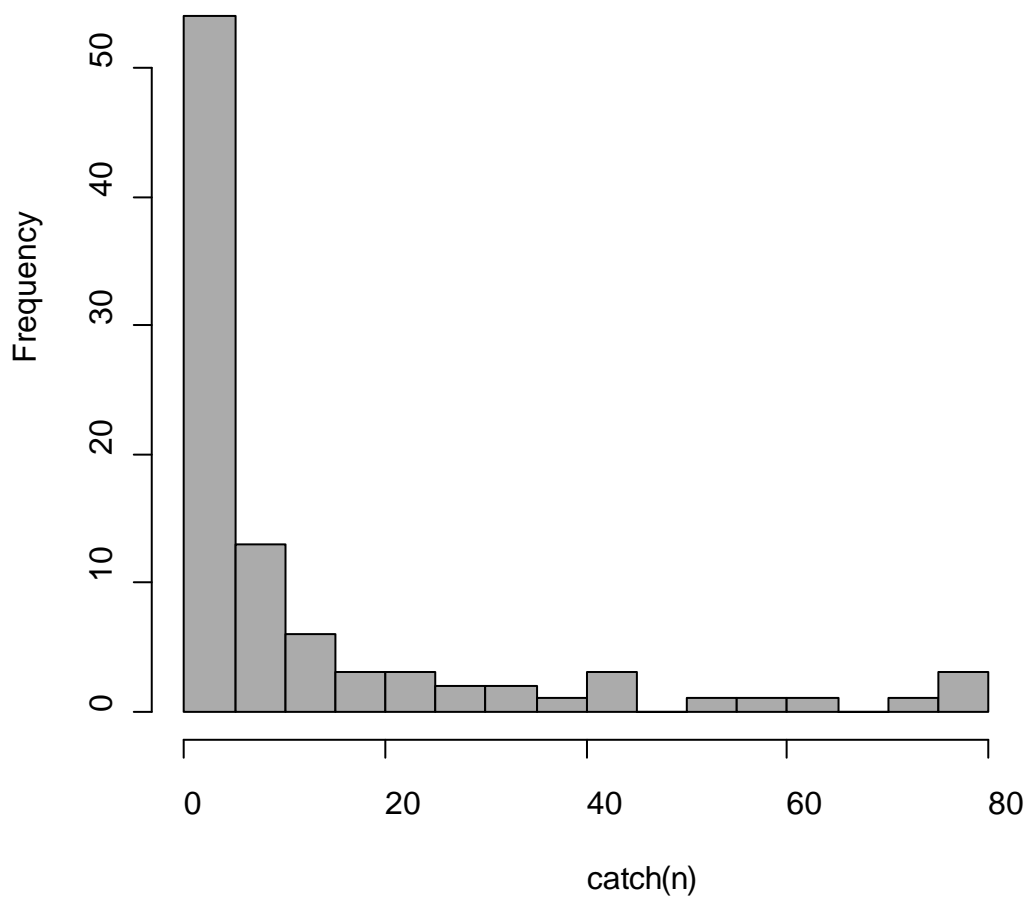


Figure 6.2 - Sailfish catch per number of boats registered per tournament day for the Brazilian sport fishery in the Atlantic Ocean from 1996 to 2008.

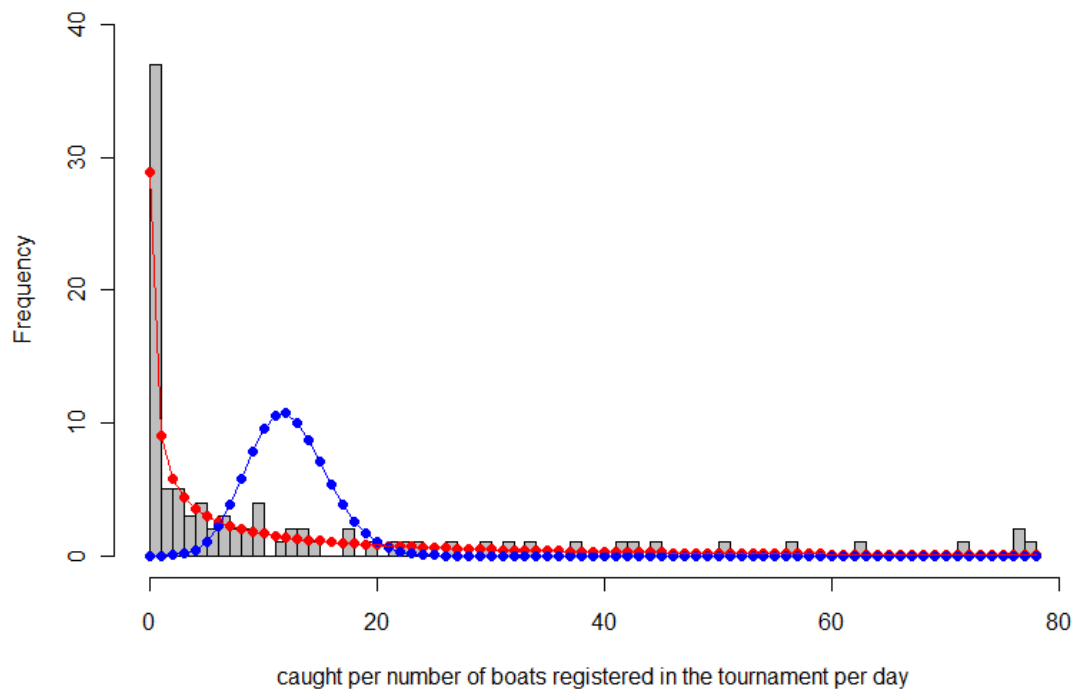


Figure 6.3 - Grey bars empirical distribution of catch per number of boats registered per tournament per day; Red line represents the theoretical negative binomial distribution and; Blue line represents the theoretical Poisson distribution.

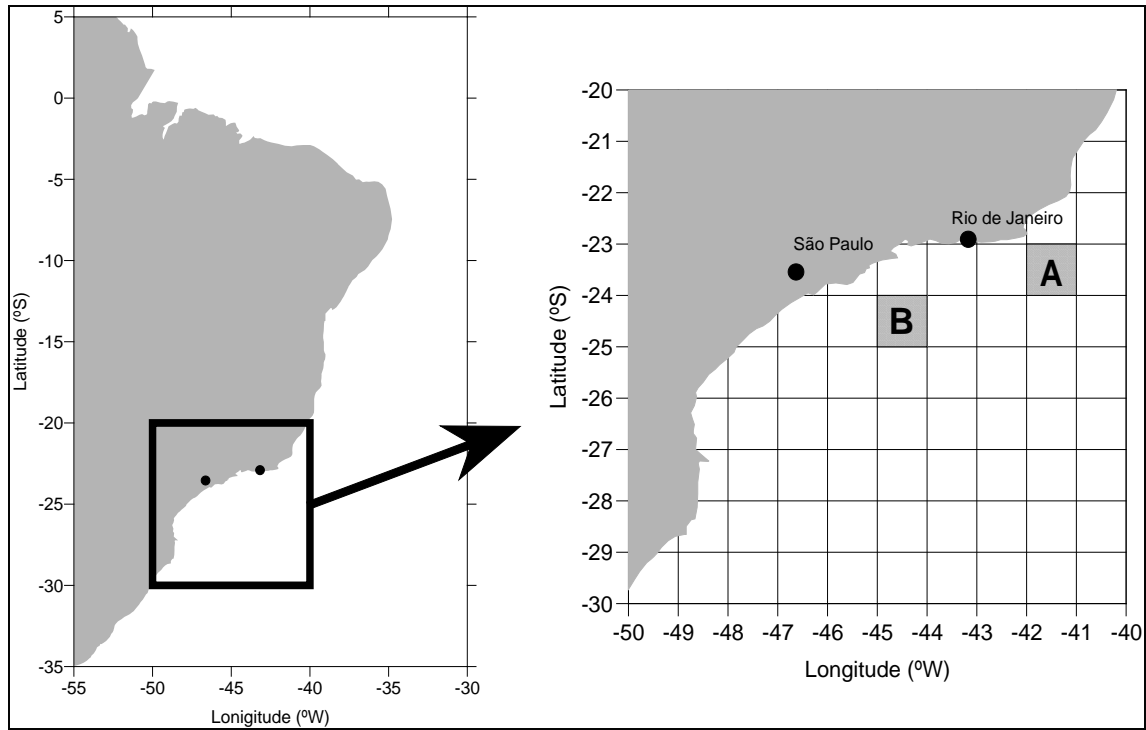


Figure 6.4 - Fishing grounds of recreational fishery in southern Brazil representing two different fishing areas about approximately 90 miles from coast, as follows: A: 23° to 24°S/ 41° to 42°W for Rio de Janeiro and B: 24° to 25°S/ 44° to 45°W for São Paulo

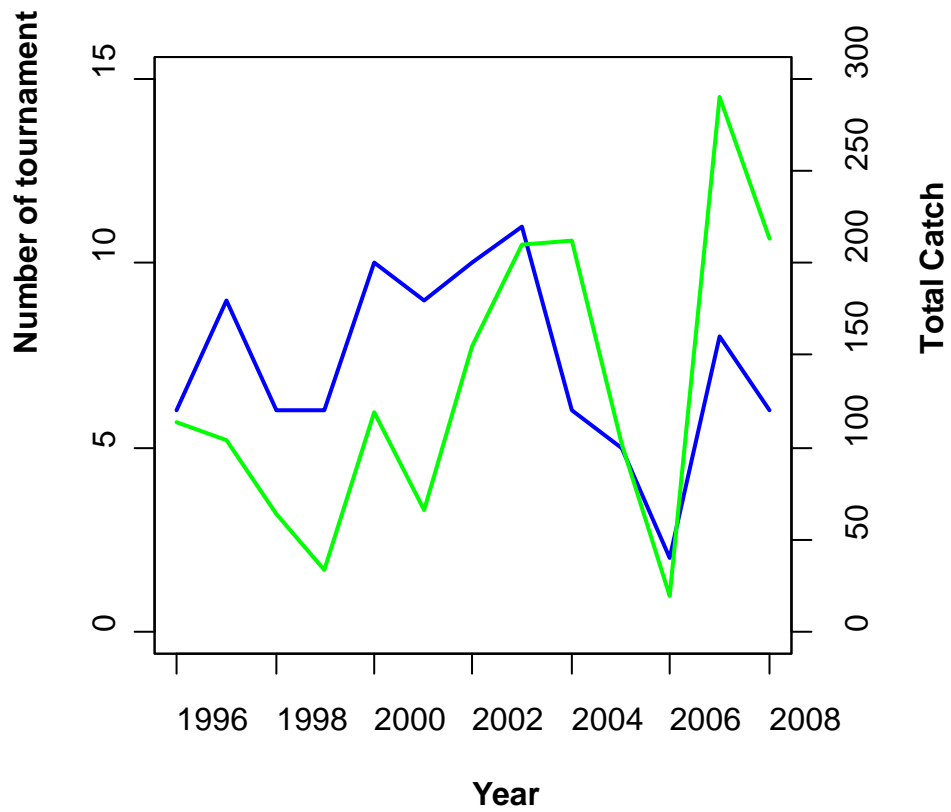


Figure 6.5 - Number of tournament days monitored and total catch by year in the Brazilian sport fishery in the Atlantic Ocean from 1996 to 2008. Blue line represents the fishing effort and green line represents the total catch.

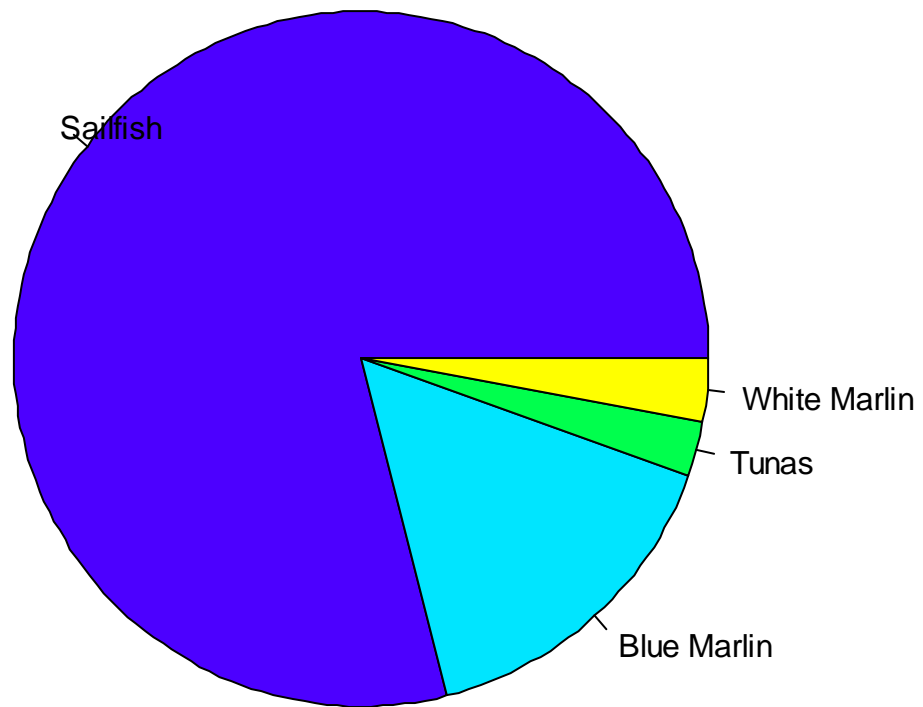


Figure 6.6 - Proportion of species regularly caught year in the Brazilian sport fishery in the Atlantic Ocean from 1996 to 2008.

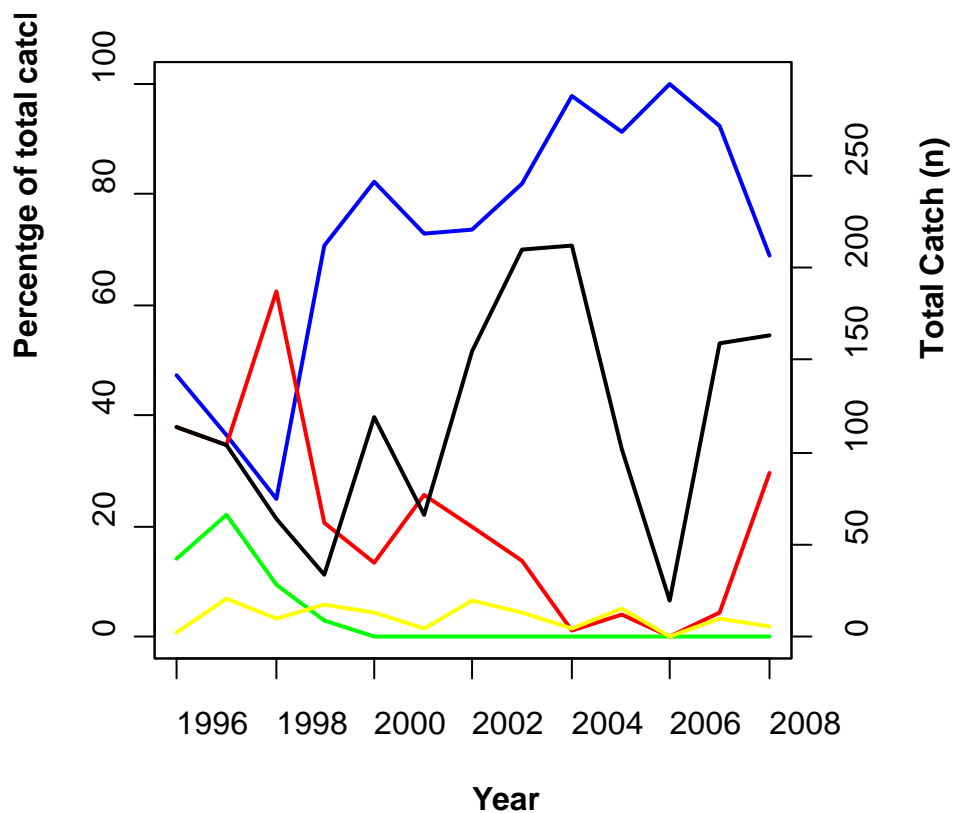


Figure 6.7 - Percentage of total catch and total catch (n) by year in the Brazilian sport fishery in the Atlantic Ocean from 1996 to 2008. Blue line: Sailfish (%); Red line: Blue marlin (%); Green line: Tunas (%); Yellow line: White marlin (%) and; Black line: Total catch (n).

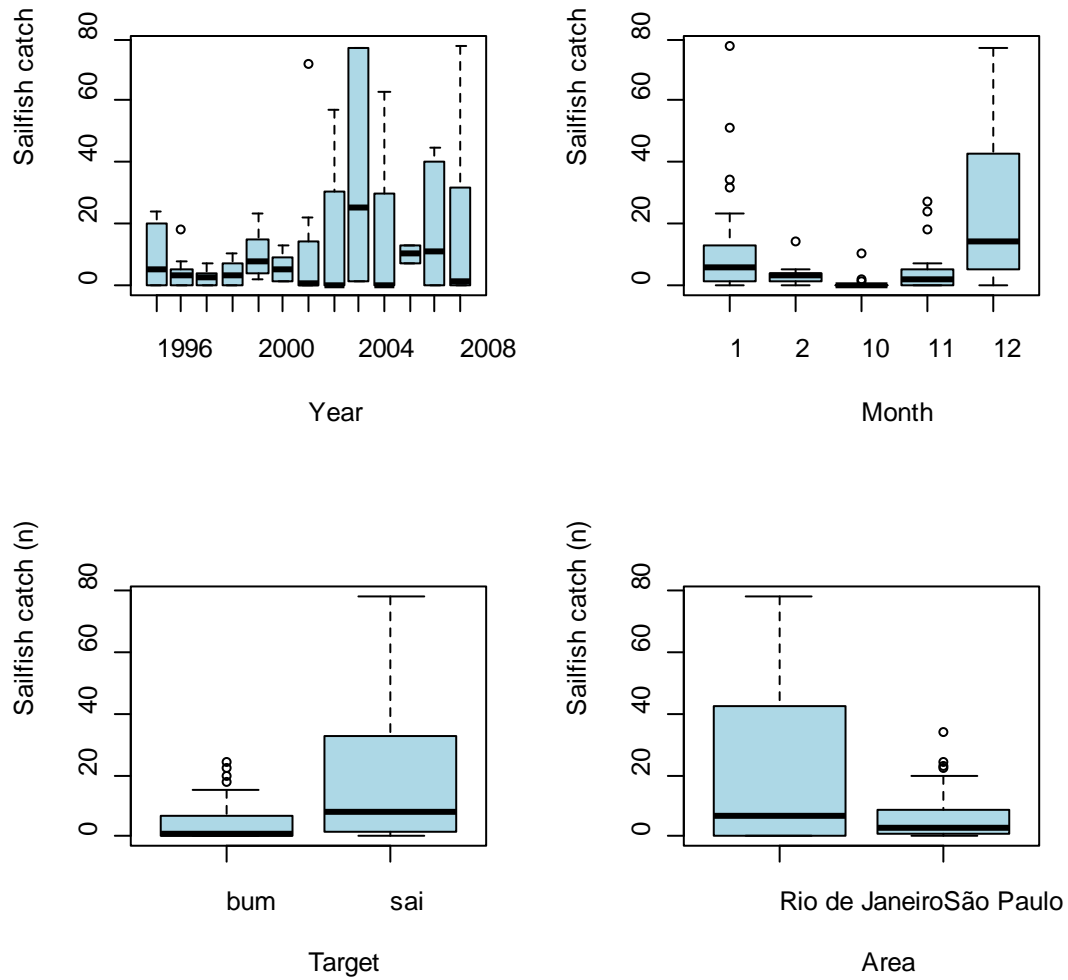


Figure 6.8 – Box plot of nominal sailfish catch (n° of fish/n° of boats/day) for each factor and level in the Brazilian sport fishery in the Atlantic Ocean from 1996 to 2008

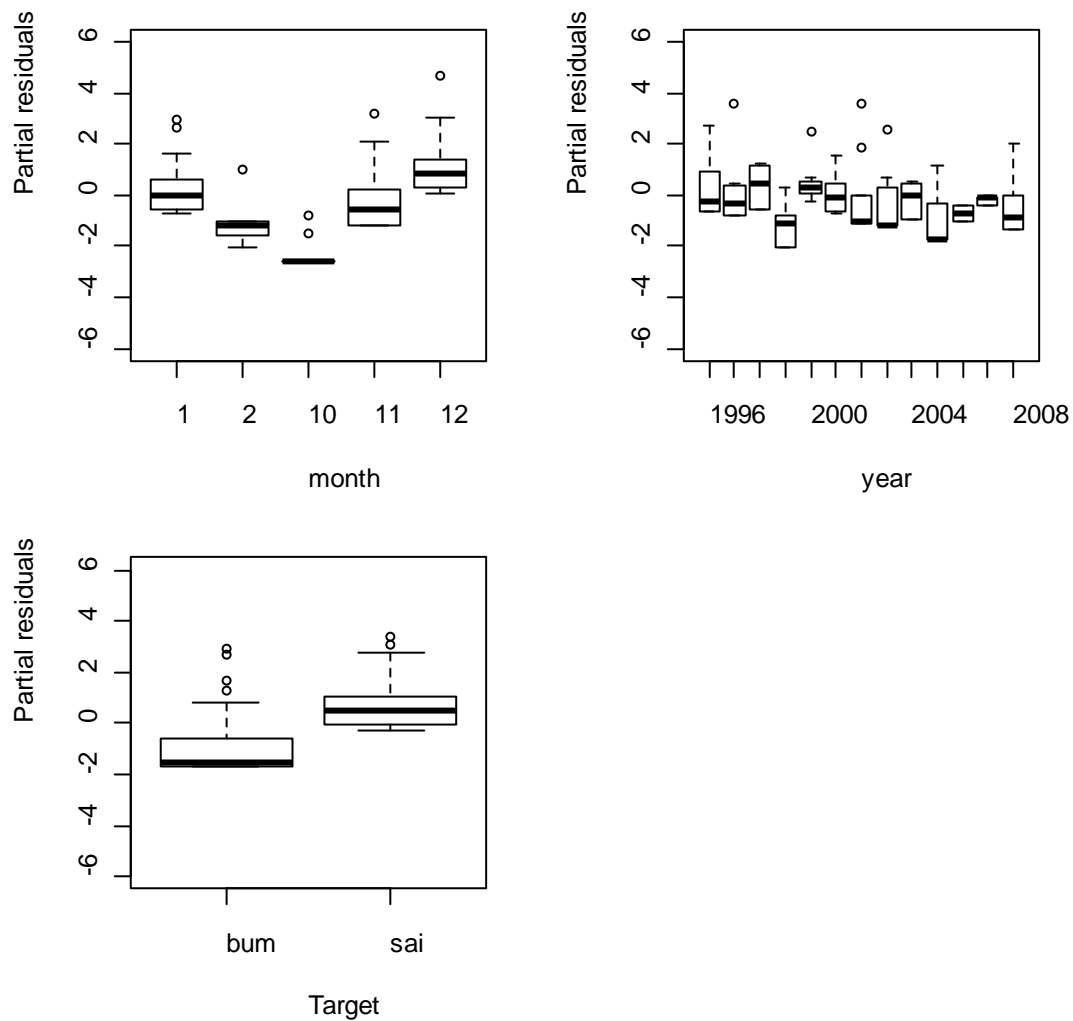


Figure 6.9 – Box plot of partial residuals for each select factor and level of the selected model for the standardization of sailfish caught by the sport fishery in Atlantic Ocean (1996-2008).

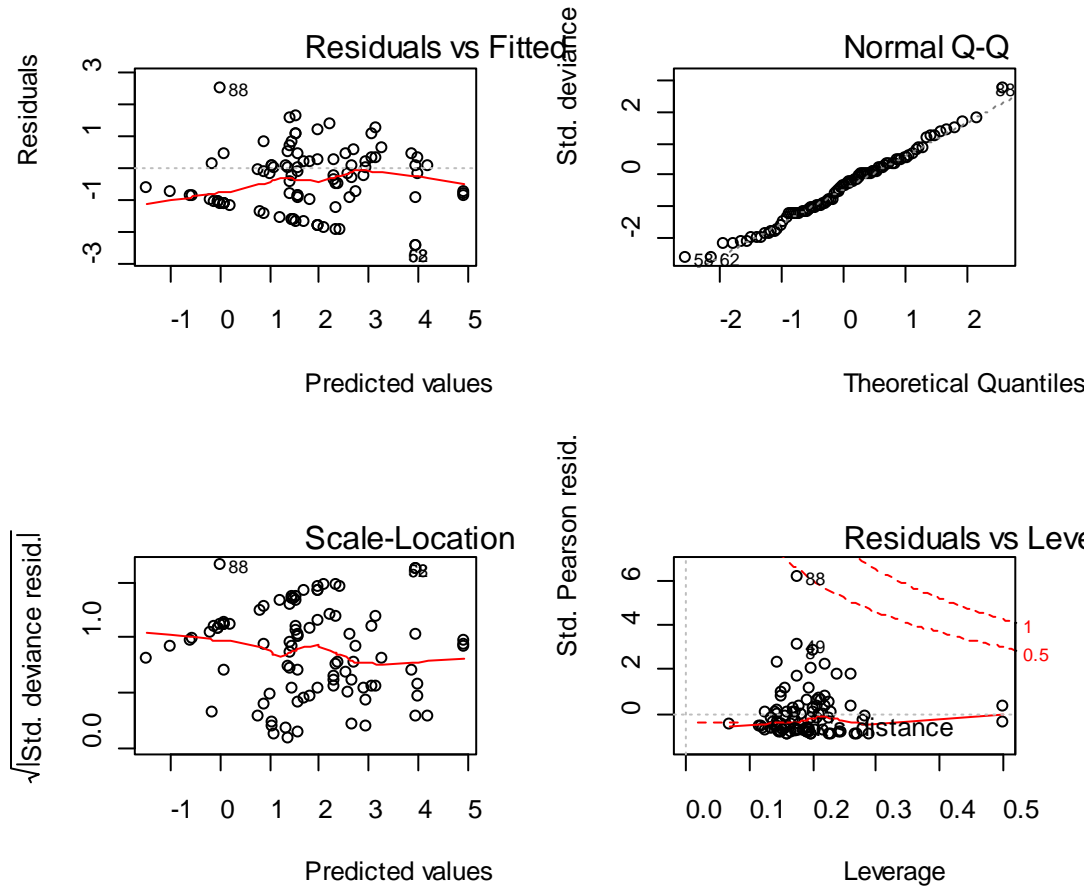


Figure 6.10 – Diagnostics plots of the fitted model for the standardization of sailfish caught by the Brazilian sport fishery in Atlantic Ocean (1996-2008). Red line represents the smooth fit and in the leverage plot dashed red line represents the Cook's distance

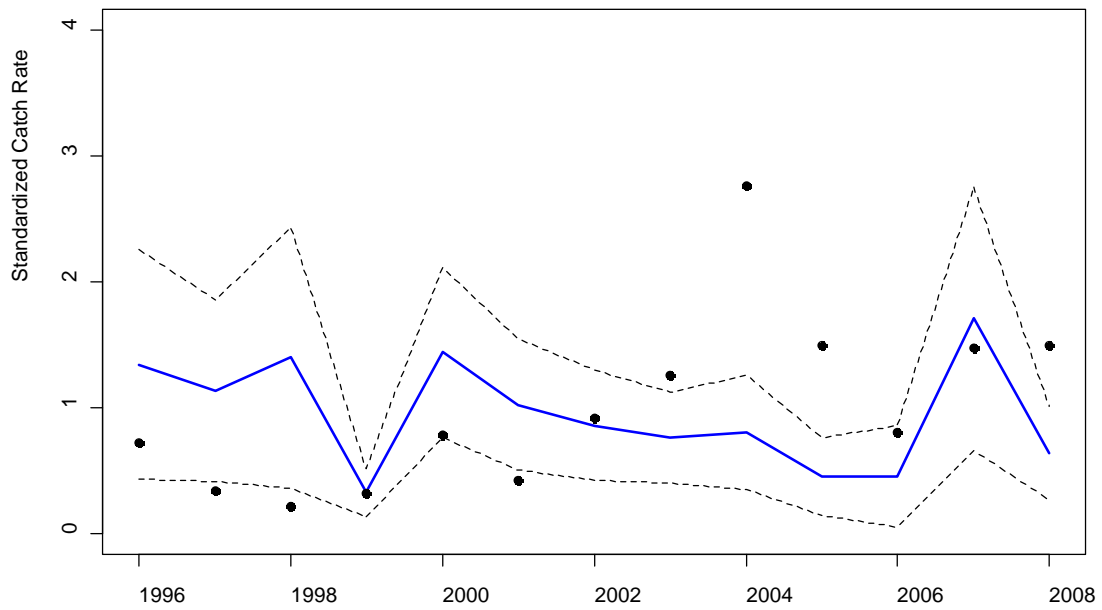


Figure 6.11 – Nominal (black points) and standardized catch rate (blue line) of sailfish caught by the Brazilian sport fishery in Atlantic Ocean. Dashed line represents the standard errors of standardized catch rate estimates.

Chapter 7 - General conclusions and recommendations

In the Atlantic Ocean, sailfish has been managed by ICCAT, which has traditionally assumed the existence of two stocks (west and east) separated arbitrarily by the meridians associated with the mid Atlantic Ridge (long. 40°W, North Atlantic; long. 20°W, South Atlantic). The results of the last sailfish stock assessment carried out by ICCAT in 2009 indicated that both stocks are probably overfished, particularly the one from the eastern Atlantic. However, the analyses in this assessment were severely hampered by an acute lack of accurate data (*i.e.* catch and effort data, ICCAT 2009). Moreover, the difference of recent trends in abundance among the different fleets, particularly after 1990, also suggested a high degree of uncertainty regarding the status of sailfish stocks in Atlantic (ICCAT 2009). Hence, despite of ICCAT work group have recommended that the catches of western stock should not exceed the current levels, no specific management or regulations were adopted.

The absence of basic life history information (*i.e.* reproductive biology and growth parameters) has precluded the application of size or age-structured models in the past sailfish stock assessments in the Atlantic Ocean. The length at first sexual maturity estimated in the present work, however, can be converted to age at first sexual maturity, being thus directly applicable to the next stock assessment. Additionally, this study also estimated various other important parameters, such as fecundity, as well as sex ratios stratified by area and season, which might be useful to arrange sailfish catch statistics by sex. Furthermore, stratifying catches by latitude during spawning and non-spawning periods could be useful to reduce the variances of abundance indices used in stock assessments. Future research, therefore, should include simulation studies to explore the quantitative effects of sex stratification by season and area on stock assessments.

Another aspect presented in this study was the spatial modeling of size at catch. Size-based indicators are progressively being used in fisheries management and could be a useful instrument for monitoring sailfish stocks during periods when stock assessments are not conducted. Monitoring the mean length and catch rates of sailfish in the pelagic longline fisheries during the spawning season in the Southeast Brazilian coast, for example, may provide

some insight into the spawning stock biomass. Although there was no indication of a declining mean size of spawning sailfish in the studied area over the duration of the present investigation, longer-term trends were not investigated.

The present results also show that the inclusion of oceanographic variables in catch rate standardization might provide a better understanding of the possible relationship between the fishing gear behavior and catchability, as a result of the physiological ecology of sailfish. Regarding the Brazilian catch rate series, despite the present results agree relatively well with previous findings, there were some discrepancies between the available times series of sailfish catch rate in southwestern Atlantic. This could be explained primarily by the different data sets used, but also by the diverse standardization procedures.

New analysis, incorporating new variables, and the development of cooperative studies could be useful to identify the causes of the differences between authors found so far. Although the present results are speculative, considering the rather limited amount of data used, they provide an additional catch rate series to be taken into account when assessing the condition of the sailfish stock in the South Atlantic. Moreover, the hotspots identified in the present analysis might serve as a basis for the delimitation of the explanatory variable “area” in the next catch rate standardization procedures, considering also a possible interaction between area and month, since there is a strong correlation of these hotspots with summer months in the southeast Brazilian coast.

The understanding of the population structure of exploited species is one of the main requirements for the proper delineation of fishery management units and consequently to an effective management and conservation of fisheries resources. In the last sailfish stock assessment the billfish working group concluded that there was a need to reevaluate the stock structure for the species (ICCAT, 2009), in light of new biological information. Some questions stemming from that are:

- (1) Are South Atlantic sailfish a separate stock from North Atlantic sailfish?
- (2) Are Southwest Atlantic sailfish a separate stock from Southeast Atlantic sailfish and North Atlantic sailfish?
- (3) Do South Atlantic sailfish constitute a single stock unit?

According to Gulland (1983), several classes of information should be considered in the delineation of stocks: (i) spatiotemporal discontinuities in fish abundance, as reflected in catch rate by fishing vessels; (ii) location and timing of spawning; (iii) differences in population parameters, such as, growth and size structure; (v) tagging data; (iv) genetic differences. The provision of new information on South Atlantic sailfish with regard to several of these categories was the primary task of the present dissertation, as discussed in the previous chapters.

Spawning areas for sailfish have been identified on the basis of gonad examination and larval distribution in the Northwest in the Straits of Florida (Voss, 1953; Jolley, 1974; Richardson *et al.*, 2009a and b) and Southeast coast of Brazil (Amorim and Arfelli, 1981; Mourato *et al.*, 2009). On these grounds, it has been generally accepted that sailfish spawn in summer in sub-tropical Atlantic waters centred on 20°N and 20°S. These spawning grounds are thus symmetrically distributed in the two hemispheres, with temporal separation of spawning seasons. On the other hand, spawning in the eastern Atlantic has been observed all year long with a peak in April on the West African shelf (Ovchinnikov, 1971). Ueyanagi *et al.* (1970) reported taking sailfish larvae off Angola and Sierra Leone between November to April. More recent preliminary information also suggests peak spawning of sailfish in the area of the Gulf of Guinea from October to December (ICCAT, 2009).

The geographical separation between Northern and Southern Hemisphere spawning grounds seems to be reasonably supported also by tagging data which have not shown any trans-equatorial movements. This information strongly suggests that South Atlantic sailfish and North Atlantic sailfish pertain to different populations. A possible separation of South Atlantic sailfish into two independent stocks, however, is not so clear. The main question remaining to be answered, thus, with regard to the Atlantic sailfish stock structure is: what is the level of connectivity between the southwestern and the eastern Atlantic sailfish?

The present results showed that, at least in part, the sailfish stock in the Atlantic Ocean is structured longitudinally according to ontogenetic stages, reflected by environmental preferences of adults and juveniles or sub-adults. This fact combined with the existence of discrete non-overlapping of spawning seasons and southwestern and eastern Atlantic and a clear continuity of sailfish catch throughout the entire equatorial Atlantic basin, together with rather narrow distance between the coast of Africa and the northeast tip of Brazil suggest that such a

longitudinal mixing is highly likely. The analysis of spatiotemporal distribution of catch rates and reproduction data have suggested a southward movement of the stock from October on, from the western central tropical Atlantic towards the southeast Brazilian coast, in order to spawn. After spawning, the sailfish is probably driven northeastward in order to return to the tropical western central tropical Atlantic.

Thus, it is likely that some interchange does happen in the equatorial region between southwestern sailfish and eastern sailfish, particularly during the second and third quarters of each year. Moreover, the difference of the mean sailfish size between the southwestern and eastern Atlantic also might be an indication that sailfish after achieving the sexual maturity spawn for the first time in the western side, spawning in the eastern side from that time onward. Although the separation of the northwest sailfish stock seems to be clear, there is still a large uncertainty about the degree of mixing between southwestern and eastern sailfish. Should it be considered a single stock for management purposes and what would be the impact of different stock structure scenarios in the results of the assessments are some of the questions that still need to be answered. Based on the information then available, during the last assessment, ICCAT used the two stocks hypothesis (east and west) for Atlantic sailfish. In light of the information hereby presented, other alternative stock structure scenarios should also be considered in the next sailfish assessments to be carried out by ICCAT, although additional studies, such as tagging studies, confirmation of timing and area of spawning in the eastern side of the Atlantic and genetic analysis are still needed to reduce the uncertainty in regard of sailfish stock structure in the Atlantic Ocean.

Bycatch in pelagic longline fisheries represents the major source of fishing mortality for sailfish stocks in the Atlantic Ocean. In this context, the development of management tools based on spatial analyses of the pelagic longline fisheries, such as time-area closures might be a good option to decrease or to ensure appropriate levels of catches. Goodyear (1999), for example, demonstrated that time-area restrictions might significantly reduce the bycatch of billfishes in US pelagic longline fisheries with minor impacts on catch of target species. Evidently that the hotspots identified in the present work could be used to form the basis for a time-area closure as a management tool for the sailfish population in the southwestern Atlantic Ocean. The overlap between peak commercial longline catches of sailfish off Southeast

Brazil and peak spawning activity encourages careful consideration of management measures required to ensure that spawning stock biomass is fished at a sustainable level.

On the other hand, it is crucial to ensure that hot-spot areas are consistent over years (*e.g.* Watson et al 2008; Bigelow and Mourato, 2010) and thus additional research using catch and effort data from different fleets (*i.e.* ICCAT data base) covering a broader area are still needed to refine the highest density areas in Atlantic Ocean prior to definition of time-area closures (*e.g.* Goodyear, 2003). Furthermore, the effectiveness of bycatch reduction measures involving time-area controls must also take in account the degree of overlap between the bycatch and target species and a possible reallocation of fishing effort, including socioeconomic aspects about the nature and dynamics of the pelagic longline fishery (Goodyear 1999, 2003; Bigelow and Mourato, 2010).

Additionally, other possible management measures that might also result in an effective reduction of fishing mortality of sailfish involve changes of fishing gear, such as the employment of circle hooks (*e.g.* Kerstetter and Graves, 2008), which has proven to increase survival of the fish caught, followed by the mandatory release of specimens that are still alive at haul-back. Another alternative to significantly reduce fishing mortality is to increase the hook fishing depths, since the present results showed a marked preference of the tagged sailfish for the upper 10m of the water column during any time of the day. Bigelow and Mourato (2010), for instance, demonstrated that the redistribution of hook depth in Hawaii-based longline fleet significantly reduced the striped marlin catches with minor impacts on the catches of the target species, such as bigeye tuna.

Finally, the results obtained by the present study have presented new information that might be used to establish new management measures aiming at ensuring the conservation of sailfish stocks in the Atlantic Ocean.

Chapter 8 - References

- Akaike, H. 1974. A new look at the statistical identification model. *IEEE transactions on Automatic Control*. 19: 716-723.
- Amorim, A.F. and Arfelli, C.A. 2001. Analysis of the Santos fleet from São Paulo, Southern Brazil (1971-1999). *Col. Vol. Sci. Pap.*, ICCAT (53):263-71.
- Amorim, A.F. and Silva, B.O. 2005. Game fisheries off São Paulo State coast, in Brazil (1996-2004). *Collect. Vol. Sci. Pap. ICCAT*, 58(5): 1574-1588.
- Amorim, A.F., Andrade, H.A. and Lins, J.E., 2006. Assessment of billfish abundance based on Brazilian sport fishing catches. *Bull. Mar. Sci.*, 79: 659-666.
- Amorim, A.F., Pimenta, E.G. and Amorim, M.C. 2011. *Peixes de bico do Atlântico*. Edição do Autor. 108pp.
- Arfelli C.A. and Amorim A.F. 1981. Estudo biológico-pesqueiro do agulhão-vela, *Istiophorus platypterus* (Shaw and Nodder, 1791), no sudeste e sul do Brasil (1971 a 1980). *B. Inst. Pesca*. 8: 9-22.
- Arfelli, C.A., Amorim, A.F., Graça-Lopes, R., 1994. Billfish sport fishery off Brazilian coast. *Collect. Vol. Sci. Pap. ICCAT*, (41): 214-217.
- Arocha, F. 2002. Oocyte development and maturity classification of swordfish from the north-western Atlantic. *J. Fish Biol.* 60, 13–27.
- Arocha, F. and Marcano, L., 2006. Life history characteristics of Blue marlin, White marlin and sailfish from the eastern Caribbean Sea and adjacent waters. *Amer. Fish. Soc. Symp.* 49:1481-1491.
- Arocha, F. and Barrios, A. 2009. Sex ratios, spawning seasonality, sexual maturity, fecundity of white marlin (*Tetrapturus albidus*) from the western central Atlantic. *Fish. Res.*, 95:98-111.
- Arnold. G. and Dewar, H. 2001. *Electronic Tags in Marine Fisheries Research: A 30-Year Perspective*. pp. 7-64. In: J Seibert & J. Nielsen (ed.) *Electronic Tagging and Tracking in Marine Fisheries*. Kluwer Academic Publishers, Dordrecht, The Netherlands.
- Augustin, N.H., Mugglestone, M.A. and Buckland, S.T. 1998. The role of simulation in modeling spatially correlated data. *Environmetrics*. 9: 175-196.
- Baranov, F.I. 1918. On the question of the biological basis of fisheries. *Nauchnyi issledovatel'skii ikhtiologicheskii Institut Izvestia* 1(1):81–128 (Translated).

- Bard, F.X., Joanny, T. and Ngoran, N.Y. 2002. Standardized Indices of Abundance of Sailfish (*Tetrapterus Albicans*) Off Côte D'ivoire, 1988-2001. *ICCAT, Col. Vol. Sci. Pap.* 54: 764-771.
- Bayliff, W.H. 1993. An indexed bibliography of papers on tagging of tunas and billfishes. Special Report N°8. Inter-American Tropical Tuna Commission. 148 pp.
- Bayliff, W.H. 1996. An indexed bibliography of papers on tagging of tunas and billfishes: Supplement 1. Status of Interactions of Pacific Tuna Fisheries in 1995. Proceedings of the Second FAO Expert Consultation on Interactions of Pacific Tuna Fisheries. Shimizu, Japan, 23-31 January.: 592-612.
- Beardsley, G.L., Merrett, N.R. and Richards W.J. 1975. Synopsis of the biology of the sailfish, *Istiophorus platypterus* (Shaw and Nodder, 1791). In: Shomura RS and Williams F (eds). Proc. Intl. Billfish Symp., Pt. 2. NOAA Tech. Rep. NMFS SSRF- 675: 335p.
- Beardsley, G.L. 1980. Size and possible origin of sailfish, *Istiophorus platypterus*, from the eastern Atlantic ocean. *Fish. Bull.* 78: 805-808.
- Becker H. 2001. *Hidrologia dos bancos e ilhas oceânicas do nordeste brasileiro. Uma contribuição ao Programa REVIZEE*. Tese de Doutorado. Universidade Federal de São Carlos, São Carlos, São Paulo, Brasil. 175p.
- Bekkby, T., Rinde, E., Erikstad, L., Bakkestuen, V., Longva, O., Christensen, O., Isaeus, M. and Isachsen, P.E. 2008. Spatial probability modelling of eelgrass (*Zostera marina*) distribution on the west coast of Norway. *ICES J. Mar. Sci.* 65: 1093–1101.
- Bigelow, A. K., Musyl, M. K., Poisson, F and Kleiber, P. 2006. Pelagic longline gear depth and shoaling. *Fish. Res.* 77: 173–183.
- Bigelow, A. K. and Maunder M.N. 2007. Does habitat or depth influence catch rates of pelagic species? *Can. J. Fish. Aquat. Sci.*, 64: 1581-1594.
- Bigelow, K. and Mourato, B. L. 2010. Evaluation of longline mitigation to reduce catches of North Pacific striped marlin in the Hawaii-based tuna fishery. *Western and Central Pacific Fisheries Commission Working Papers*. 1 - 23.
- Block, B.A. 1986. Structure of the brain and eye heater tissue in marlins, sailfish, and spearfishes. *J.Morphology* 190:169-189.
- Block, B.A., Booth, D.T. and Carey, F.G .1992a. Depth and temperature of the blue marlin, *Makaira nigricans*, observed by acoustic telemetry. *Mar Biol.*, 114: 175-183.

- Block, B.A., Booth, D.T. and Carey, F.G. 1992b. Direct measurement of swimming speeds and depth of blue marlin. *J Exp Biol.*, 166: 267-284.
- Block, B.A., Dewar, H., Farwell, C. and Prince, E.D. 1998. A new satellite technology for tracking the movements of Atlantic bluefin tuna. *Proc Natl Acad Sci USA*, 95:9384–9389.
- Brill, R.W. and Lutcavage, M.E. 2001. Understanding environmental influences on movements and depth distributions of tunas and billfishes can significantly improve population assessments. *Amer. Fish. Soc. Symp.* 25: 179-198.
- Brill, R.W., Holts, D.B., Chang, R.K.C., Sullivan, S., Dewar, H. and Carey, F.G. 1993 Vertical and horizontal movements of striped marlin (*Tetrapturus audax*) near the Hawaiian Islands, determined by ultrasonic telemetry, with simultaneous measurement of oceanic currents. *Mar Biol*, 117: 567-574.
- Brinson, A., Alcalá, A., Die, D. and Shivilani, M. 2006. Contrasting socioeconomic indicators for two fisheries that target Atlantic billfish: southeast Florida recreational charter boats and Venezuelan artisanal gill-netters. *Bull. Mar. Sci.* 79: 635–646.
- Brown-Peterson, N. J., Wyanski, D.M. Fran Saborido-Rey, B. J., Macewicz, S and Lowerre-Barbieri, K. 2011. A Standardized Terminology for Describing Reproductive Development in Fishes. *Marine and Coastal Fisheries: Dynamics, Management, and Ecosystem Science*, 3:52–70.
- Cadrin, S.X. and Secor, D.H. 2009. Accounting for spatial population structure in stock assessment: past, present, and future. In: *The future of fisheries science in North America*. Beamish RJ, Rothschild BJ (eds) Springer, New York, pp. 405-426.
- Carey, F.G. 1990. *Further acoustic telemetry observations of swordfish*. In Stroud, Richard H. (editor), *Planning the Future of Billfishes: Research and Management in the 90s and Beyond*. Proceedings of the Second International Billfish Symposium, Kailua-Kona, Hawaii, August 1-5, 1988, Part 2: Contributed Papers, National Coalition for Marine Conservation, Inc., Savannah, Georgia: 103-122.
- Carey, F.G. and Robison, B.H. 1981. Daily patterns in the activities of swordfish, *Xiphias gladius*, observed by acoustic telemetry. *Fish. Bull.*, 79, 277–292.
- Chiang, W.C., Musyl, M.K., Sun, C.L., Chen, S., Chen, W., Liu, D.C., Su, W.C., Yeh, Su-Zan, F., Fu, S. and Huang, T. 2011. Vertical and horizontal movements of sailfish (*Istiophorus*

- platypterus*) near Taiwan determined using pop-up satellite tags. *Journal of Experimental Marine Biology and Ecology*. 397 (2): 129-135.
- Chiang, W., Sun, C., Yeh, S., Cheng, W., Liu, D., Chen, W. 2006a. Sex ratio at sexual maturity and spawning seasonality of sailfish *Istiophorus platypterus* from eastern Taiwan. *Bul. Mar. Science*, 79(3): 727-737.
- Chiang, W. C., Sun, C. L., Yeh, S. Z., Su, W. C. and D. C. Liu. 2006b. Spawning frequency and batch fecundity of the sailfish (*Istiophorus platypterus*) (Istiophoridae) in waters off Eastern Taiwan. *Zool. Stud.* 45:483–491.
- Cayré, P. and Laloé, F. 1986. Review of the gonad index (GI) and an introduction to the concept of its "critical value": Application to the skipjack tuna, *Katsuwonus pelamis*, in the Atlantic Ocean. *Marine Biology*, 90:345-351.
- Carvalho, F., Murie, D., Hazin, F. H.V., Hazin, H., Leite-Mourato, B. and Burgess, G. 2011. Spatial predictions of blue shark CPUE and catch probability of juveniles in the Southwest Atlantic. *ICES J. Mar. Sci.*, 68(5): 901-910.
- Ciannelli, L., Fauchald, P., Chan, K.S., Agostini, V.N. and Dingsør, G.E. 2008. Spatial fisheries ecology: Recent progress and future prospects. *Journal of Marine Systems*, 71: 223–236.
- Cleveland, W. S., and Delvin. S. J. 1988. Locally weighted regression: an approach to regression analysis by local fitting. *J. Am. Stat. Ass.* 83: 596 -610.
- De Sylva, D. and Breder, P.R. 1997. Reproduction, gonad histology and spawning cycles of North Atlantic billfishes (Istiophoridae). *Bull. Mar. Sci.* 60, 668–697.
- Dunn, P.K. and Smyth, G. K. 2005 Series evaluation of Tweedie exponential dispersion model densities. *Statistics and Computing*. 15(4): 267–280.
- Diouf, T. 1994. Les istiophoridés en Atlantique est: Etude des pêcheries et quelques aspects de La biologie du voilier au Sénégal . *ICCAT, Col. Vol. Sci. Pap.* 41: 442- 457.
- Duffett-Smith, Peter. 1988. *Practical astronomy with your calculator*. Cambridge University Press (Cambridge Cambridgeshire and New York). 3rd edition. 185p.
- Figueiras, A., Roca-Pardiñas, J. and Suárez, C.C. 2005. A Bootstrap Method to Avoid the Effect of Concurvity in Generalized Additive Models in Time Series Studies of Air Pollution. *Journal of Epidemiology and Community Health*. 59: 881-884.
- Fielding, A.H. and Bell, J.F. 1997. A review of methods for the assessment of prediction errors in conservation presence/absence models. *Environ. Conserv.* 24: 38–49.

- Finnerty, J.R. and Block, B.A. 1995. Evolution of cytochrome *b* in the Scombroidei (Teleostei): molecular insights into billfish (Istiophoridae and Xiphiidae) relationships. *Fish. Bull.* 93: 78-96.
- Fraser, K.W., Overton, J.M., Warburton, B. and Rutledge, D.T. 2005. Predicting spatial patterns of animal pest abundance. *Sci. Conserv. Ser.* 236: 1–57.
- Fréon, P. and Misund, O.A. 1999. *Dynamics of pelagic fish distribution and behaviour: effects on fisheries and stock assessment*. First Edition, Science, B.S. Fishing News Books, Oxford.
- Garstang, W. 1900. The impoverishment of the sea. *J. Mar. Biol. Assoc.*, 6: 1-69.
- Garza-Pérez, J.R., Lehmann, A. and Arias-González, J.E. 2004. Spatial prediction of coral reef habitats: integrating ecology with spatial modeling and remote sensing. *Mar. Ecol. Prog. Ser.* 269: 141–152.
- Gaertner, D., Ménard, F., Develter, C., Ariz, J. and Delgado de Molina, A. 2002. Bycatch of billfishes by the European tuna purse-seine fishery in the Atlantic Ocean. *Fish. Bull.* 100: 683–689.
- Goodyear, C.P. 1999. An analysis of the possible utility of time–area closures to minimize billfish bycatch by U.S. pelagic longlines. *Fish. Bull.*, 97: 243–255.
- Goodyear, C.P. 2003. Spatio-temporal distribution of longline catch per unit effort, sea surface temperature and Atlantic marlin. *Marine and Freshwater Research*, 54, 409–417.
- Goodyear, C.P., Luo, J., Prince, E.D., Hoolihan, J.P., Snodgrass, D., Orbesen, E.S. and Serafy, J.E. 2008. Vertical habitat use of Atlantic blue marlin *Makaira nigricans*: interaction with pelagic longline gear. *Mar. Ecol. Prog. Ser.* 365: 233-245.
- Graves, J.E. 1998. Molecular insights into the population structures of cosmopolitan marine fishes. *The Journal of Heredity*. 89: 427-437.
- Graves, J.E., Luckhurst, B.E. and Prince, E.D. 2000. An evaluation of pop-up satellite tag technology to estimate post-release survival of blue marlin (*Makaira nigricans*). *Inter. Comm. Cons. Atlan. Tunas, Coll. Vol. Sci. Pap.*, 51: 910-922.
- Graves, J.E., Luckhurst, B.E. and Prince, E.D. 2002. An evaluation of pop-up satellite tags for estimating postrelease survival of blue marlin (*Makaira nigricans*) from a recreational fishery. *Fish. Bull.* 100: 134-142.
- Graves, J.E. and MacDowell, J.R. 2003 Stock structure of the world's istiophorid billfishes: a genetic perspective. *Mar. Fresh Res.* 54: 287-298.

- Gulland, J. A. 1983. *Fish stock assessment: a manual of basic methods*, New York.
- Gunn, J.S., Patterson, T.A. and Pepperell, J.G. 2003 Shortterm movement and behaviour of black marlin, *Makaira indica* in the Coral Sea as determined through a pop-up satellite archival tagging experiment. *Mar. Freshw. Res.* 54:515–525.
- Hazin, F.H.V. 1993, *Fisheries-oceanographical study on tunas, billfishes and sharks in the Southwestern Equatorial Atlantic Ocean*. Tese de Doutorado. Universidade de Pesca de Tóquio, Tóquio, Japão. 286p.
- Hazin, F.H.V., Lessa, R.P.T., Amorim, A.F., Arfelli, C.A. and Antero-Silva, J.N. 1994. Sailfish (*Istiophorus albicans*) fisheries off Brazilian coast by national and leased longliners (1971-91). *Collect. Vol. Sci. Pap. ICCAT*, 41: 199-207.
- Hazin, H. G. and Erzini, K. 2008. Assessing swordfish distribution in the South Atlantic based on spatial predictions. *Fish. Res.*, 90: 45-55.
- Hastie, T. and Tibshirani, R. 1990. *Generalized additive models*. UK: Chapman and Hall, London.
- Hernandez, A. and Ramírez, M., 1998. Spawning seasonality and length at maturity of sailfish (*Istiophorus platypterus*) off the Pacific coast of Mexico. *Bull. Mar. Sci.*, 63:459-467.
- Hernández, A., Ramírez, M. and Muhlia-Melo, A. 2000. Batch fecundity and spawning frequency of sailfish (*Istiophorus platypterus*) off the Pacific coast of Mexico. *Pac. Sci.* 54: 189-194.
- Hilborn, R. and Walters, C. J. 1992. *Quantitative Fisheries Stock Assessment: Choice, Dynamics and Uncertainty*. Chapman and Hall, Inc., London, New York: 570p.
- Hinton, M.G. and Nakano, H. 1996. Standardizing catch and effort statistics using physiological, ecological, or behavioral constraints and environmental data, with an application to blue marlin (*Makaira nigricans*) catch and effort data from Japanese longline fisheries in the Pacific. *Bull. Inter-Amer. Trop. Tuna Comm. Bull.* 21: 169-200.
- Holland, K., Brill, R.W. and Chang, R.K.C. 1990. Horizontal and vertical movements of Pacific blue marlin captured and released using sportfishing gear. *Fish Bull US*, 88: 397-402.
- Holts, D. and Bedford, D. 1990. *Activity patterns of striped marlin in the southern California bight*. In: Stroud, RS (Ed) *Planning the future of billfishes*. National Coalition for Marine Conservation, Inc., Savannah, Georgia, pp 81-93.

- Hoolihan, J.P. 2004. Horizontal and vertical movements of sailfish (*Istiophorus platypterus*) in the Arabian Gulf, determined by ultrasonic and pop-up satellite tagging. *Mar. Biol.* 146: 1015-1029.
- Hoolihan, J.P. and Luo, J. 2007. Determining summer residence status and vertical habitat use of sailfish (*Istiophorus platypterus*) in the Arabian Gulf. *ICES J. Mar. Sci.* 64:1-9.
- Hoolihan, J.P., Luo, J., Richardson, D.E., Snodgrass, D., Orbesen, E.S. and Prince, E.D. 2009. Vertical movement rate estimates for Atlantic istiophorid billfishes derived from high resolution pop-up satellite archival data. *Bull. Mar. Sci.* 83:257–264.
- Hoolihan, J.P., Luo, J., Richardson, C.P. Goodyear D., Orbesen, E.S. and Prince, E.D. (2011) Vertical habitat use of sailfish (*Istiophorus platypterus*) in the Atlantic and eastern Pacific, derived from pop-up satellite archival tag data. *Fish. Oceanogr.* 20:3, 192–205.
- Horodysky, A.Z. and Graves, J.E. 2005. Application of pop-up satellite archival tag technology to estimate postrelease survival of white marlin (*Tetrapturus albidus*) caught on circle and straight-shank ('J') hooks in the western North Atlantic recreational fishery. *Fish. Bull.* 103:84–96.
- Horodysky, A.Z., Kerstetter, D.W., Latour, R.J. and Graves, J.E. 2007. Habitat utilization and vertical movements of white marlin (*Tetrapturus albidus*) released from commercial and recreational fishing gears in the western North Atlantic Ocean: inferences from short duration pop-up archival satellite tags. *Fish. Oceanogr.*, 16: 240–256.
- Hunter, J. R., and B. J. Macewicz. 1985. *Measurement of spawning frequency in multiple spawning fishes*. In: Lasker, R. (Ed.) *In An Egg Production Method for Estimating Spawning Biomass of Pelagic Fish: Application to the Northern Anchovy*, *Engraulis mordax*. U.S. National Marine Fisheries Service, National Oceanic and Atmospheric Administration Technical Report 36, pp. 79–94.
- Hunter, J.R., Lo, N.C. and Leong, R.J., 1985. *Batch fecundity in multiple spawning fishes*. In: Lasker, R. (Ed.) *In An Egg Production Method for Estimating Spawning Biomass of Pelagic Fish: Application to the Northern Anchovy*, *Engraulis mordax*. U.S. National Marine Fisheries Service, National Oceanic and Atmospheric Administration Technical Report 36, pp. 67–78.
- Hunter, J.R., Macewicz, B. and Sibert, J.R., 1986. The spawning frequency of skipjack tuna, *Katsuwonus pelamis*, from the South Pacific. *Fish. Bull.* 84, 895–903.

- Ibe, A.C. and Ajayi, T.O. 1985. Possible upwelling phenomenon off the Nigerian coast. *Technical Paper of the Nigerian Institute for Oceanography and Marine Research*, 25: 1-30.
- ICCAT, 2009. International Commission for the Conservation of Atlantic Tunas: Report of the 2009 sailfish assessment. 117p.
- Jolley, J.W. 1977. The biology and fishery of Atlantic sailfish *Istiophorus platypterus*, from southeast Florida. *Fla. Mar. Res. Publ.*, 28: 1-31.
- Jolley, J.W. and Irby, E.W. 1979. Survival of tagged and released Atlantic sailfish (*Istiophorus platypterus*: Istiophoridae) determined with acoustic telemetry. *Bull. Mar. Sci.* 29: 155-169.
- Kerstetter, D.W. and Graves, J.E. 2008. Post-release survival of sailfish caught by commercial pelagic longline gear in the southern Gulf of Mexico. *North American Journal of Fisheries Management* 28: 1578-1586.
- Kerstetter, D.W., Luckhurst, B.E., Prince, E.D. and Graves, J.E. 2003. Use of pop-up satellite archival tags to demonstrate survival of blue marlin (*Makaira nigricans*) released from pelagic longline gear. *Fish. Bull.* 101:939–948.
- Kume, S. and Joseph, J. 1969. Size composition and sexual maturity of billfish caught by the Japanese longline fishery for tunas and billfishes in the Pacific ocean east of 130°W. *Bull. Far Seas Fish. Res. Lab.*, 2: 115-162.
- Laevastu, T. and Hayes, M.L. 1981. *Fisheries Oceanography and Ecology*. Fishing News Books Ltd. London. 200 pp.
- Laurs, R.M. 1983. The north pacific albacore-an important visitor to California current waters, *CalCOFI Rep.* 24: 99-106.
- Lehmann, A., Overton, J.M. and Leathwick, J.R. 2002. GRASP: Generalized regression analysis and spatial predictions. *Eco. Model.*, 157: 189-207.
- Lehodey, P., Andre, J.M., Bertignac, M., Hampton, J., Stoens, A., Menkes, C., Memery, L. and Grima, N. 1998. Predicting skipjack tuna forage distributions in the equatorial Pacific using a coupled dynamical bio-geochemical model. *Fish. Oceanogr.* 7: 317–325.
- Longhurst, A.R. 1962. A review of the oceanography of the Gulf of Guinea. *Bull. de L.I.F.A.N.* 24: 633-663.
- Lutcavage, M.E., Brill, R.W, Skomal, G.B, Chase, B.C, Goldstein, J.L. and Tutein, J. 2000. Tracking adult North Atlantic bluefin tuna (*Thunnus thynnus*) in the northwestern Atlantic using ultrasonic telemetry. *Marine Biology*, 137, 347-358.

- Luthy, S.A. 2004. *Billfish larvae of the Straits of Florida*. Ph.D. Dissertation, Miami, FL: University of Miami, pp. 112.
- Maravelias, C.D., Reid, D.G. and Swartzman, G. 2000. Modeling spatio-temporal effects of environment on Atlantic herring, *Clupea harengus*. *Env. Biol. Fish.*, 58: 157-172.
- Marr, J. C. 1953. On the use of the terms abundance, availability, and apparent abundance in fishery biology. *Copeia*, 2:163–169.
- Mather, F.J. 1963. Tags and tagging techniques for large pelagic fishes. In ‘North Atlantic Fish Marking Symposium’. Woods Hole, Mass. Pp. 288-293. (*International Commission for the Northwest Atlantic Fisheries, Special Publication 4.*)
- Matsuura, Y. 1986. Contribuição ao estudo da estrutura oceanográfica da Região Sudeste entre Cabo Frio (RJ) e Cabo de Santa Marta Grande (SC). *Ciênc. Cult.* 38(8):1439-1450.
- Maunder, M.N. and Punt, A.E. 2004. Standardizing catch and effort data: a review of recent approaches. *Fish. Res.* 70: 141-159.
- Mohammed, E., Parker, C. and Willoughby A. 2003. Barbados: Reconstructed fisheries catches and fishing effort, 1940-2000. *Fisheries Centre Research Reports*, 11(6): 45-66.
- Mourato, B.L., Pinheiro, P., Hazin, F.H.V., Melo, V.B., Amorim, A.F., Pimenta, E. and Guimarães, C. 2009a. Preliminary analysis of gonadal development, spawning period, sex ratio and length at first sexual maturity of sailfish, *Istiophorus platypterus* in Brazilian coast. ICCAT, *Col. Vol. Sci. Pap.* 64: 1927-1940.
- Mourato, B.L., Amorim, A.F., Arfelli, C.A, Hazin, H.G., Hazin, F.H.V. and Lima, C.W. 2009b. Standardized CPUE of atlantic sailfish (*Istiophorus platypterus*) caught by recreational fishery in southern Brazil. ICCAT, *Col. Vol. Sci. Pap.* 64: 1941-1950.
- Mourato, B.L., Hazin, H.G., Wor, C., Travassos, P., Arfelli, C.A., Amorim, A.F. and Hazin, F.H.V. 2010a. Environmental and spatial effects on the size distribution of sailfish in the Atlantic Ocean. *Ciencias Marinas*. 36(3): 225–236
- Mourato, B.L., Carvalho, F.C., Hazin, F.H.V., Pacheco J.C., Hazin, H.G., Travassos, P. and Amorim, A.F. (2010b) First observations and habitat preference of atlantic sailfish, *Istiophorus platypterus* in the southwestern Atlantic ocean. ICCAT, *Col. Vol. Sci. Pap.* 65: 1740-1747.

- Musyl, M and L. M. McNaughton. 2007. Report on Pop-up Satellite Archival Tag (PSAT) Operations, Conducted on Sailfish, *Istiophorus platypterus*, by Research Scientists of the Fisheries Research Institute, Eastern Marine Biology Research Center, and Institute of Oceanography, College of Science, National Taiwan University, 6-7 June 2007, Chengkong, Taiwan, R.O.C.17p.
- Musyl, M. K., Domeier, M.L., Nasby-Lucas, N., Brill, R.W., McNaughton, L.M., Swimmer, J. Y.M., Lutcavage, S., Wilson, S.G., Galuardi, B. and Liddle, J. B. 2011. Performance of pop-up satellite archival tags. *Mar Ecol Prog Ser.*, 433: 1–28.
- Murua, H., Kraus, G., Saborido-Rey, F., Witthames, P.R., Thorsen, A. and Junquera, S. 2003. Procedures to estimate fecundity of marine fish species in relation to their reproductive strategy. *J. Northw. Atl. Fish. Sci.*, 33, 33–54.
- Nakamura, I. 1985. FAO species catalogue. Vol. 5: Billfishes of the world. An annotated and illustrated catalogue of marlins, sailfishes, spearfishes and swordfishes known to date. FAO Fish. Synop., Rome, n.125. 65p.
- Orbesen, E.S., Hoolihan, J.P., Serafy, J.E., Snodgrass, D., Peel, E.M. and Prince, E.D. 2008. Transboundary movement of Atlantic istiophorid billfishes among international and U.S. domestic management areas inferred from mark-recapture studies. *Mar. Fish. Rev.*, 70: 14-23.
- Ortiz, M. and Arocha, F. 2004. Alternative error distributions models for standardization of catch rates of non-target species from a pelagic longline-fishery: billfish species in the Venezuelan tuna longline fishery. *Fish. Res.*, 70: 275-294.
- Ortiz, M., Prince, E.D., Serafy, J.E., Holts, D.B., Dary, K.B., Pepperell, J.G., Lowry, M.B. and Holdsworth, J.C. 2003. Global overview of the major constituent-based billfish tagging programs and their results since 1954. *Mar. Freshwater Res.* 54: 489-507.
- Ovchinnikov, V.V. 1971 Swordfishes and billfishes in the Atlantic Ocean. Trad. H. Mills. Jerusalém, *Israel Prog. for Sci. Transl.* 77pp.
- Peel, E., Nelson, R. and Goodyear, P.C. 2003. Managing Atlantic marlin as bycatch under ICCAT. The fork in the road: recovery or collapse. *Mar. Fresh. Res.*, 54: 575-584.
- Pepperel, J.G. and Davis, T.L.O. 1999. Post-release mortality of black marlin, *Makaira indica*, caught off the great barrier reef with sportfishing gear. *Marine Biology*, 135: 369-380.

- Peterson, R.G. and Stramma, L. 1991 Upper-level circulation in the South Atlantic Ocean. *Progr. Oceanogr.* 26(1): 1-73.
- Prince, E.D. and Goodyear, C.P. 2006 Hypoxia-based habitat compression of tropical pelagic fish. *Fish. Oceanogr.* 15: 451-464.
- Prince, E.D., Luo, J., Goodyear, C.P., Hoolihan, J.P., Snodgrass, D., Orbesen, E. S., Serafy, J. E., Ortiz, M. and Schirripa, M.J. (2010) Ocean scale hypoxia-based habitat compression of Atlantic istiophorid billfishes. *Fish. Oceanogr.* 19(6): 448-462.
- Pikitch, E. K., Santora, C., Babcock, E. A., Bakun, A., Bonfil, R., Conover, D. O., Dayton, P., Doukakis, P., Fluharty, D., Heneman, B., Houde, E. D., Link, J., Livingston, P. A., Mangel, M., Macallister, M. K., Pope, J. and Sainsbury, K. J. 2004. Ecosystem-based fishery management. *Science*, 305: 346-347.
- Pimenta, E.G., Lima, G., Cordeiro, C.J., Tardelli, M., Amorim, A.F., 2005. Reproduction and stomach content analysis of sailfish *Istiophorus platypterus*, off Rio de Janeiro State, RJ, Brazil. *Collect. Vol. Sci. Pap. ICCAT*, 58(5): 1589-1596.
- Picaut J. 1983. Propagation of the seasonal upwelling in the eastern equatorial Atlantic. *J. Phys. Oceanogr.*, 13: 18-37.
- Post, J.T., Serafy, J.E., Ault, J.S., Capo, T.R. and De Sylva, D.P. 1997. Field and laboratory observations on larval Atlantic sailfish (*Istiophorus platypterus*) and swordfish (*Xiphias gladius*). *Bulletin of Marine Science*, 60(3):1026-1034.
- R Development Core Team. 2010. R: A language and environment for statistical computing. R Foundation for Statistical Computing, Vienna, Austria. ISBN 3-900051-07-0, URL <http://www.R-project.org/>.
- Ramsay, T.O., Burnett, R.T., and Krewski, D. (2003) The Effect of Concurvity in Generalized Additive Models Linking Mortality to Ambient Particulate Matter. *Epidemiology*. 14: 18-23.
- Reine, K. 2005. An overview of tagging and tracking technologies for freshwater and marine fishes, *DOER Technical Notes Collection, ERDC TN-DOER-E18*, U.S. Army Engineer Research and Development Center, Vicksburg, MS.
- Restrepo, V., Prince, E.D., Scott, G.P. and Uozumi, Y. 2003. ICCAT stock assessments of Atlantic billfish. *Mar. Fresh. Res.* 54: 361-367.

- Richardson, D. E., Cowen, R. K., Prince, E. D., and Sponaugle, S. 2009. Importance of the Straits of Florida spawning ground to Atlantic sailfish (*Istiophorus platypterus*) and blue marlin (*Makaira nigricans*). *Fish. Oceanogr.*, 18(6), 402-418.
- Richardson, D.E., Llopiz, J.K., Leaman, K.D., Vertes, P.S., Muller-Karger, F.E. and Cowen, R.K. 2009b. Sailfish (*Istiophorus platypterus*) spawning and larval environment in a Florida Current frontal eddy. *Prog. Oceanogr.*, 82(4): 252-264.
- Ricker, W. E. 1940. Relation of “catch per unit effort” to abundance and rate of exploitation. *Journal of the Fisheries Research Board of Canada*, 5: 43–70.
- Shono, H. 2008. Application of the Tweedie distribution to zero-catch data in CPUE analysis. *Fish. Res.* 93: 154–162.
- Sibert, J.R., Musyl, M.K. and Brill, R.W. 2003. Horizontal movements of bigeye tuna (*Thunnus obesus*) near Hawaii determined by Kalman filter analysis of archival tagging data. *Fish Oceanogr.* 12 (3), 141–151
- Schwarz, G. 1978. Estimating the dimension of a model. *Ann. Stat.* 6: 461–464.
- Sun, C.L., Chang, Y.J., Tszeng, C.C., Yeh, S.Z. and Su, N.J. 2009. Reproductive biology of blue marlin (*Makaira nigricans*) in the western Pacific Ocean. *Fish. Bull. US*. 107, 420–432.
- Swartzman, G., Huang, C. and Kaluzny, S. 1992. Spatial analysis of Bering Sea groundfish survey data using generalized additive models. *Can. J. Fish. Aquat. Sci.* 49: 1366-1378.
- Ueyanagi, S., Kikawa, S., Uto, M. and Nishikawa, Y. 1970 Distribution, spawning and relative abundance of billfishes in the Atlantic Ocean. *Bull. Far Seas Fish. Res. Lab.* 3:15-55.
- Uozumi, Y. 2003. Historical perspective of global billfish stock assessment. *Mar. Fresh. Res.* 54: 555-565.
- Vaske-Junior, T. 2005. Cefalópodes oceânicos da zona econômica exclusiva do nordeste do Brasil. *B. Inst. Pesca, São Paulo*, 31(2): 137 – 146.
- Vaske-Junior, T., Vooren, C.M. and Lessa, R.P. 2004. Feeding habits of four species of Istiophoridae (Pisces: Perciformes) from northeastern Brazil. *Environ. Biol. Fish.* 70: 293–304.
- Valavanis, V.D., Georgakarakos, S., Kapantagakis, A., Palialexis, A., Katara, I. 2004. A GIS environmental modelling approach to essential fish habitat designation. *Ecol. Model.* 178: 417-427.

- Valavanis, V.D., Pierce, G.J., Zuur, A.F., Palialexis, A., Saveliev, A., Katara, I. and Wang, J. 2008. Modelling of essential fish habitat based on remote sensing, spatial analysis and GIS. *Hydrobiologia*, 612: 5-20.
- Venables, W.N and Dichmont C.M. 2004. GLMs, GAMs and GLMMs: an overview of the theory for applications in fisheries research. *Fish. Res.* 70: 319-337.
- Voss, G.L. 1953. A contribution to the life history and biology of the sailfish, *Istiophorus americanus* Cuv and Val., in Florida waters. *Bull. Mar. Sci. Gulf Caribb.* 3: 206-240.
- Walsh, W.A., Howell, E.A., Bigelow, K.A. and McCracken, M.L. 2006. Analyses of Observed Longline Catches of Blue Marlin , *Makaira nigricans*, using Generalized Additive Models with Operational and Environmental Predictors. *Bull. Mar. Sci.* 79(3): 607-622.
- Wares, P.G. and Sakagawa, T. 1974. Some morphometrics of billfishes from the eastern Pacific ocean. *In: R.S. Shomura RS, Williams F (eds.), Proc. Intl. Billfish Symp., Pt. 2. NOAA Tech. Rep. NMFS SSRF- 675.* 335p.
- Watson, J.T., Essington, T.E., Lennert-Cody, C. E. and Hall, M.A. 2008. Trade-Offs in the Design of Fishery Closures: Management of Silky Shark Bycatch in the Eastern Pacific Ocean Tuna Fishery. *Conservation biology*, 1-10.
- West, G. 1990. Methods of assessing ovarian development in fishes: a review. *Aust. J. Mar. Freshw. Res.* 41, 199–222.
- Wood, S.N. 2006. *Generalized additive models: an introduction with R*. Chapman & Hall/CRC, Boca Raton, FL.
- Wood, S.N. and Augustin, N.H. 2002. GAMs with integrated model selection using penalized regression splines and applications to environmental modeling. *Ecological Modelling.* 157: 157-177.
- Wor, C., Mourato, B. L., Hazin, H. G., Hazin, F. H. V, Travassos, P., Andrade, H. A. 2010. Standardized catch rate of sailfish (*Istiophorus platypterus*) caught by Brazilian longliners in the Atlantic Ocean (1978-2008). *Col. Vol. Sci. Pap., ICCAT* .65 -1762 - 1771.
- Zerger, A., Gibbons, P., Seddon, J., Briggs, S. and Freudenberger, D. 2009. A method for predicting native vegetation condition at regional scales. *Landsc. Urban Plann.* 91: 65-77.
- Zheng, X., Pierce, J.G., Reid, D.G., Jolliffe, I.T. 2002. Does the North Atlantic current affect spatial distribution of whiting? Testing environmental hypotheses using statistical and GIS techniques. *ICES J. Mar. Sci.*, 59: 239 – 253.

- Zuur, A.F., Ieno, E.N., Saveliev, A.A. and Smith, G.M. 2009. *Mixed effects models and extensions in ecology with R*. 1st Edition, Springer. 574pp.
- Zuur, A.F., Ieno, E.N. and Elphick, C.S. 2010. A protocol for data exploration to avoid common statistical problems. *Methods in Ecology & Evolution*. 1: 3-14.